

TIP-OVER STABILITY ANALYSIS OF CRAWLER CRANES IN HEAVY LIFTING APPLICATIONS

A Thesis
Presented to
The Academic Faculty

by

Sima Rishmawi

In Partial Fulfillment
of the Requirements for the Degree
Master of Science in Mechanical Engineering in the
The George W. Woodruff School of Mechanical Engineering

Georgia Institute of Technology
May 2016

Copyright © 2016 by Sima Rishmawi

TIP-OVER STABILITY ANALYSIS OF CRAWLER CRANES IN HEAVY LIFTING APPLICATIONS

Approved by:

Professor William Singhose, Advisor
The George W. Woodruff School of
Mechanical Engineering
Georgia Institute of Technology

Professor Aldo Ferri
The George W. Woodruff School of
Mechanical Engineering
Georgia Institute of Technology

Professor Alper Erturk
The George W. Woodruff School of
Mechanical Engineering
Georgia Institute of Technology

Date Approved: April 1, 2016

To my family,

especially my mother and father,

Thank you for your endless love, sacrifices,

prayers, support and advice.

ACKNOWLEDGEMENTS

I am thankful ...

For the Author and Giver of life for His constant care and blessings, for I learned that all is possible through faith and prayer ...

For all that I have given and all that I have received ...

For everything I have obtained and for not having everything I desire, If I did, what would there be to look forward to ...

For all the knowledge I have acquired and for everything I do not know, for it gives me the opportunity to learn ...

For the good times and the bad times, during these times I grow ...

For my limitations, because they give me the chance to improve ...

For each new challenge, because it will build and strengthen my character ...

For my mistakes, for they teach me valuable lessons ...

For the time when I am tired and worn-out, for it means I made a difference ...

For my parents, my family, my teachers and friends whose presence and encouragement was a candle burning to light my way.

TABLE OF CONTENTS

ACKNOWLEDGEMENTS	iv
LIST OF TABLES	viii
LIST OF FIGURES	ix
SUMMARY	xv
I INTRODUCTION	1
1.1 Construction Crane Types	1
1.1.1 Mobile Cranes	2
1.1.2 Advantages and Disadvantages of Mobile Cranes	3
1.2 Crane Accidents	6
1.2.1 Modes of Crane Failure	7
1.2.2 Crane Accident Causes between 2011 and 2015	9
1.3 Tip-Over Stability of Mobile (Crawler) Cranes	10
1.4 Previous Work	12
1.5 Thesis Overview	14
1.6 Thesis Contributions	15
II STATIC TIP-OVER STABILITY OF CRAWLER CRANES WITH MOVABLE COUNTERWEIGHTS	16
2.1 Overview	16
2.2 Tip-over Stability Based on Sum of Moments about Possible Tip-over Axes	19
2.3 Case Study - Terex CC 2800-1	22
2.3.1 Effect of Parameters in the Boom-Mast Configuration	23
2.3.2 Effect of Parameters in the No-Mast Configuration	31
2.3.3 Effect of Parameters when a Jib is Added to the Configuration	32
2.4 Summary	39

III PSEUDO-DYNAMIC TIP-OVER STABILITY OF CRAWLER CRANES WITH MOVABLE COUNTERWEIGHTS	41
3.1 Description of the Approach	41
3.2 Straight Base Motion	43
3.2.1 Mathematical Model and Payload Swing Dynamics	43
3.2.2 Tip-over Stability Analysis of Straight Base Motion	47
3.2.3 Effect of Hoist Cable Length	55
3.3 Boom Luffing Motion	60
3.3.1 Mathematical Model and Payload Swing Dynamics	60
3.3.2 Tip-over Stability Analysis of Boom Luffing	63
3.3.3 Effect of Counterweight Mass and Payload Mass	68
3.4 Boom Slewing Motion	69
3.4.1 Mathematical Model and Payload Swing Dynamics	70
3.4.2 Experimental Verification - Tower Crane	73
3.4.3 Tip-over Stability Analysis of Boom Slewing	79
3.5 Summary	84
IV EXPERIMENTAL VERIFICATION	85
4.1 Introduction	86
4.2 Components	86
4.2.1 Truss Set Members (ME-6993)	86
4.2.2 #6 I-Beam Spares (ME-7008)	87
4.2.3 Flat Structures Members (ME-6987)	87
4.2.4 Full Round Connectors Spares (ME-6997)	88
4.2.5 Angle Connectors (ME-6999A)	89
4.2.6 Axle Spares (ME-6998A)	89
4.2.7 Cord Lock Spares (ME-6996)	89
4.3 Crane Model Specifications	90
4.4 Experimental Procedure	93

4.4.1	Effect of Crawler Crane Slew Angle on Minimum Counterweight Position Required to Prevent Forward Tip-over	93
4.4.2	Effect of Payload Swing	95
4.5	Results	95
4.5.1	Effect of Crawler Crane Slew Angle on Minimum Counterweight Position Required to Prevent Forward Tip-over	95
4.5.2	Effect of Payload Swing	98
4.6	Limitations and Challenges	100
4.7	Summary	101
V	CRAWLER CRANES IN TANDEM LIFTING	102
5.1	Overview	102
5.2	Tip-over Stability Based on the Sum of Moments About the Forward Tip-over Axis	104
5.3	Case Study - Terex CC 2800-1	108
5.3.1	Boom Luffing Angle vs. Swing Angle	109
5.3.2	Payload Mass vs. Swing Angle	113
5.3.3	Separation Distance vs. Swing Angle	115
5.3.4	Effect of Hoist Length	117
5.4	Summary	118
VI	CONCLUSIONS AND FUTURE WORK	120
6.1	Conclusions	120
6.2	Future Work	121
	APPENDIX A — MATLAB SOURCE CODES	123
	REFERENCES	226

LIST OF TABLES

1	Crane Accident Statistics (2011- June, 2015) [4].	7
2	Parameters of the Terex CC 2800-1 [34].	24
3	Geometrical Parameters of the Terex CC 2800-1 (Jib Configuration) [34].	34
4	Summary of Stability Trends.	40
5	Guidelines to Choose the Acceleration Command Generating Minimum Vibrations for Different Hoist Lengths.	58
6	Parameters of the Tower Crane.	76
7	Truss Members Set [26].	86
8	Parameters of the Experimental Crane Model.	92
9	Parameters of the Terex CC 2800-1.	108

LIST OF FIGURES

1	Construction Crane Types.	2
2	Crawler Crane Parts [32].	3
3	Scene of crane collapse at 40 Worth St & W Bdwy in Manhattan [3].	5
4	Boom Damage of the Collapsed Crane in Manhattan [3].	5
5	Crane Accident Causes during the Past Five Years [4].	11
6	Tandem Lift Accident [4].	12
7	Crawler Crane Tip-Over Accident [23].	13
8	Counterweights on Rotating Bed and on Trailer, Modified from [34]. .	17
9	Crane with movable counterweight patented by Wigglesworth [37]. . .	18
10	Top View of the Horizontal Plane Formed by the Possible Tip-over Axes.	20
11	Schematic Diagram for a Crawler Crane with movable Counterweight (Mast included).	21
12	Terex CC 2800-1 Crawler Crane [34].	23
13	Sample Load Chart for the Terex CC 2800-1 Crawler Crane [34]. . . .	25
14	Minimum Counterweight Position to Prevent Forward Tip-over for a Boom Luffing Angle of 62° and a Payload Mass of $110 t$, (m_4 is the Movable Counterweight Mass).	26
15	Maximum Counterweight Position to Prevent Backward Tip-over for a Boom Luffing Angle of 62° , (m_4 is the Movable Counterweight Mass).	27
16	Backward and Forward Tip-over Limits for a Boom Luffing Angle of 62° , a Payload Mass of $110 t$, and a Movable Counterweight Mass of $200 t$	28
17	The Effect of Changing the Luffing Angle ϕ_1 on the Minimum Counter- weight Position to Prevent Forward Tip-over for a Payload mass of $110 t$ and a Counterweight Mass of $200 t$	29
18	The Effect of Changing the Luffing Angle ϕ_1 on the Maximum Counter- weight Position to Prevent Backward Tip-over for a Counterweight Mass of $200 t$	30
19	The Effect of Changing the Payload Mass on the Minimum Counter- weight Position to Prevent Forward Tip-over for a Boom Luffing Angle of 62° and a Counterweight Mass of $200 t$, (m_5 is the Payload Mass).	30

20	Minimum Counterweight Position to Prevent Forward Tip-over (No Mast Configuration) for a Boom Luffing Angle of 62° and a Payload Mass of $110 t$, (m_4 is the Movable Counterweight Mass).	31
21	Maximum Counterweight Position to Prevent Backward Tip-over (No Mast Configuration) for a Boom Luffing Angle of 62° , (m_4 is the Movable Counterweight Mass)..	32
22	Schematic Diagram for a Crawler Crane with Movable Counterweight (Mast and Jib included).	33
23	Minimum Counterweight Position to Prevent Forward Tip-over (Jib included) for a Boom Luffing Angle of 62° and a Payload Mass of $110 t$, (m_4 is the Movable Counterweight Mass).	35
24	Minimum Counterweight Position to Prevent Forward Tip-over (Jib included) for a Boom Luffing Angle of 62° and a Payload Mass of $65 t$, (m_4 is the Movable Counterweight Mass)..	35
25	Maximum Counterweight Position to Prevent Backward Tip-over (Jib included) for a Boom Luffing Angle of 62° , (m_4 is the Movable Counterweight Mass).	36
26	The Effect of Changing the Luffing Angle ϕ_1 on the Minimum Counterweight Position to Prevent Forward Tip-over (Jib included) for a Payload Mass of $110 t$ and a Movable Counterweight Mass of $200 t$	37
27	The Effect of Increasing the Payload Mass on the Minimum Counterweight Position (Jib included) for a Boom Luffing Angle of 62° and a Movable Counterweight Mass of $200 t$, (m_5 is the Payload Mass).	38
28	The Effect of Decreasing the Payload Mass on the Minimum Counterweight Position (Jib included) for a Boom Luffing Angle of 62° and a Movable Counterweight Mass of $200 t$, (m_5 is the Payload Mass).	39
29	Schematic Diagram of a Crawler Crane with a Movable Counterweight Showing Payload Swing.	42
30	Bang-Coast-Bang Acceleration Command.	45
31	Vector Diagram for the Acceleration Command Resulting in Maximum Residual Vibrations.	46
32	Free Body Diagram of Crawler Crane with Inertial Forces during Deceleration.	48
33	Payload Swing Angle in Bang-Coast-Bang Motion vs. Time with Different Acceleration Durations.	49
34	Payload Swing Response to a Bang-Coast-Bang Acceleration Command vs. Time (Maximum Oscillation).	50

35	Minimum Counterweight Position to Prevent Forward Tip-Over in the Static and Dynamic Cases with a Payload of 110 t.	51
36	Static and Dynamic Safety Regions for a 200 t Counterweight and Boom Luffing Angle of 60°.	52
37	Length of Static and Dynamic Safety Regions for a 200 t Counterweight and Boom Luffing Angle of 60°.	53
38	Minimum Counterweight Position to Prevent Forward Tip-over in the Static and Dynamic Case with a Payload of 110 t (Independent Effects of Payload Swing and Inertial Forces).	54
39	Minimum Counterweight Position to Prevent Forward Tip-over in the Dynamic Case with a Payload of 110 t, (m_4 is the Counterweight Mass).	55
40	Minimum Counterweight Position to Prevent Forward Tip-Over in the Dynamic Case with a Counterweight of 200 t, (m_5 is the Payload Mass).	56
41	Maximum Residual Payload Swing Angle vs. Hoist Length.	56
42	Vector Diagram for the Acceleration Command Resulting in Minimum Residual Vibrations.	57
43	Payload Swing Response to a Bang-Coast-Bang Acceleration Command vs. Time (Minimum Oscillation).	58
44	Payload Swing Response to a Bang-Coast-Bang Acceleration Command vs. Time (Reduced Oscillation).	59
45	Dynamics in Constant Luffing Down Motion - Side View.	61
46	Payload Swing Angle in Constant Luffing Down Motion vs. Time.	64
47	Minimum Counterweight Position to Prevent Forward Tip-over for a Range of Initial Boom Luffing Angles with a Payload of 110 t.	65
48	Minimum Counterweight Position to Prevent Forward Tip-over in the Static and Dynamic Boom-Luffing Cases with a Payload of 110 t.	65
49	Static and Dynamic Safety Regions for a 200 t Counterweight and an Initial Boom Luffing Angle of 60°.	67
50	Static and Dynamic Safety Regions for a 200 t Counterweight and an Initial Boom Luffing Angle of 60°.	67
51	Minimum Counterweight Position to Prevent Forward Tip-over in the Dynamic Case with a Payload of 110 t, (m_4 is the Counterweight Mass).	68
52	Minimum Counterweight Position to Prevent Forward Tip-over in the Dynamic Case with a Counterweight of 200 t, (m_5 is the Payload Mass).	69

53	Dynamics in Boom Slewing Motion.	71
54	Tower Crane used in Experiments.	74
55	Radial Swing of the Payload when the Tower Crane was Slewed a Distance of 75°	75
56	Tangential Swing of the Payload when the Tower Crane was Slewed a Distance of 75°	75
57	Maximum Radial Swinging Angle of the Payload vs. Slewing Distance (Experimental and Simulation Results).	77
58	Maximum Tangential Swinging Angle of the Payload vs. Slewing Distance (Experimental and Simulation Results).	77
59	Experimental and Simulated Radial Swinging Angle of the Payload for a Moving Distance of 60°	78
60	Experimental and Simulated Tangential Swinging Angle of the Payload for a Moving Distance of 60°	79
61	Maximum Swinging Angles of the Payload vs. Slewing Distance.	81
62	Minimum Counterweight Position to Prevent Forward Tip-over for Different Slewing Distances.	82
63	Minimum Counterweight Position to Prevent Sideways Tip-over for Different Slewing Distances.	82
64	Minimum Counterweight Position to Prevent Front and Sideways Tip-over for Different Slewing Distances for a Counterweight Mass of 200 <i>t</i>	83
65	Experimental Scale Crane Model.	85
66	Truss Set Members (ME-6993) [26].	87
67	Flat Structures Members (ME-6987) [26].	88
68	Full Round Connectors Spares (ME-6997) [26].	88
69	Angle Connectors (ME-6999A) [26].	89
70	Axle Spares (ME-6998A) [26].	90
71	Cord Lock Spares (ME-6996) [26].	90
72	Acrylic Plates Specifications (Units are in inches).	91
73	Slewing Mechanism in the Experiment.	92
74	Experimental Crane Setup - Slew Angle is 30°	94
75	Experimental Crane Setup - Slew Angle is 90°	94

76	Minimum Counterweight Position to Prevent Forward Tip-over [Boom Luffing Angle of 66° , Payload Mass of 1 <i>kg</i> , and Counterweight Mass of 1 <i>kg</i>].	96
77	Minimum Counterweight Position to Prevent Forward Tip-over [Boom Angle of 66° , Payload Mass of 1.1 <i>kg</i> , and Counterweight Mass of 1 <i>kg</i>	97
78	Minimum Counterweight Position to Prevent Forward Tip-over for Both Payload Masses.	98
79	Maximum Payload Swing Angle to Prevent Forward Tip-over.	99
80	Tandem Lifting Cranes [36].	103
81	Top View of the Horizontal Plane Formed by the Possible Tip-over Axes.	104
82	Schematic Diagram for Tandem Crawler Cranes (load is swinging)	105
83	Schematic Diagram for Tandem Crawler Cranes (load is pulled)	106
84	Free Body Diagram of Payload.	107
85	Minimum Boom Angle to Prevent Forward Tip-over vs. Swing Angle for a Payload Mass of 220 <i>t</i>	109
86	Minimum Boom Angle to Prevent Forward Tip-over vs. Swing Angle for Different Payload Masses for Crane A, (m_4 is the Payload Mass).	110
87	Critical Payload Swing Angle vs. Payload Mass for a Boom Angle of 82°	111
88	Schematic Diagram for Tandem Crawler Cranes (Triangular Payload).	112
89	Minimum Boom Angle to Prevent Forward Tip-over vs. Swing Angle for a Triangular Payload with a Mass of 220 <i>t</i>	112
90	Maximum Payload Mass to Prevent Forward Tip-over vs. Swing Angle for a Boom Angle of 77°	113
91	Maximum Payload Mass to Prevent Forward Tip-over vs. Swing Angle for Different Boom Angles.	114
92	Minimum Boom Angle and Maximum Payload Mass to Prevent Forward Tip-over vs. Swing Angle.	115
93	Minimum Boom Angle to Prevent Forward Tip-over vs. Separation Distance for a Payload Mass of 220 <i>t</i>	116
94	Minimum Boom Angle to Prevent Forward Tip-over vs. Separation Distance for a Payload Mass of 220 <i>t</i> and Different Hoist Cable Lengths L_4	117

95	Critical Separation Distance vs. Different Hoist Cable Lengths for a Boom Angle of 82°	118
----	--	-----

SUMMARY

Cranes are often the most conspicuous machines on a construction site. This is due to their large size, in addition to the important role they have in transporting heavy payloads vertically and horizontally.

There are two major families of construction cranes: tower cranes and mobile cranes. Mobile cranes that are mounted on tracks are a subgroup referred to as “crawler cranes”. Crawler cranes are widely used on construction sites, and are a backbone of the United States construction industry, thus a detailed study of these cranes’ behavior is essential.

This research studies the tip-over stability of crawler cranes in heavy-lifting applications. Two major applications are discussed: crawler cranes using movable counterweights and crawler cranes in tandem lifting.

1. Crawler cranes with movable counterweights

Crawler cranes introduce the advantage of mobility and versatility on the construction site, which provides faster and more accurate positioning of payloads. However, the massive size and weight of these machines create a large tip-over hazard. A small force with a large moment arm can create a huge moment that can cause the crane to tip-over. Crane counterweights provide balancing forces so that the crane does not tip over as it picks up and moves heavy payloads.

To increase the stability of the crawler crane and help support a heavier payload, a larger counterweight may seem like a straight-forward solution, however there are important trade-offs to consider. Larger counterweights are more difficult to transport from one location to another, and they require ground preparation to properly support the large compressive load that these counterweights cause. Also, a larger

counterweight results in a slower, and more difficult to move crawler crane, thus compromising the mobility advantage of the crawler crane. Therefore, the concept of a movable counterweight has been introduced as a solution to these problems.

Movable counterweights provide several advantages in terms of reducing the total machine weight, increasing mobility, and improving ease of use. However, introducing a movable counterweight complicates the design and control of the crane. Furthermore, the difficulty of performing the static and dynamic analyses of the crawler crane is increased.

This research provides a detailed static and pseudo-dynamic analyses to calculate the limits of the counterweight position to ensure stability and prevent tip-overs for various crane parameters and configurations. Additionally, a guideline is given to crane operators to prevent accidents, and define safety regions of operation.

First, the crane is considered to be stationary, and the effect of different parameters on the counterweight's position is examined. Then, the effect of different motion scenarios is studied, and a comprehensive stability analysis is performed, taking into consideration the payload swing induced by different motions.

All the results presented in this research provide general guidelines for crane operators, so that they can make reasonable decisions regarding the placement of the movable counterweight during operation. These guidelines help prevent tip-over accidents, and improve the operation for crawler cranes in general.

2. Crawler Cranes in Tandem Lifting

One common problem in crane lifting operations is the need to transport a bulky or irregular-shaped payload. In such case, it may be necessary to handle these items by tandem lifting with two cranes. The complexity of such a configuration is discussed, and a static tip-over analysis of the two cranes in tandem lifting operation is studied.

These cranes have a large tendency to tip-over creating bigger catastrophes, since the tipping of one crane causes the other crane to tip as well. Also, it is often difficult

to synchronize the behavior of the two cranes because they are operated with two different operators, who can have difficulties perceiving what the other crane is doing. Thus it is important to provide a set of guidelines that can simplify the procedure and minimize accidents. This challenge is what the final chapter of this thesis focuses on.

The prediction model and the results in this thesis provide a significant tool for practical application of tip-over stability analysis for crawler cranes with heavy lifting applications, whether a movable counterweight is used, or tandem lifting. Experimental results are provided to verify some of the key theoretical results.

CHAPTER I

INTRODUCTION

Modern building construction projects are highly mechanized and becoming more so everyday. On construction sites, production equipment is being replaced by *transportation* equipment, because structural elements are being prefabricated off-site and then installed or assembled on site. Material handling and lifting equipment now dominate building construction sites more than ever before, and they constitute a critical element in achieving high productivity [31].

The typical building construction site will include several or all of the following equipment: cranes, material handlers, concrete pumps, hoists and lifts, and forming systems. However, *cranes* are the most conspicuous machines on site, not only because of their size, but also due to the important role they have in transporting materials and elements vertically and horizontally [31].

1.1 Construction Crane Types

There are two major families of construction cranes: tower cranes and mobile cranes. Examples of these two families are shown in Figure 1. The term “mobile cranes” can be used to refer to *truck-mounted* mobile cranes only, while *track-mounted* mobile cranes are a subgroup referred to as “crawler cranes” [31].

Traditionally, the number of mobile cranes used on construction sites in the United States has been far greater than the number of tower cranes. They are by and large the backbone of the United States construction industry, and will be the focus of this thesis. However, it should be mentioned that tower cranes, the icon of construction in Europe and the Far East are also in wide spread use at United States building sites [31].



(a) Mobile Crane [21]



(b) Tower Crane [35]

Figure 1: Construction Crane Types.

1.1.1 Mobile Cranes

A mobile crane is a self-propelled mobile machine, capable of moving freely about the job site, and in most cases from one job site to another. The span of machine size ranges from mini machines fitting in the back of a small truck to huge models used in shipyards, wind farms, construction sites, ports, and other manufacturing facilities. The type of mobile cranes included in this research is the track-mounted mobile crane, also known as “crawler cranes” [31].

A crawler crane is composed of several parts, as illustrated in Figure 2. The base of the machine has the crawling tracks and the propulsion system. On top of the track, are the engine, control area, and the operator cab. The lifting cables run up through the end of the boom and hang downward to the hook. Objects to be lifted

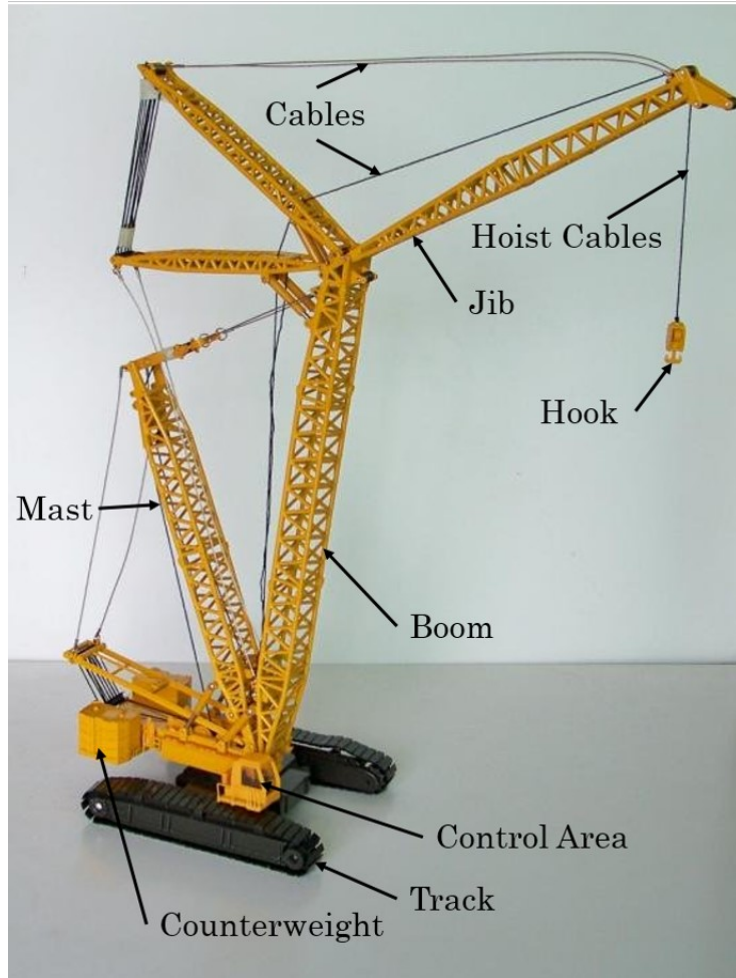


Figure 2: Crawler Crane Parts [32].

are attached to the hook. Sometimes the crane boom has an extension that sticks out at an angle from the boom. This “jib” extension allows the crane to move objects further away from its center and to higher heights. Finally, the counterweight, which can weigh hundreds of tons, allows the crane to lift very heavy loads. Crawler cranes can lift thousands of tons depending on their components and configuration [38].

1.1.2 Advantages and Disadvantages of Mobile Cranes

There are many reasons that make crawler cranes popular and widely used. These cranes are maneuverable and versatile while on the job site. Due to the stability of

their steel track design, they can lift heavier loads than those of rubber tire-equipped models with similar attachments. Finally, crawler cranes can travel while carrying a load, provided that the crane is operating on firm level ground to within 1% gradient, which is about a slope of 0.6° [39]. This is a highly recommended common practice in crane operations. Also, crawler cranes sometimes have booms that can reach several hundred feet in the air, which makes them perfect for large construction sites [38, 9].

On the other hand, crawler cranes cannot be transported from one construction site to another without additional equipment. Usually, they need to be dismantled into pieces and transported by trucks, rails, or other vehicles. This increases the cost of using a crawler crane as compared to other types of mobile cranes [38, 9].

Also, the massive size and weight of these cranes create a larger tip-over hazard. Given the massive height of such cranes, a small force with a large moment arm can create a huge moment that can cause the crane to tip over. Therefore, as the crane gets taller the counterweight generally needs to be larger. Massive counterweights need special ground preparation to properly support the large compressive loads that they generate [38, 9].

To better understand the danger of forces and moments that cause tip-overs, one of the recent crane tip-over accidents is discussed. This accident happened in Manhattan, New York City on February 5th, 2016. One person was killed and three were injured. The crane was being secured when it tipped over, letting the extremely long boom fall along Worth Street in Tribeca, a roadway that is normally swarming with people during the morning rush hours. Luckily, injuries were lessened because construction workers were guiding people away from the street when the collapse happened [3]. Figures 3 and 4 show the dramatic tip-over, and the huge fall zone of the boom. This is an example of how severe tip-over accidents are and emphasizes the need to study their causes.



Figure 3: Scene of crane collapse at 40 Worth St & W Bdwy in Manhattan [3].



Figure 4: Boom Damage of the Collapsed Crane in Manhattan [3].

Nevertheless, modern industrialization and construction is driving the need for heavy cargo, and this includes components used in renewable and sustainable energy developments, such as wind turbines. Wind turbine components provide an excellent example of challenging crane lifts due to their considerable mass. The machinery housings, called nacelles, are very heavy, while the rotor blades are extremely bulky and awkward to manipulate [7].

Consequently, moving heavy or over-sized loads is posing new challenges for the crane industry. It is not only the demand for more powerful cranes that is growing. There is a growing need for alternative methods of lifting. When payloads are heavy, mobile cranes with movable counterweights are a convenient alternative. Given the problems posed by large and awkward shapes, it may be necessary to handle some items by tandem lifting with two cranes [7].

As a result, it is evident that improving lifting capacity will require more safety features to prevent tipping over and guarantee larger stable workspaces [38, 9].

1.2 Crane Accidents

The construction industry in the US has a high injury and fatality rate when compared with other industries [22]. The reason is that this industry involves complex and dynamic work environments that present hazards to workers on a daily or even hourly basis.

Though there are a number of factors that cause this high rate of accidents in the construction industry, many injuries and fatalities can be attributed to the heavy machinery. Cranes, with their numerous types and configurations are a critical component of most construction projects, and are the reason behind one-third of all construction and maintenance fatalities and injuries resulting in permanent disability [22].

Nevertheless, the volume of crane accidents can only be estimated because the

Table 1: Crane Accident Statistics (2011- June, 2015) [4].

Year	Accidents	Deaths
2011	106	93
2012	235	99
2013	193	61
2014	215	78
2015	103	38
Average	189.3	82

definition of *accident* is not universal. That is, some businesses may report only events resulting in injuries or deaths, while others report only accidents resulting from certain causes.

On the website CraneAccidents.com [4], a large number of crane accidents are voluntarily archived each year. Table 1 shows the number of accidents reported on this website in each of the past five years, as far as the end of June, 2015. It also shows the number of fatalities in each year.

It should be mentioned however, that a major crane accident occurred on September 11th, 2015 in Mecca, Saudi Arabia. This accident took place in Mecca’s Grand Mosque, which was crowded with people a few days before Hajj season, thus causing 107 deaths on its own.

In order to study the causes of these accidents, it is essential to first examine the reasons why cranes fail.

1.2.1 Modes of Crane Failure

Cranes fail, sometimes catastrophically, in a number of different ways. One generally accepted list of 13 failure modes was presented by David MacCollum in 1980 and then in his book in 1993 [17, 18]. These modes are:

1. **Overloading:** Combination of boom length, angle, and lifted load that exceeds the rated capacity and safety margin of a crane and results in a crane upset.
2. **Side Pull:** Lateral boom loading encountered when a load is turned or lifted can buckle the boom.
3. **Outrigger Failure:** Outriggers fail to keep crane stabilized, or are never deployed to begin with.
4. **Hoist Limitations:** Hoist line parts while being reeled in or suspending a load.
5. **Two-Blocking:** Load is lifted too high and the hook block strikes the boom tip.
6. **Killer Hooks:** Worn hook fails and drops a load unexpectedly.
7. **Boom Buckling:** Boom deformation due to suddenly applied strains (i.e. abrupt release of load, raising the boom beyond the safe angle, boom striking a structure), or compromise during shipping.
8. **Upset/Overturn:** Due mainly to operator failure to extend outriggers, although also possible while moving a load on unstable/uneven terrain.
9. **Unintentional Turntable Turning:** Load is lifted without operator locking cab onto chassis.
10. **Oversteer/Crabbing:** Can occur in some rough terrain cranes where rear wheel steering can be engaged accidentally, resulting in an unexpected halving of the crane's turning radius.
11. **Control Confusion:** Can occur due to lack of control standardization among different crane makes and models, or insufficient distance and illogical placement of controls.

12. **Access/Egress:** Footholds allowing operators to access the cab are frequently located in areas where hydraulic leaks occur, resulting in slippery footrests and subsequent falls.
13. **Unintentional Power Line Contact:** Accidental contact between line and boom or crane chassis.

Other modes which have been identified include improper assembly/dismantling, fall of load or lifting tackle, being struck by a moving load, and being struck by the crane itself [22].

However, my research brings up some other modes that need to be mentioned, such as payload swinging and payload pulling in tandem lifting which increase the risk of tipping over, in addition to wind load which can be unpredictable in some cases. Finally, when mobile cranes travel on the streets, they are subject to traffic accidents.

1.2.2 Crane Accident Causes between 2011 and 2015

Looking through the reported accidents archived in [4] and mentioned in Table 1, I was able to make a list of the causes behind these accidents. This list includes causes for accidents that actually happened in the last five years. These causes do not include the whole list of MacCollum, which covers broader categories. They are as follows:

- (A) Payload falling on victims or equipment.
- (B) Unintentional power line contact and electrocutions.
- (C) Improper assembly or dismantling of the crane.
- (D) Mechanical failure including buckling.
- (E) Overturning or tipping over of the crane.

- (F) Victims struck by moving load or crane parts.
- (G) Victims falling from crane.
- (H) Other miscellaneous causes including traffic accidents and fires.

Figure 5 demonstrates the percentage of the above cases with respect to the whole number of accidents in each year from January, 2011 to October, 2015. It is clear in the charts that the main reason a crane accident occurs is the case of the crane overturning or tipping over. This is a very wide category that can happen as a consequence of numerous events. Studying crane tip-overs, their causes, and how to prevent them is a very important research topic that can contribute to improving safety at construction sites.

1.3 Tip-Over Stability of Mobile (Crawler) Cranes

Being such huge machines, and having to carry heavy loads from one place to another, crawler cranes obviously pose a significant stability hazard. If the payload weight is more than the weight specified in load charts, then it can create a moment decreasing the stability of the crane in the forward direction. Also, positioning the boom at an angle that is too low would change the lever arm of the payload and boom weight forces, thereby creating a tip-over moment in the forward direction. Another interesting case is when the payload suddenly falls off. In such cases, if the counterweight is too large, then it creates a moment causing the crane to tip over backwards. And finally, weather sometimes plays a role. Higher wind speeds than those stated in load charts can lead to catastrophic consequences, similar to the Manhattan tip-over accident mentioned earlier.

An example of a recent serious crane accident is the one that took place at VT Halter Marine in Pascagoula, Mississippi. On June 25th, 2014, three crawler cranes were in tandem lifting trying to move a section of a boat. One of them failed and

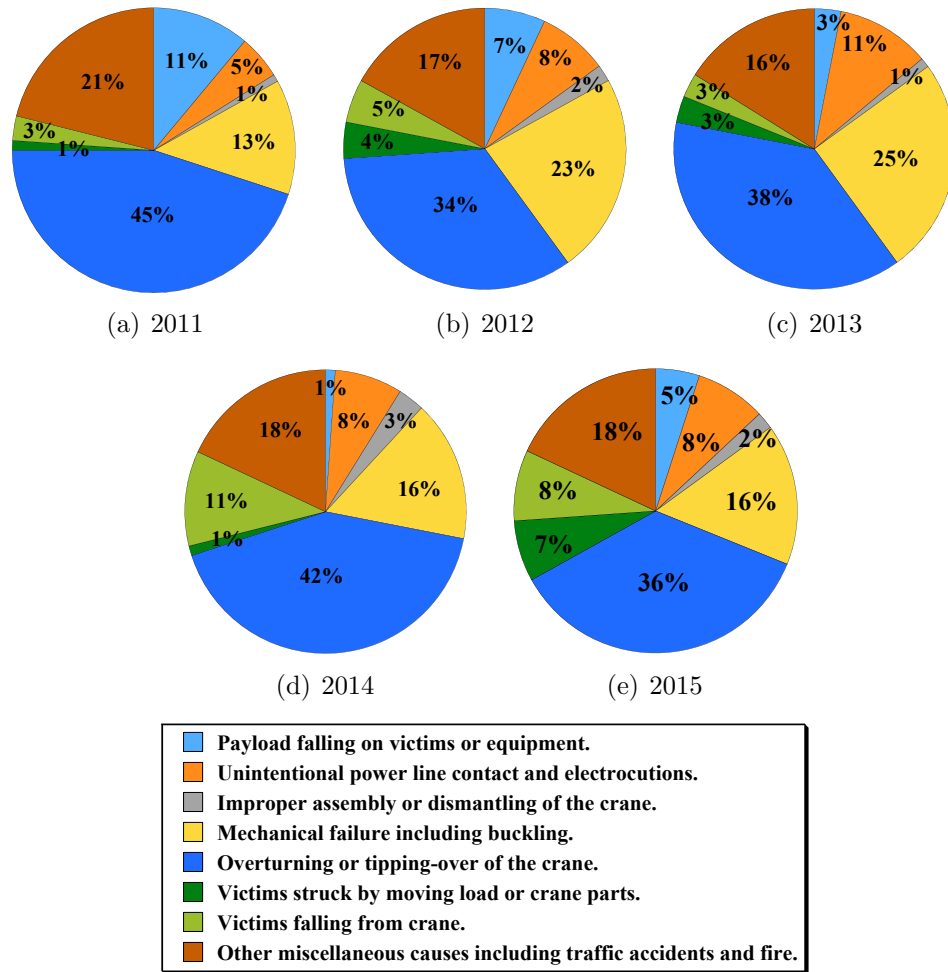


Figure 5: Crane Accident Causes during the Past Five Years [4].

tipped over forwards, which caused the hoists attached to the shared payload to break. Thus, the second crane suddenly lost its payload and tipped over backwards. This was a catastrophic incident that led to the death of one person, while four others were injured. Figure 6 shows a picture taken at the scene [10].

Moreover, when the crane is in motion, things get more complicated. Base acceleration and boom motions cause the payload to swing, and these oscillations increase the payload moment arm and add a centripetal force to the gravity forces. The time-varying sum of these forces creates a moment that, if not somehow counterbalanced,



Figure 6: Tandem Lift Accident [4].

will decrease the crane's stability.

When a crane tips over it can completely destroy itself, cause great damage to the surrounding environment, and can cost lives of humans operating the crane, working in the fall zone, or even just passing nearby. Figure 7 shows a crawler crane that has tipped over. The boom falls a long way from the base of the crane. Therefore, the potential fall zone around a tall crawler crane is massive.

1.4 Previous Work

There have been several investigations of the tip-over stability of cranes. Neitzel et al. [22] reviewed available information on crane-related injuries, and gave recommendations for improving crane injury prevention and future crane safety research. Jeng, Yang, Chieng [8] introduced two indices, a moment-index and a force-index, to quantify the tip-over behavior of mobile cranes. They also examined the bearing capacity of outriggers. The force-angle stability measure [24, 25], which is easily computed



Figure 7: Crawler Crane Tip-Over Accident [23].

and is sensitive to changes in the center of mass height, provides an indication of proximity to tip-over.

The tip-over stability of a mobile crane considering the payload oscillations was investigated by Rauch et al. in [29]. The comparison between the static stability and the full-dynamic stability revealed that a simple semi-dynamic analysis provides good approximations for the tip-over stability properties. A dynamic model for the control of a flexible mobile crane with a flexible boom was derived by Kiliçaslan [11]. The goal was to determine safe loads and prevent tipping.

In addition to cranes, several investigations of related machinery have been conducted. A small-scale cherrypicker was constructed to investigate the dynamics and stability of aerial lifts [19]. Vibration-control techniques were used to improve system response. Manning et al. [20] used an input-shaping control method to suppress double-pendulum oscillations created by a payload with distributed-mass properties.

Furthermore, tip-over of a mobile manipulator was determined as a function of inertia, gravity, and acceleration [15]. An online fuzzy logic self-motion planner was used to generate desired motions in real-time.

Korayem et al. [12] derived kinematic and dynamic models of a mobile manipulator. Ghasempoor and Sepehri [6] showed that the amount of impact energy that can be sustained by a vehicle without tipping-over can be used to compute the tip-over potential of a vehicle carrying a manipulator. Lee and Yi [14] investigated a fuzzy logic roll stability control system to prevent the rollover of sport utility vehicles. The maximum payload path for a specified payload was generated using an optimal control approach. Zhaofa et al. [41] studied a scheme for stability monitoring of large-scale hoisting transfer equipment. The hydraulic leg force was measured by a weight sensor to judge safety for the hoisting equipment. Abo-Shanab and Sepehri [1] developed a simulation model for studying the tip-over stability of a typical heavy-duty hydraulic log-loader machine. Their results showed that the flexibility at the manipulator joints due to the hydraulic compliance improved the machine stability.

1.5 Thesis Overview

In this thesis, the tip-over stability of a crawler crane is analyzed under various conditions. In Chapter 2, a tip-over prediction model of a crawler crane equipped with a movable counterweight is presented. The crane is assumed to be stationary, with a single-pendulum point-mass payload. A method to determine the limits of the counterweight position that prevent forward and backward tip-overs is explained. A static stability analysis is then performed to provide insights on the effect of different parameters on the counterweight position, such as the counterweight mass, the boom luffing angle, the payload mass, and the presence of a mast or jib.

Chapter 3 introduces a pseudo-dynamic stability analysis that is used to study the tip-over stability of a crawler crane with a movable counterweight when it performs

simple motions. The analysis considers the dynamics and payload swing introduced by motions such as: straight base motion, boom luffing motion, and boom slewing motion.

A small-scale experimental crane model was built and presented in Chapter 4. Experiments were performed on this model to support the results obtained in Chapter 2. In Chapter 5, the process of tandem lifting is studied. A static stability analysis is performed to develop guidelines for operating these cranes safely. The chapter also provides an introduction to a wide scope of future research in tandem lifting.

Finally, Chapter 6 summarizes the results obtained during this research project, and suggests some possible future work in the area of tip-over stability in heavy lifting applications.

1.6 Thesis Contributions

This thesis contributes to the knowledge of crawler cranes' tip-over stability by:

1. Developing a computational tool that can estimate the safety region in which a movable counterweight can be placed to prevent forward and backward tip-overs.
2. Determining the effect of the crane's parameters on the counterweight positioning required to prevent tip-over.
3. Examining the effect of different configurations of the crawler crane on the counterweight positioning.
4. Extending the developed computational tool to include the effect of acceleration and payload swing as the crane undergoes simple motions, which can also be easily expanded to apply to other types of machinery.
5. Studying the static performance of cranes in tandem lifting, and providing some guidelines that can improve the performance and reduce accidents.

CHAPTER II

STATIC TIP-OVER STABILITY OF CRAWLER CRANES WITH MOVABLE COUNTERWEIGHTS

2.1 Overview

Crane counterweights provide balancing forces so that the crane does not tip over as it picks up and moves heavy payloads. As cranes get taller, their counterweight masses increase significantly. This makes the crane more expensive, harder to transport, and more difficult to erect. Massive counterweights also require extensive ground preparation to properly support the large compressive loads. In order to decrease the required counterweight, crane manufacturers have been developing cranes with movable counterweights. Some of the recent patented models are described in [27], [28], [33], and [40].

The mobile platform of a crane can provide a significant counterweight. However, the width of the base is often limited by the need to transport the crane on roads. To increase side-to-side stability, outriggers can be used, however, this eliminates mobility during lifts. To improve stability in the fore-aft direction of the boom, additional mass can be added directly on the rotating bed, or mass can be attached through an auxiliary platform or trailer. Such auxiliary counterweights are shown in Figure 8.

Movable counterweights provide several advantages in terms of reducing the total machine weight, increasing mobility, and improving ease of use, when compared with similar cranes with fixed counterweights. A crane with a movable counterweight has less total mass because it can move the weight to various locations to change the moment arm. Given the reduced counterweight mass, the crane is easier to move,

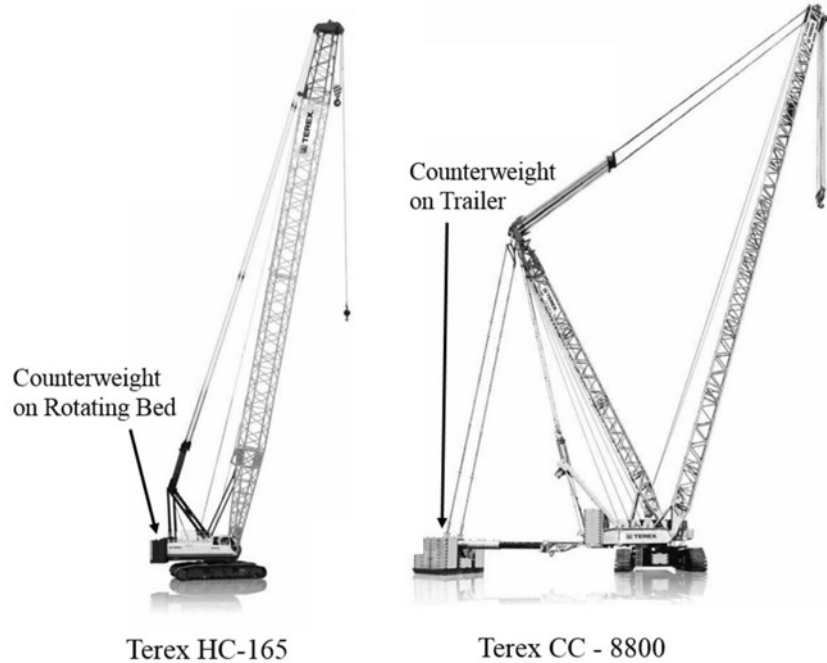
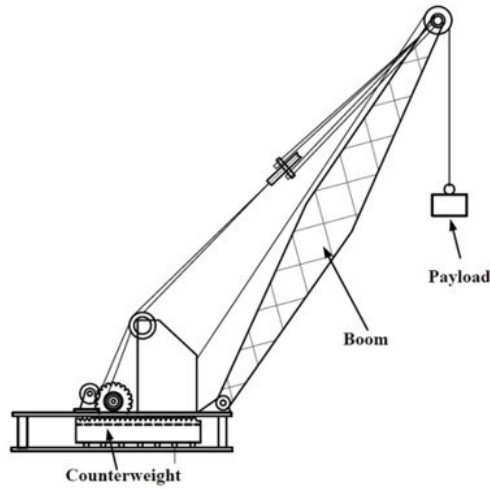


Figure 8: Counterweights on Rotating Bed and on Trailer, Modified from [34].

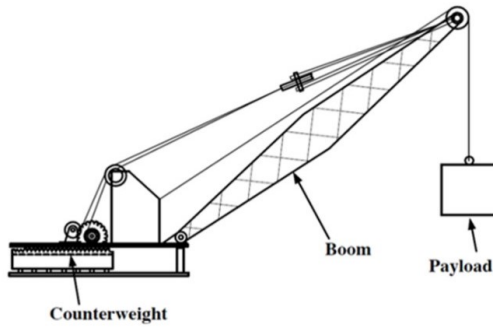
both from one job site to another and around any given job site.

Movable counterweights for heavy machinery have been well documented for about 100 years. For example, Figure 9 shows a boom crane patented in 1922. In Figure 9(a) the counterweight is in a retracted position near the center of the crane. While in Figure 9(b) the counterweight is extended rearward to provide more resistance to forward tipping. This resistance is needed when the boom is lowered or when a larger payload is connected to the hook. The counterweight should not be kept in the rearward position all the time though, because it would cause the crane to tip-over backwards in certain configurations including the case where the payload suddenly falls off. This means that the position should be chosen in a way that prevents both forward and backward tip-overs.

Previous research showed that the design and control of a crane with movable counterweights is more complex than cranes with fixed counterweights [16]. The



(a) Counterweight Retracted



(b) Counterweight Extended

Figure 9: Crane with movable counterweight patented by Wigglesworth [37].

counterweight should be moved in coordination with both the configuration of the crane and the weight of the attached load. In order to achieve this counterbalancing effect, the crane must be equipped with sensors that measure the boom angle, the counterweight position, and the payload weight. This sensor information is then used by a control system that automatically adjusts the counterweight position.

This chapter investigates the tip-over stability of a crawler crane with a movable counterweight. In order to determine the appropriate position of the counterweight, the sum of moments method is used.

The maximum and minimum safe positions of the counterweight are calculated for a wide range of conditions including:

1. Various boom-mast configurations.
2. Various payload masses and counterweight masses.
3. Various slew angles and boom angles.

The analysis demonstrates that the stability properties are complex functions of the crane and payload parameters.

2.2 Tip-over Stability Based on Sum of Moments about Possible Tip-over Axes

Crawler crane structures are complex and subject to multiple forces arising from inertia, gravity, wind, payload swing, ground undulations, etc. In this chapter, static tip-over stability is investigated; therefore the moment created by each gravitational force about a corresponding tip-over axis is calculated. The sum of these moments about each possible tip-over axis should be less than or equal to zero for the crane to be stable.

Figure 10 shows the general geometry of the possible tip-over axes of a crawler crane. The possible tip-over axes run along the toes and heels, as well as the outside edges of the crawler tracks. Vectors \vec{a}_1 and \vec{a}_3 represent the forward and backward tip-over axes respectively, while \vec{a}_2 and \vec{a}_4 represent the sideways tip-over axes.

Figure 11 illustrates a representative model of a crawler crane with a movable counterweight. The model is composed of a mobile base, m_1 , a rotational boom, m_2 , a mast, m_3 , a movable counterweight, m_4 , and a suspension cable with a payload mass, m_5 . The base is modeled as a thin plate and has a center of gravity at the geometric center of the base. As illustrated in Figure 11(b), the boom arm and mast can rotate through a slew angle β about a vertical axis located at the geometric

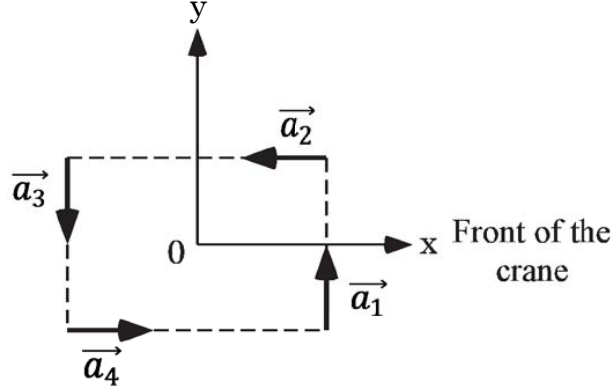


Figure 10: Top View of the Horizontal Plane Formed by the Possible Tip-over Axes.

center of the crawler. The boom has a length of L_2 . Its center of mass is located in the middle of the boom arm. The boom is elevated at an angle ϕ_1 relative to the horizontal plane. This angle is known as the luffing, or boom, angle. The mast forms an angle ϕ_2 with the horizontal plane and its length is L_3 . The position of the counterweight is measured by a distance, L_4 , from the slew axis. To calculate the moment generated by each of the gravitational forces about a certain axis we use:

$$\vec{M}_{ij} = \vec{a}_j \cdot (\vec{r}_i \times \vec{f}_i) \quad (2.1)$$

where:

$i = 1, \dots, 5$ and $j = 1, \dots, 4$.

\vec{M}_{ij} is the moment generated by the force \vec{f}_i about the axis \vec{a}_j [Nm].

\vec{f}_i is the gravitational force acting on body i at its gravitational center [N].

\vec{a}_j is a unit vector along the j^{th} tip-over axis.

\vec{r}_i is a position vector pointing from any point on the tip-over axis to any point on the line of action of the force [m].

The individual moments found using (2.1) are combined to get the total moment

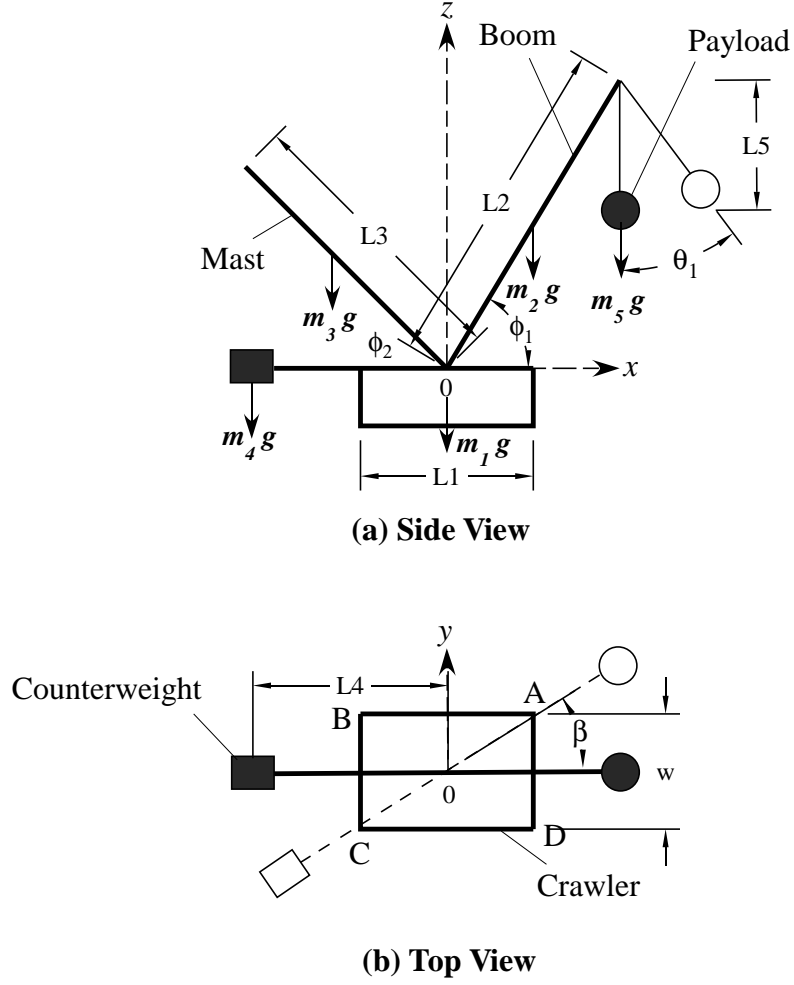


Figure 11: Schematic Diagram for a Crawler Crane with movable Counterweight (Mast included).

about each tip-over axis:

$$\vec{M}_j = \sum_{i=1}^5 \vec{M}_{ij} = \sum_{i=1}^5 \vec{a}_j \cdot (\vec{r}_i \times \vec{f}_i) \quad (2.2)$$

Therefore, the moment creating a forward tip-over is:

$$\begin{aligned} \vec{M}_f = & m_2 g \left(\frac{L_2}{2} \cos \beta \cos \phi_1 - \frac{L_1}{2} \right) + m_5 g \left(L_2 \cos \beta \cos \phi_1 - \frac{L_1}{2} \right) \\ & - m_3 g \left(\frac{L_3}{2} \cos \beta \cos \phi_2 + \frac{L_1}{2} \right) - m_1 g \frac{L_1}{2} - m_4 g \left(L_4 \cos \beta + \frac{L_1}{2} \right) \quad (2.3) \end{aligned}$$

If the counterweight is too heavy or placed too far backwards, or even if the

payload suddenly falls off, then the crane might tip over backwards. The moment creating the backward tip-over is:

$$\begin{aligned} \vec{M}_b = & -m_2g\left(\frac{L_2}{2} \cos \beta \cos \phi_1 + \frac{L_1}{2}\right) - m_5g\left(L_2 \cos \beta \cos \phi_1 + \frac{L_1}{2}\right) \\ & + m_3g\left(\frac{L_3}{2} \cos \beta \cos \phi_2 - \frac{L_1}{2}\right) - m_1g\frac{L_1}{2} + m_4g\left(L_4 \cos \beta - \frac{L_1}{2}\right) \quad (2.4) \end{aligned}$$

It should be noted that tip-overs could occur about any of the four axes shown in Figure 81, depending on the value of the slew angle β , keeping in mind that a forward tip-over is one that occurs in the direction in which the boom is pointing, while a backward tip-over is one that occurs in the direction in which the counterweight is pointing.

To avoid tipping, the load moment acting to overturn the crane should be less than or equal to the maximum moment of the crane available to resist overturning. In other words, the moments calculated using (2.3) and (2.4) should be less than or equal to zero.

Using these conditions, the range of counterweight positions that stabilize the crane can be calculated.

2.3 Case Study - Terex CC 2800-1

One of the well-known crawler cranes with movable counterweights that is currently in use is the TEREX CC 2800-1 shown in Figure 12. Based on the datasheet found in [34], its geometrical and mass parameters are listed in Table 2.

It should be noted that the counterweight used in this crane is divided into two parts, the first has a fixed mass and is located at a fixed distance from the center of the crawler. The second is the movable counterweight, whose mass can be varied, as well as moved away or towards the center of the crane.

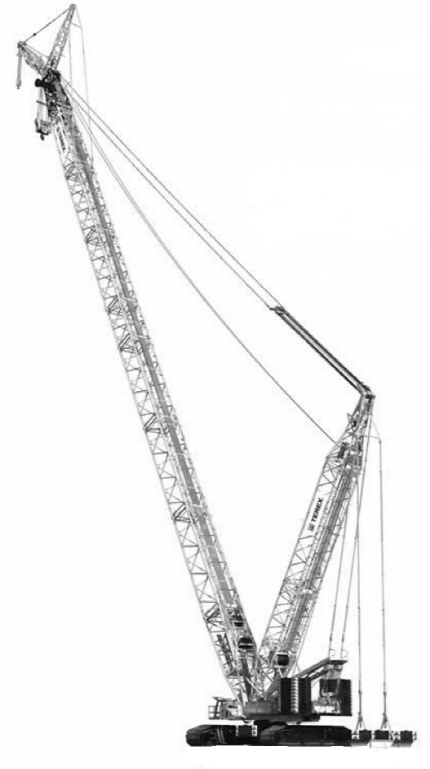


Figure 12: Terex CC 2800-1 Crawler Crane [34].

2.3.1 Effect of Parameters in the Boom-Mast Configuration

When a crawler crane is slewed about the vertical axis, its stability properties change because the moment arm of each mass element changes, as does the tip-over axis. In order to isolate the effect of the slew angle, the length of the boom and the mass of the payload were fixed. The parameters were chosen using the crane's load chart, which is shown in Figure 13.

To explain how a load chart is used, first the required configuration should be determined. For example, in this case study, the boom mast configuration is used. This configuration is denoted by HSSL_S7 for the Terex CC 2800-1. Thus the load chart corresponding to this configuration is the one shown in Figure 13. The second step is determining the boom length which is shown in the first row of the chart (84

Table 2: Parameters of the Terex CC 2800-1 [34].

Parameter	Item	Numerical Data
w	Width of base	8.4 <i>m</i>
h	Height of base	2.45 <i>m</i>
L_1	Length of base	10.33 <i>m</i>
L_2	Length of boom	102 <i>m</i>
L_3	Length of mast	30 <i>m</i>
L_{4F}	Length of fixed counterweight	7 <i>m</i>
L_5	Length of hoist	10 <i>m</i>
m_1	Mass of base	125 <i>t</i>
m_2	Mass of boom	60 <i>t</i>
m_3	Mass of mast	13 <i>t</i>
m_{4F}	Mass of fixed counterweight	240 <i>t</i>
m_5	Mass of payload	110 <i>t</i>

to 108 *m* here). The length used in this case study is 102 *m*, therefore the 4th column is the one needed.

The second row displays the configuration, the third shows the range of allowed movable counterweights, and the fourth shows the range of allowed movable counterweight positions. Each of the remaining entries represents the rated payload mass corresponding to various horizontal distances between the slewing axis and the hook connected to the payload.

The horizontal distances listed in the first column of the chart are directly related to the boom luffing angle for a fixed boom length. For instance, a boom luffing angle of 62° requires the horizontal distance between the slewing axis and the hook connected to the load to be 48 *m*, thus the value of 50 *m* is chosen which has a rated payload mass of 107.3 *t*. And this is why the payload mass was set to 110 *t*. It should be mentioned however, that the maximum load given in a crane’s load chart is 75% of its theoretical maximum load for the given configuration [2].

Finally, the load chart also contains other information in its header, such as the

SSL / HSSL_S7

CC 2800-1

		180 t + 60 t ZB				8,40 m		9.8 m/s		360°		EN13000 / ISO	
		84 m		90 m		96 m		102 m		108 m			
		SSL		HSSL_S7		HSSL_S7		HSSL_S7		HSSL_S7		HSSL_S7	
		0 t		0 t-300 t		0 t-300 t		0 t-300 t		0 t-300 t		0 t-300 t	
		11-15m		17m		11-15m		11-15m		11-15m		11-15m	
m	t	t	t	t	t	t	t	t	t	t	t	t	t
12	253,0	281,0	281,0	307,0	289,0	254,0	-	-	-	-	-	-	-
13	224,0	281,0	281,0	307,0	288,5	253,5	218,0	191,0	191,0	191,0	191,0	191,0	191,0
14	195,0	281,0	281,0	307,0	288,0	253,0	218,0	191,0	191,0	191,0	191,0	191,0	191,0
16	157,0	281,0	281,0	307,0	287,0	250,0	215,0	189,0	189,0	189,0	189,0	189,0	189,0
18	130,0	281,0	281,0	307,0	286,0	248,0	212,0	187,0	187,0	187,0	187,0	187,0	187,0
20	110,0	278,0	278,0	307,0	285,0	246,0	210,0	184,0	184,0	184,0	184,0	184,0	184,0
22	94,5	271,0	271,0	305,0	274,0	242,0	208,0	182,0	182,0	182,0	182,0	182,0	182,0
24	82,0	265,0	265,0	284,0	264,0	236,0	203,0	179,0	179,0	179,0	179,0	179,0	179,0
26	72,0	259,0	259,0	260,0	254,0	231,0	198,0	174,0	174,0	174,0	174,0	174,0	174,0
28	63,5	240,0	241,0	238,0	237,0	226,0	193,0	170,0	170,0	170,0	170,0	170,0	170,0
30	56,0	219,0	223,0	218,0	217,0	213,0	188,0	165,0	165,0	165,0	165,0	165,0	165,0
34	44,8	186,0	192,0	186,6	186,3	183,6	173,3	155,6	155,6	155,6	155,6	155,6	155,6
38	35,6	160,0	168,0	160,3	160,3	158,3	156,0	144,6	144,6	144,6	144,6	144,6	144,6
42	28,4	140,0	148,0	139,0	139,0	137,0	136,0	132,0	132,0	132,0	132,0	132,0	132,0
46	22,7	124,0	132,0	123,6	123,6	121,6	120,6	118,0	118,0	118,0	118,0	118,0	118,0
50	18,0	111,0	119,0	110,3	110,1	108,1	107,3	105,5	105,5	105,5	105,5	105,5	105,5
54	14,1	100,0	106,0	99,0	98,5	96,5	96,0	94,5	94,5	94,5	94,5	94,5	94,5
58	10,9	91,0	95,5	90,0	89,5	87,3	86,8	85,0	85,0	85,0	85,0	85,0	85,0
62	8,2	83,0	85,5	81,9	81,0	79,3	78,8	76,8	76,8	76,8	76,8	76,8	76,8
66	5,9	76,0	76,5	74,0	74,0	72,0	71,5	69,5	69,5	69,5	69,5	69,5	69,5
70	-	68,0	68,0	65,6	67,0	65,6	65,5	63,5	63,5	63,5	63,5	63,5	63,5
74	-	60,0	60,0	57,5	60,0	59,3	59,6	58,0	58,0	58,0	58,0	58,0	58,0
75	-	-	-	56,0	58,2	57,7	58,2	56,5	56,5	56,5	56,5	56,5	56,5
78	-	-	-	-	53,0	53,0	54,0	52,0	52,0	52,0	52,0	52,0	52,0
80	-	-	-	-	50,0	49,5	51,2	49,5	49,5	49,5	49,5	49,5	49,5
82	-	-	-	-	-	46,6	48,4	47,0	47,0	47,0	47,0	47,0	47,0
85	-	-	-	-	-	43,0	44,2	43,3	43,3	43,3	43,3	43,3	43,3
86	-	-	-	-	-	-	42,9	42,1	42,1	42,1	42,1	42,1	42,1
90	-	-	-	-	-	-	38,2	37,3	37,3	37,3	37,3	37,3	37,3
91	-	-	-	-	-	-	37,5	36,1	36,1	36,1	36,1	36,1	36,1
94	-	-	-	-	-	-	-	33,0	33,0	33,0	33,0	33,0	33,0
96	-	-	-	-	-	-	-	31,6	31,6	31,6	31,6	31,6	31,6

For HSSL_S7 a boom power-kit is required · Für HSSL_S7 ist ein Ausleger-Verstärkungs-Kit erforderlich ·
 Un kit à fortifier de flèche principale est nécessaire pour HSSL_S7

Figure 13: Sample Load Chart for the Terex CC 2800-1 Crawler Crane [34].

mass of the fixed counterweight, the width of the crane base, the allowed wind speed, etc.

After choosing and setting the crane's parameters, the slewing angle β and the counterweight position were changed, while calculating the stability properties. Figure 14 shows the result for the minimum¹ position of the movable counterweight to

¹The minimum counterweight position is the position closest to the vertical axis of rotation

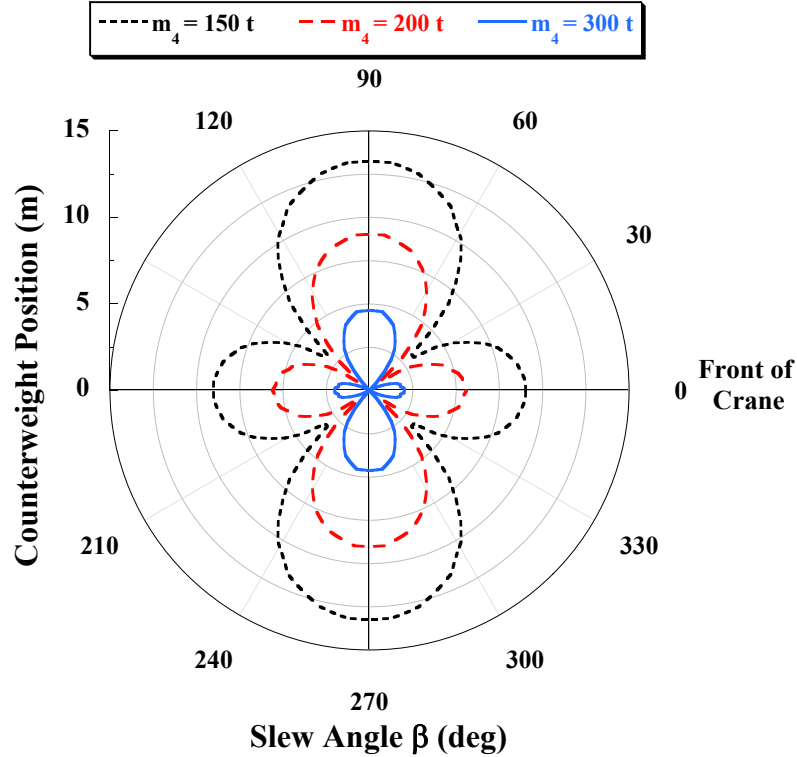


Figure 14: Minimum Counterweight Position to Prevent Forward Tip-over for a Boom Luffing Angle of 62° and a Payload Mass of 110 t , (m_4 is the Movable Counterweight Mass).

guarantee static stability and prevent forward tip-over, when the mass of the moving counterweight is 150 t , 200 t and 300 t . Note that $\beta = 0$ corresponds to the case when the boom is pointing directly forward. The figure clearly shows that as the mass of the counterweight increases, the distance needed to counterbalance the mass of the payload decreases. However, the most interesting effect is the flower shape that indicates the crane is most stable when the boom is pointing at a corner of the mobile base.

If the payload suddenly falls off, then the crane can tip over backwards. Figure 15 shows the maximum possible location of the movable counterweight that will prevent

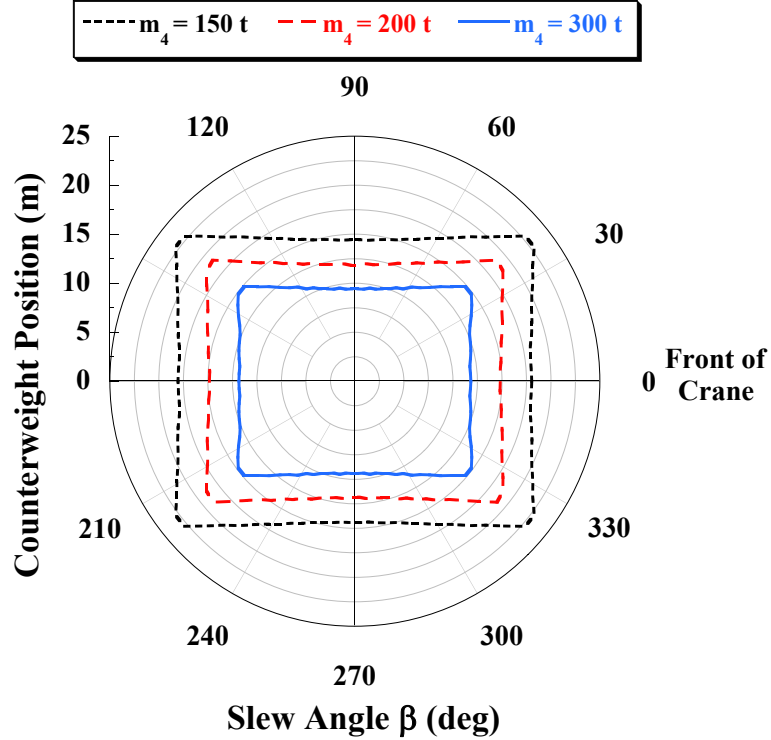


Figure 15: Maximum Counterweight Position to Prevent Backward Tip-over for a Boom Luffing Angle of 62° , (m_4 is the Movable Counterweight Mass).

backward tip-over if the payload suddenly drops to zero. The heavier the counterweight, the greater the risk of tipping over backwards and the smaller the allowable rearward position of the counterweight.

If the two previous graphs are combined for a counterweight mass of 200 t, then the result is the graph shown in Figure 16. This graph shows that the smallest possible counterweight safe positioning region is represented by the length A, while the largest possible counterweight region is represented by the region B. This means that the crane is least stable when the boom is rotated 90° , in the sense that the counterweight has to be more accurately positioned within the small safety zone.

The luffing angle of the boom is one of the most important stability parameters.

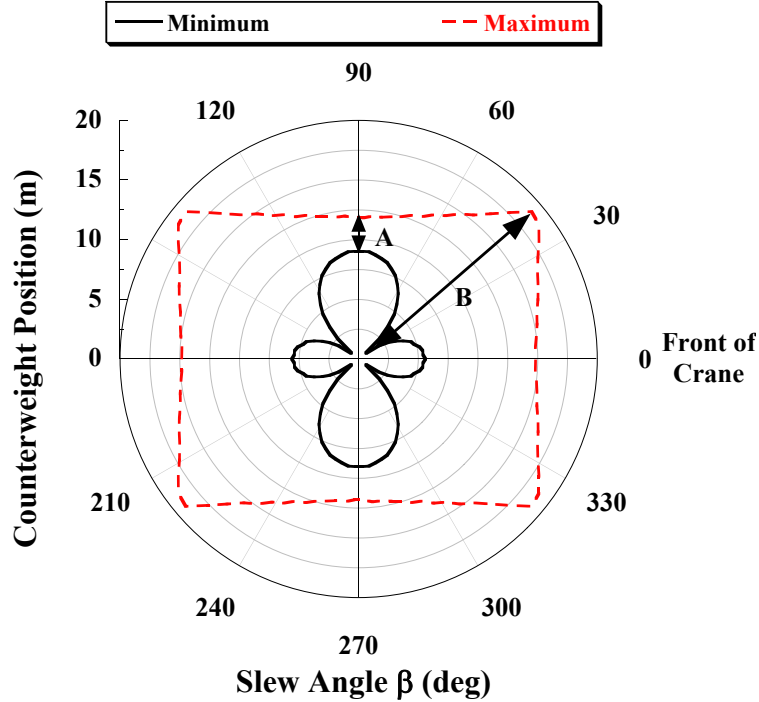


Figure 16: Backward and Forward Tip-over Limits for a Boom Luffing Angle of 62° , a Payload Mass of $110 t$, and a Movable Counterweight Mass of $200 t$.

In fact, it is the primary variable in the load charts that companies provide to characterize their machine's stability. The luffing angle ϕ_1 was changed to see its effect on the stable ranges of counterweight positions. The result is shown in Figure 17, which shows that, for forward tip-over, as the luffing angle increases, the rearward position of the counterweight needed to counterbalance the mass of the payload decreases. Also, it is noted that the stability of the crane is very sensitive to a change in the value of the luffing angle, that is, a change of 15° in the luffing angle requires almost a 10 m change in the counterweight position. Another interpretation of the data is that the crane stability increases along with the boom angle. This is a well-known property that is confirmed by our calculations.

In cases where the payload falls off, or suddenly drops to zero (like when it is set on the ground or the lift cable breaks) the luffing angle value has an important effect

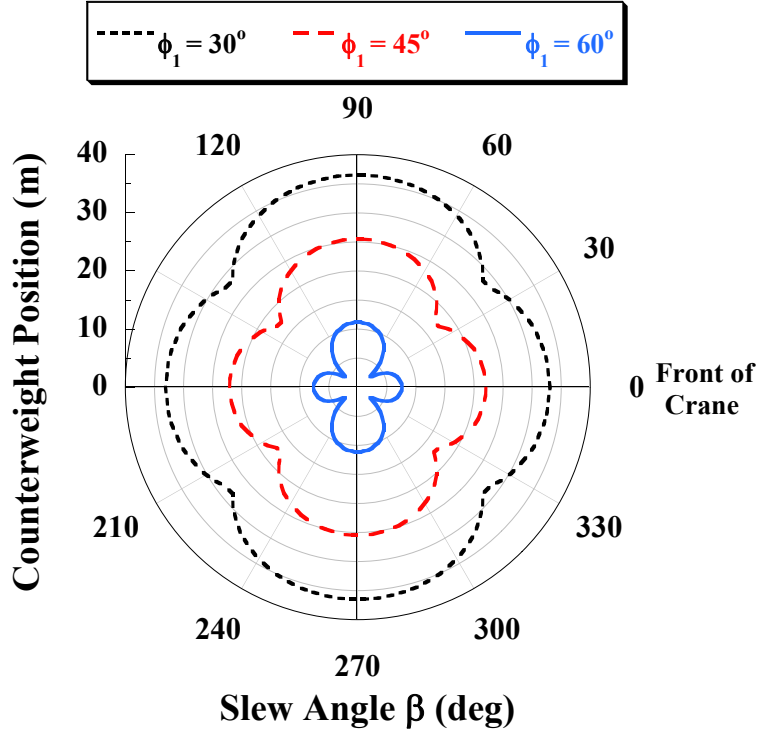


Figure 17: The Effect of Changing the Luffing Angle ϕ_1 on the Minimum Counterweight Position to Prevent Forward Tip-over for a Payload mass of 110 t and a Counterweight Mass of 200 t.

as well regarding backward tip-over. Figure 18 shows the maximum possible location for the counterweight corresponding to different luffing angle values. The higher the value of the luffing angle, the larger the risk of tipping over backwards.

The effect of the payload mass was also investigated. One counterweight mass was used: 200 t, the luffing angle ϕ_1 value was set to 62° again and the payload mass was varied. Figure 19 shows that the larger the payload is, the further the counterweight has to be moved backwards. For the special case of the Terex CC 2800-1 considered here, the maximum allowable payload mass is 110 t, according to the load chart. When the payload was changed to 210 t the counterweight had to be moved about 25 m rearward. This is physically impossible for this crane, which means that a payload that heavy, lift at that boom angle, would almost certainly cause a tip-over accident.

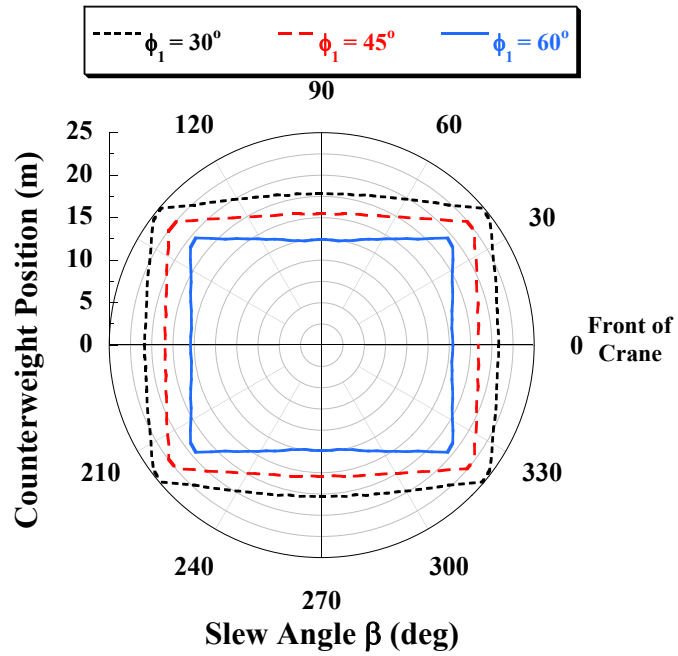


Figure 18: The Effect of Changing the Luffing Angle ϕ_1 on the Maximum Counterweight Position to Prevent Backward Tip-over for a Counterweight Mass of 200 t.

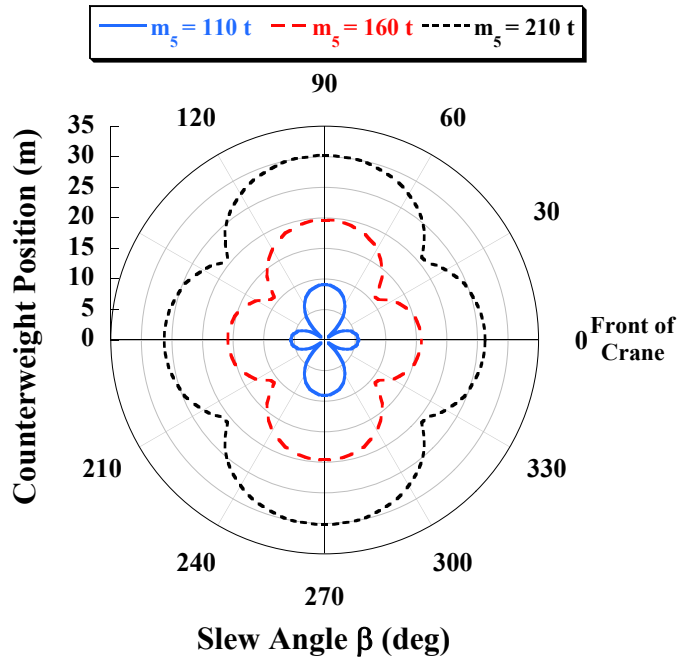


Figure 19: The Effect of Changing the Payload Mass on the Minimum Counterweight Position to Prevent Forward Tip-over for a Boom Luffing Angle of 62° and a Counterweight Mass of 200 t, (m_5 is the Payload Mass).

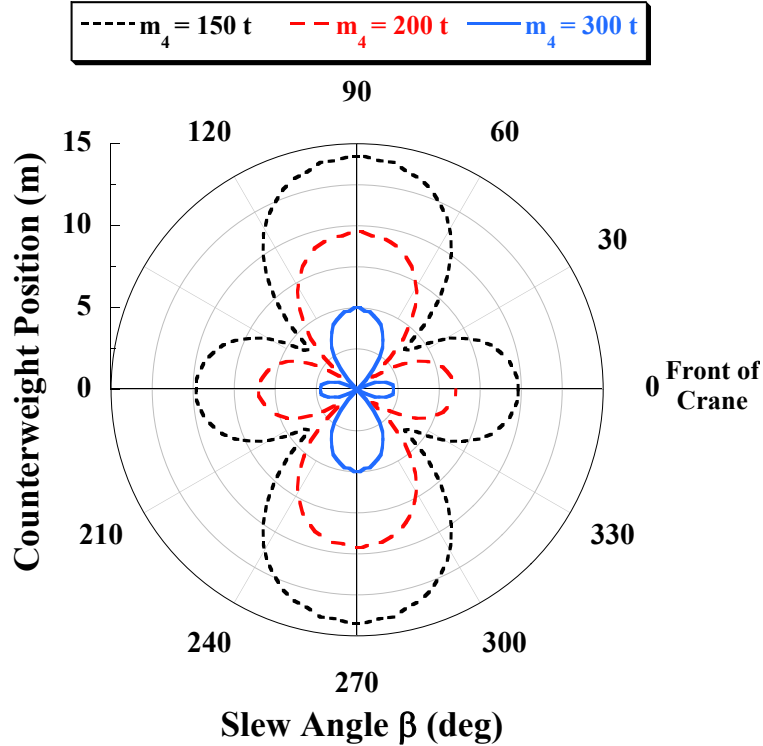


Figure 20: Minimum Counterweight Position to Prevent Forward Tip-over (No Mast Configuration) for a Boom Luffing Angle of 62° and a Payload Mass of 110 t , (m_4 is the Movable Counterweight Mass).

2.3.2 Effect of Parameters in the No-Mast Configuration

Some crawler cranes do not have the significant lattice mast that is shown in Figures 11 and 12. Therefore, the mast was removed from the model and the effect of the slew angle was recalculated. First, the forward tip-over stability was examined and the result is shown in Figure 20. Compared with Figure 14, the counterweight has to be moved a little further backwards. This is expected because the mast functions as a counterweight to counterbalance the payload carried by the crane.

Next, backward tip-over stability was examined in the case of no mast. Figure 21 shows that it is similar to when the mast was attached. This is due to the fact that the mass of the mast is small compared to mass of both the fixed and movable

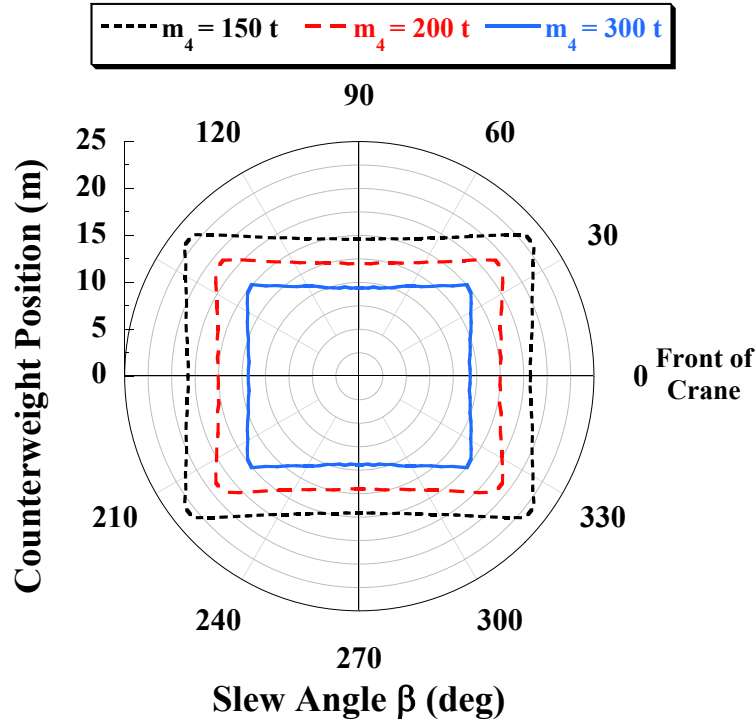


Figure 21: Maximum Counterweight Position to Prevent Backward Tip-over (No Mast Configuration) for a Boom Luffing Angle of 62° , (m_4 is the Movable Counterweight Mass)..

counterweights, so it does not make a significant difference. However, if the mast had a larger mass, then removing it will decrease the risk of backward tip-over.

2.3.3 Effect of Parameters when a Jib is Added to the Configuration

A jib is a boom extension that increases its accessibility both vertically and horizontally. When a jib is used, the crane can reach areas that are higher and further away from its center. However, it increases the complexity of the machine and poses a higher tip-over risk. In the case of a movable counterweight, a jib introduces another level of complexity in determining where the counterweight should be positioned.

For these reasons, the previous case study was repeated for the same Terex crane (CC 2800-1), but this time a jib was added. Figure 22 shows a schematic diagram

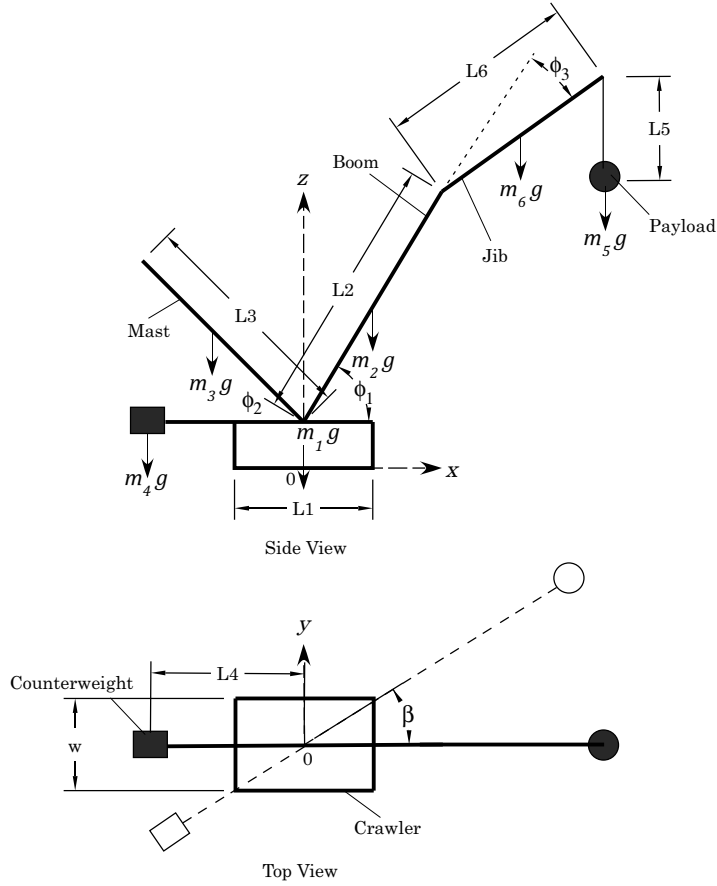


Figure 22: Schematic Diagram for a Crawler Crane with Movable Counterweight (Mast and Jib included).

of this configuration in both the side and top views. Some crane parameters had to be changed to suit this configuration, while using the same payload and the same counterweight masses. These parameters are listed in Table 3.

To study the effect of the slew angle, the lengths of the boom and jib, and the mass of payload were fixed. The mass of the payload was set to 110 t. The minimum boom luffing angle taken from the load chart is 65° , and the angle between the jib and the boom was set to 15° . The slewing angle β and the counterweight position were changed.

Table 3: Geometrical Parameters of the Terex CC 2800-1 (Jib Configuration) [34].

Parameter	Item	Numerical Data
w	Width of base	8.4 <i>m</i>
h	Height of base	2.45 <i>m</i>
L_1	Length of base	10.33 <i>m</i>
L_2	Length of boom	96 <i>m</i>
L_3	Length of mast	30 <i>m</i>
L_{4F}	Length of fixed counterweight	7 <i>m</i>
L_5	Length of hoist	50 <i>m</i>
L_6	Length of jib	96 <i>m</i>
m_1	Mass of base	125 <i>t</i>
m_2	Mass of boom	56 <i>t</i>
m_3	Mass of mast	13 <i>t</i>
m_{4F}	Mass of fixed counterweight	240 <i>t</i>
m_5	Mass of payload	110 <i>t</i>
m_6	Mass of jib	40 <i>t</i>
ϕ_3	Angle between jib and boom	15°

Figure 23 shows the minimum counterweight positions that guarantee static stability and prevent forward tip-over, when the mass of the counterweight is 150 t, 200 t, and 300 t. The figure follows the same trend as the case with no jib; however the values are notably higher. This is due to the fact that the jib creates an additional weight creating a forward tip-over moment that requires the counterweight to be moved further backwards to counterbalance its effect. It can also be inferred from Figure 23 that the mass of the counterweight has to be above 200 t for it to be moved within the allowable distance of this specific crane model. If a mass less than that is used, then the payload of 110 t will cause a forward tip-over.

The value of the payload mass was decreased to 65 t and Figure 24 was generated. In this figure we notice that the minimum counterweight position is close to that of the no jib case when it is lifting 110 t. This means that the jib considered here decreases the allowable payload mass by almost 50%, if all other conditions are to be

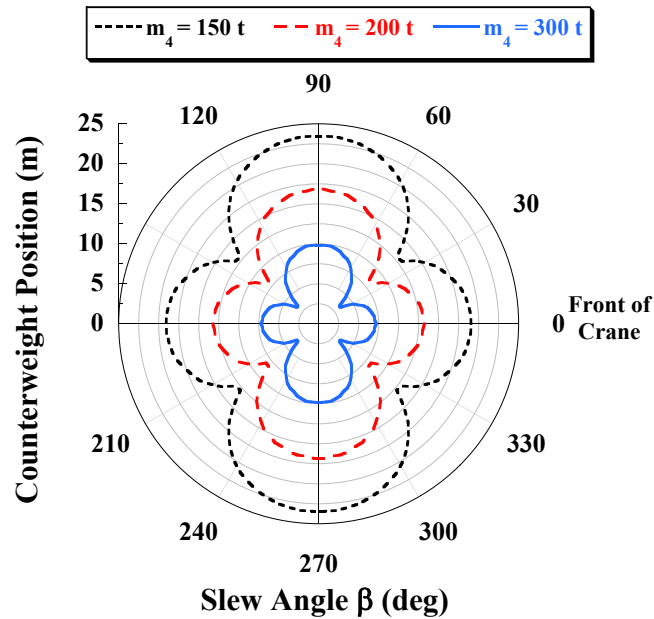


Figure 23: Minimum Counterweight Position to Prevent Forward Tip-over (Jib included) for a Boom Luffing Angle of 62° and a Payload Mass of 110 t , (m_4 is the Movable Counterweight Mass).

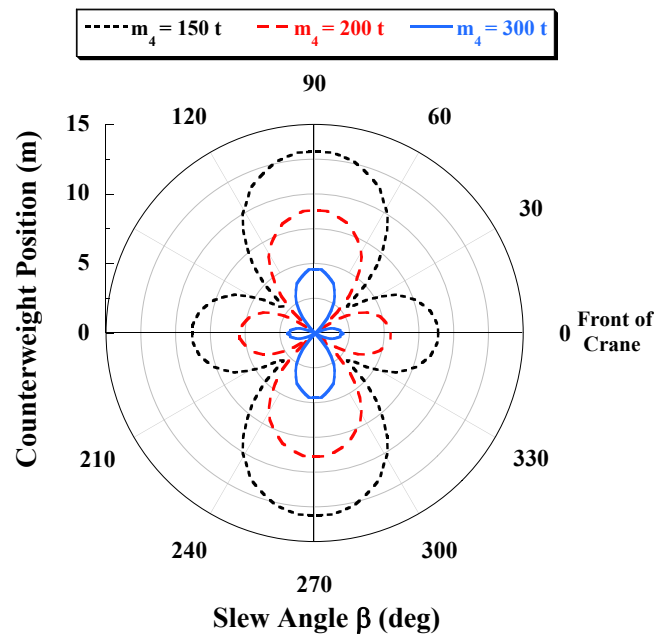


Figure 24: Minimum Counterweight Position to Prevent Forward Tip-over (Jib included) for a Boom Luffing Angle of 62° and a Payload Mass of 65 t , (m_4 is the Movable Counterweight Mass).

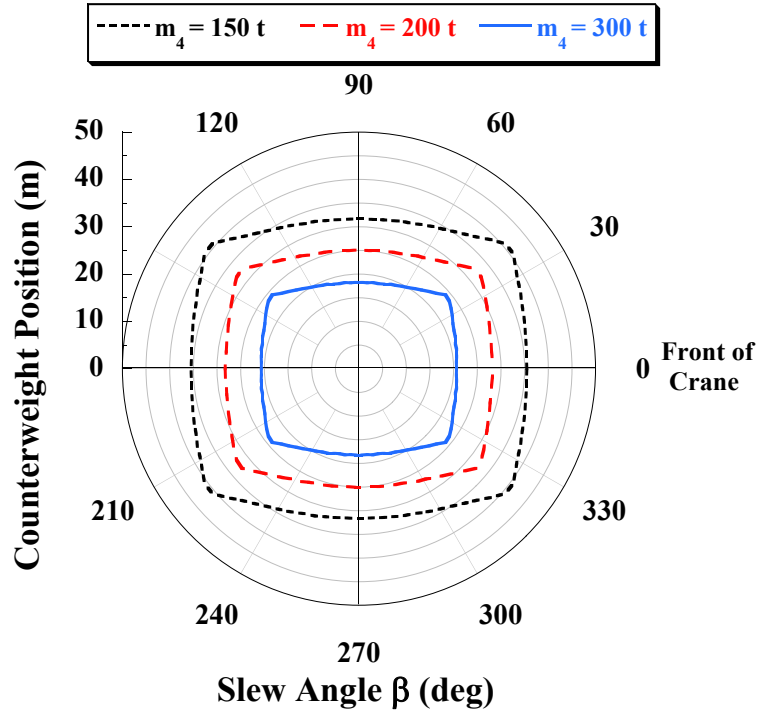


Figure 25: Maximum Counterweight Position to Prevent Backward Tip-over (Jib included) for a Boom Luffing Angle of 62° , (m_4 is the Movable Counterweight Mass).

kept fixed.

If the payload suddenly falls off, then the crane can tip-over backwards. However, having the jib fixed to the front side of the crane would make that more difficult. This is demonstrated in Figure 25. This figure implies that the counterweight of 200 t has to be placed at a distance of approximately 17 m for it to cause backward tip-over. This is rarely the case, thus the jib can be considered as a protection measure against rearward tipping. Again in this case, the greater the counterweight, the greater the risk of tipping over backwards and the smaller the allowable rearward position of the counterweight.

Figure 26 shows the effect of the luffing angle value on the crane's tip-over stability when a jib is used, and while the value of the counterweight mass is 200 t. The forward tip-over characteristics are the same as the no-jib case, which means that as

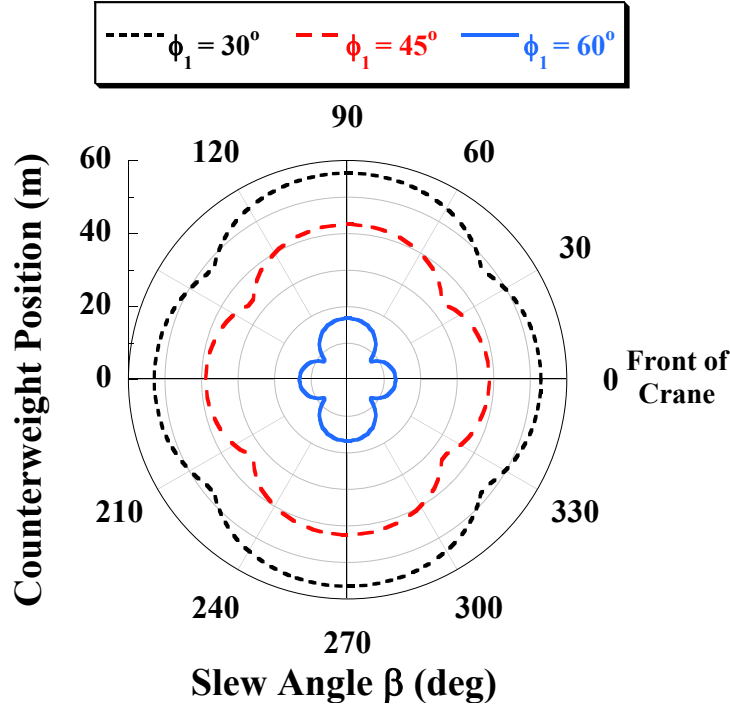


Figure 26: The Effect of Changing the Luffing Angle ϕ_1 on the Minimum Counterweight Position to Prevent Forward Tip-over (Jib included) for a Payload Mass of 110 t and a Movable Counterweight Mass of 200 t.

the luffing angle decreases, the counterweight should be moved further backwards to prevent tipping over. The problem is that stability is affected significantly by changes in the luffing angle value. A change of 20° requires the counterweight to be moved an extra 20 m backwards, which is physically impossible. Thus, the operator should be very precise when changing the luffing angle value as it is the most critical parameter when it comes to the crane's stability, especially when a jib is used.

Finally, the effect of the payload mass was investigated. The luffing angle value was set to 65° , and the value of the counterweight mass was set to 200 t. Figure 27 shows the result for the same payload masses used with the no-jib configuration. The flower shape appears again; however, the minimum counterweight's position to prevent tip-over is much larger in this case. Also, increasing the payload mass above

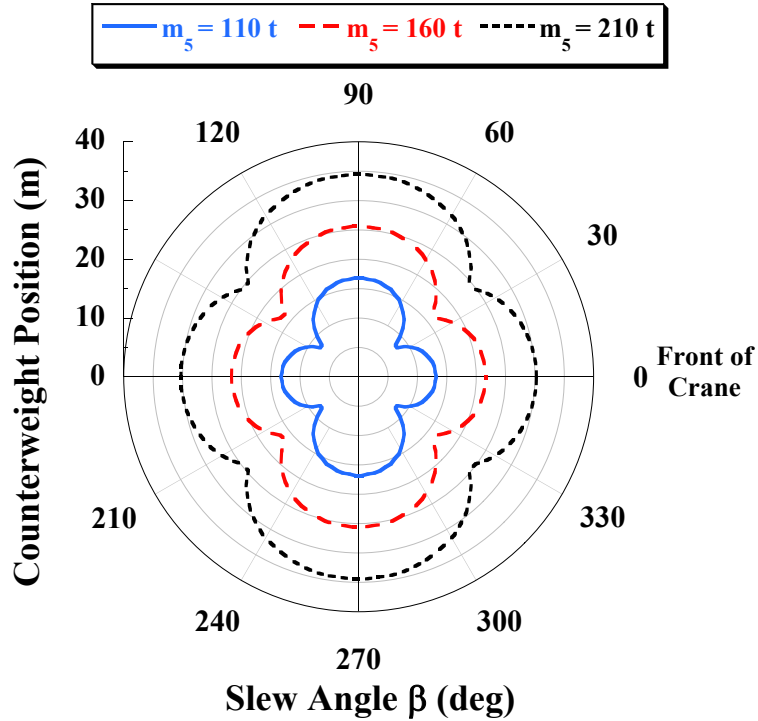


Figure 27: The Effect of Increasing the Payload Mass on the Minimum Counterweight Position (Jib included) for a Boom Luffing Angle of 62° and a Movable Counterweight Mass of 200 t , (m_5 is the Payload Mass).

110 t will cause a forward tip-over for this model.

Figure 28, on the other hand, shows that, in order to keep the minimum counterweight's position within the same range as the no-jib configuration, the payload mass must be reduced by almost 50%.

In conclusion, using a jib can be beneficial in terms of increasing the access area of the crane, and preventing, to a certain degree, backward tip-overs; however it compromises the stability of the crane in the forward direction.

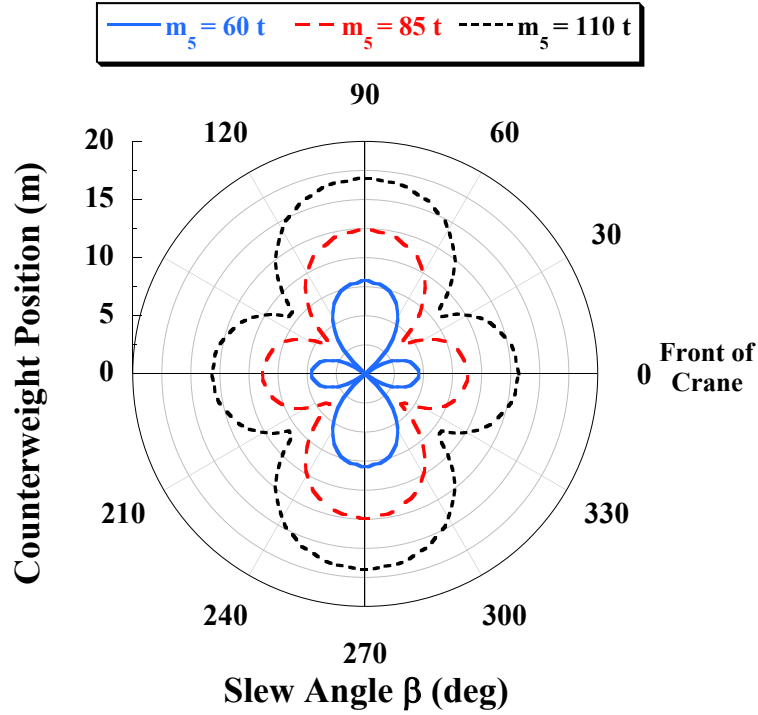


Figure 28: The Effect of Decreasing the Payload Mass on the Minimum Counterweight Position (Jib included) for a Boom Luffing Angle of 62° and a Movable Counterweight Mass of 200 t , (m_5 is the Payload Mass).

2.4 Summary

Mobile cranes are very important and useful machines that can be improved by adopting the principle of movable counterweights. However, their tip-over stability properties are extremely critical, and they become more complex functions of the machine configuration and payload mass. Therefore, care must be taken to fully understand their tip-over stability and develop a control system that can properly position the counterweight at a suitable location. In this chapter, the suitable position of the counterweight was calculated for various crane parameters. Table 4 summarizes the stability trends demonstrated in this chapter.

Table 4: Summary of Stability Trends.

Parameter	Parameter Change	Forward Stability	Backward Stability	Sideways Stability	Counter-weight Position
Counter-weight Mass	increase	increase	decrease	increase	decrease
Luffing Boom Angle	increase	increase	decrease	increase	decrease
Payload Mass	increase	decrease	increase	increase	increase
Mast Mass	increase	decrease	increase	decrease	decrease
Jib Mass	increase	decrease	increase	decrease	increase

CHAPTER III

PSEUDO-DYNAMIC TIP-OVER STABILITY OF CRAWLER CRANES WITH MOVABLE COUNTERWEIGHTS

3.1 Description of the Approach

Crawler cranes are often moved around the job site. Therefore, it is essential to study how different motions of the crane affect the tip-over stability in the presence of a movable counterweight. To achieve this understanding, the static analysis has to be extended to include dynamic effects. One of the main dynamic effects that needs to be considered is payload swing.

Figure 29 shows that the payload swings in two different directions; radial swinging expressed by θ_1 , and tangential swinging expressed by θ_2 . Because one of the goals of this research is to develop a simple tool with minimal computational cost to predict the tip-over stability of crawler cranes, the two swing angles are assumed to be constant in a Pseudo-Dynamic Stability Analysis. This means that when the suspension cable is deflected by the swinging payload, it remains fixed in the maximum deflected position.

More assumptions are made to further simplify calculations; the time-dependent centripetal and gravitational forces derived from the pendulum swing are considered time-invariant constant forces, in addition to the inertia forces acting on the crane at its center of mass, which are considered constant as well. Also, payload damping was ignored (frictionless pivot and no air drag). Thus it is obvious that this pseudo-dynamic estimation method does not study the full dynamics of the payload swing. However, it does provide a reasonable upper bound on the dynamic effects induced

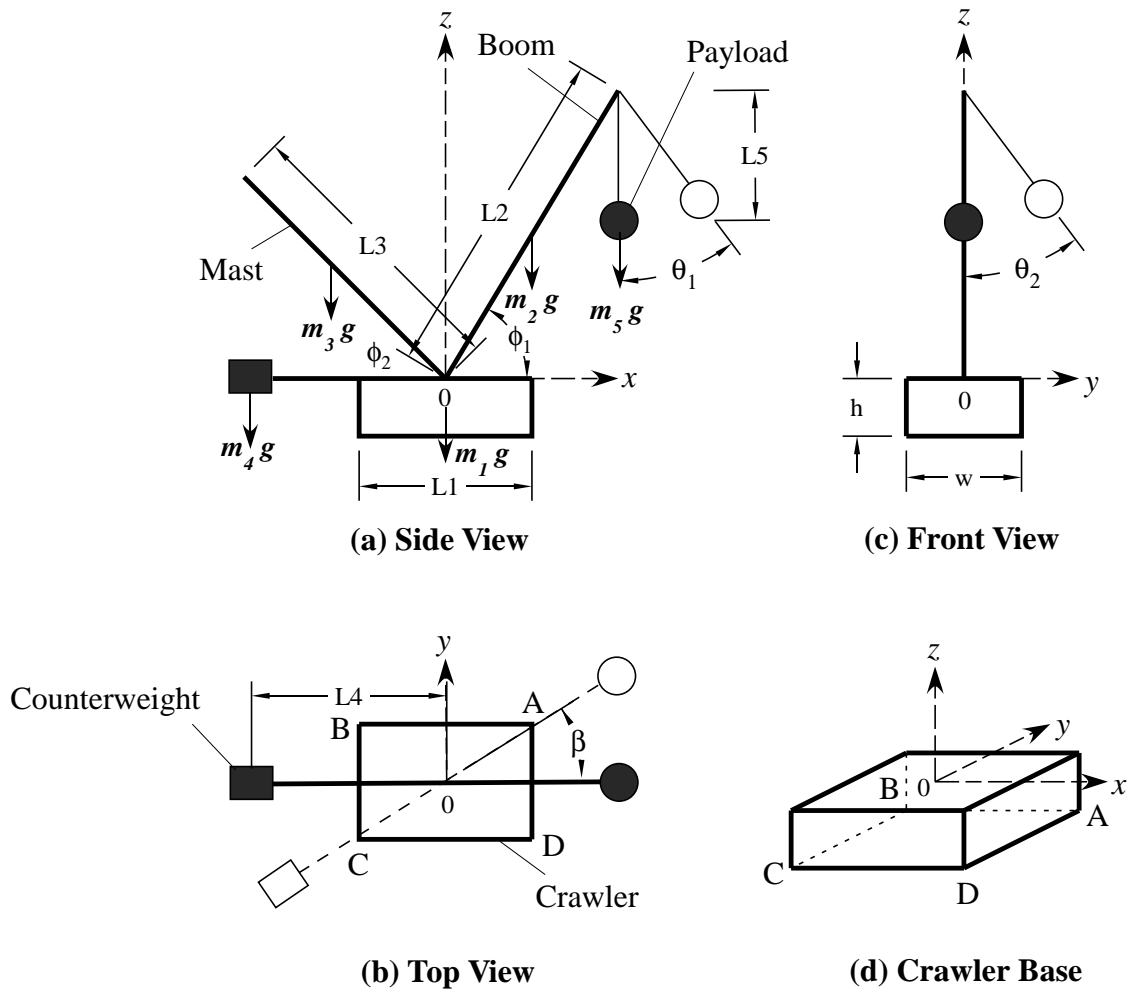


Figure 29: Schematic Diagram of a Crawler Crane with a Movable Counterweight Showing Payload Swing.

by crane motion.

A comparison between a full dynamic analysis method and the suggested pseudo-dynamic estimation method was performed twice before in [30] and [5]. The torque caused by the weight and swing of the payload about the boom angle was calculated for both radial and tangential swinging directions using both approaches. It turned out that the error between the two torque values was insignificant for a small range

of swing angles (θ_1 and θ_2). Nevertheless, to make the analysis more inclusive, the magnitude of the maximum swing angle is computed and applied to the model. This corresponds to the worst case scenario when the payload swing most aggressively compromises the crane's tip-over stability.

Finally, it should be noted that the swing deflection reduces the crane's tip-over stability because it moves the payload mass outwards. This creates a horizontal force on the boom tip that acts through the very long moment arm formed by the boom. As a result, the crane cannot support as much payload as it can in the static case. Furthermore, the counterweight has to be moved further backwards to prevent tipping-over when the payload swings out, away from the crane body.

3.2 Straight Base Motion

The simplest motion of a crawler crane is driving the base from one point to another, along a straight line, under a constant acceleration and a limited maximum speed.

3.2.1 Mathematical Model and Payload Swing Dynamics

To estimate the swing angle resulting from a base-acceleration, a closed-form solution of the swing angle needs to be derived. A few assumptions are made to derive the equation of motion of the swinging payload. First of all, the payload is assumed to be an undamped single pendulum connected to an accelerating pivot point. The pivot point is located at the external end of the luffing boom, and because the base acceleration is the only input acting on the crane, then the various parts of the crane can be regarded as one rigid body, where the acceleration of the pivot point is assumed to be the same as the acceleration of the crane's base as it moves from one point to another. Finally, as the base accelerates, it causes the payload to swing in the radial direction. Tangential swinging is ignored.

Based on these assumptions, the equation of motion for the swinging payload is:

$$\ddot{\theta}_1(t) + \omega_n^2 \sin(\theta_1(t)) = \frac{-\ddot{x}(t)}{L_5} \cos(\theta_1(t)) \quad (3.1)$$

where θ_1 is the radial swinging angle, ω_n is the natural frequency of the swinging payload, L_5 is the hoist length and x is the position of the pivot point. Assuming the swing angle is relatively small at all times, then (3.1) can be linearized using a small angle approximation for θ_1 ($\sin \theta_1 \approx \theta_1$ and $\cos \theta_1 \approx 1$) as follows:

$$\ddot{\theta}_1(t) + \omega_n^2 \theta_1(t) = \frac{-\ddot{x}(t)}{L_5} \quad (3.2)$$

Defining $\ddot{x}(t) = a(t)$, (3.2) can be expressed as:

$$\ddot{\theta}_1(t) + \omega_n^2 \theta_1(t) = \frac{-a(t)}{L_5} \quad (3.3)$$

Taking the Laplace transformation of (3.3) gives:

$$s^2 \Theta_1(s) + \omega_n^2 \Theta_1(s) = \frac{-A(s)}{L_5} \quad (3.4)$$

Rearranging the equation, the transfer function of the system can be expressed as:

$$G(s) = \frac{\Theta(s)}{A(s)} = \frac{1}{L_5(s^2 + \omega_n^2)} \quad (3.5)$$

The time-optimal command with a limited velocity and acceleration is a bang-coast-bang command, as shown in Figure 30. It is used as an input to move the base in a point-to-point motion. The bang-coast-bang command can be described as an acceleration step command with a magnitude A that consists of four steps; two positive and two negative.

The bang-coast-bang command creates a trapezoidal velocity profile. In the Laplace domain, the command can be expressed as:

$$A(s) = \frac{A}{s}(1 - e^{-t_2s} - e^{-t_3s} + e^{-t_4s}) \quad (3.6)$$

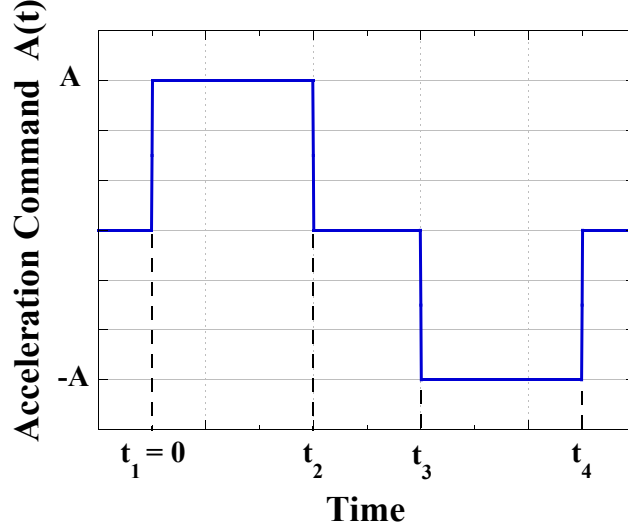


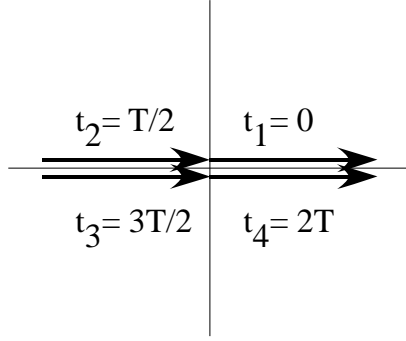
Figure 30: Bang-Coast-Bang Acceleration Command.

where A is the magnitude of the acceleration input and t_i is the corresponding timing of the i^{th} step in the command.

Now, to find a solution for the payload swing angle, the acceleration expression in the Laplace domain expressed in (3.6) is substituted into the transfer function expressed in (3.5). The resulting expression for $\Theta_1(s)$ is then transformed back into the time domain by taking the inverse Laplace transformation to get:

$$\begin{aligned} \theta_1(t) = \frac{-A}{L_5 \omega_n^2} & \left(\left(1 - \cos \omega_n t \right) - \left(1 - \cos \omega_n (t - t_2) \right) \sigma(t - t_2) \right. \\ & \left. - \left(1 - \cos \omega_n (t - t_3) \right) \sigma(t - t_3) + \left(1 - \cos \omega_n (t - t_4) \right) \sigma(t - t_4) \right) \end{aligned} \quad (3.7)$$

It can be noticed from (3.7) that the maximum swing angle occurs when all four cosine terms are in phase, and the multiplying step functions σ are all equal to 1 (i.e. the running time is long enough to complete an entire profile of the bang-coast-bang command). In that case the maximum swing angle can be calculated using the



- * Magnitude of each arrow is A.
- * T is the period of oscillation of the payload.

Figure 31: Vector Diagram for the Acceleration Command Resulting in Maximum Residual Vibrations.

following expression:

$$\theta_{1max} = \frac{4A}{g} \quad (3.8)$$

Figure 31 displays a vector diagram, where each vector represents an impulse that is convolved with a step command to create the desired bang-coast-bang acceleration. Based on this vector diagram, the maximum swing angle occurs if t_{gap} , which is the period of time between the acceleration and deceleration pulses defined as $t_3 - t_2$, is equal to the period of oscillation of the payload, while the duration of each of the two pulses is equal to half the period of oscillation.

Due to the acceleration and deceleration commands, the crawler crane experiences inertia forces acting on the crane's center of mass. These forces significantly influence the tip-over stability of the crane. The higher the center of mass of the crane is, the longer the moment arm is, and the bigger the effect of these inertial forces on the tip-over stability of the crane. The location of the center of mass can be raised by luffing the boom upwards. The effect of these forces increases with increasing the boom mass and length, and with moving the counterweight inwards. Therefore, the

inertia effects must be included to obtain a reliable estimation of the tip-over stability margin of the crane.

The inertia force effect can be included in the analysis as a force acting on the center of mass of the crane in the horizontal direction. During the acceleration phase, the inertia force acts towards the center of mass, in a direction opposite to that of motion, thus, it contributes positively to the crane's forward tip-over stability. On the other hand, the forward tip-over stability is compromised when the crane base is decelerating. Thus, the prediction model takes into account the inertial effects during the deceleration of the crane, this will take into account the worst case scenario.

D'Alembert Principle states that if the dynamic behavior of a mass is analyzed in an accelerated, body-fixed reference frame, then the inertia forces, which are fictitious forces in general, have to be regarded as real forces acting on the mass. Applying this concept, Figure 32 shows the free body diagram with the inertia forces acting horizontally on the crane system during deceleration.

The inertia force acting on the crane center of mass and the braking force F_b acting on the crawler tracks cancel each other in the horizontal direction. However, they create a couple that contributes to the tip-over instability. This couple is determined by multiplying the inertia force by the height of the center of mass above the ground h_{CM} . Since it is assumed that the crane decelerates at a constant rate, A , the couple is also assumed to be constant.

3.2.2 Tip-over Stability Analysis of Straight Base Motion

When the base of the crane moves in a straight line under the effect of the bang-coast-bang acceleration command discussed previously, it induces oscillations of the payload. Two major factors affect the value of the swinging angle of the payload; which are the total distance traveled by the crane base, and the width of the two pulses in the acceleration command.

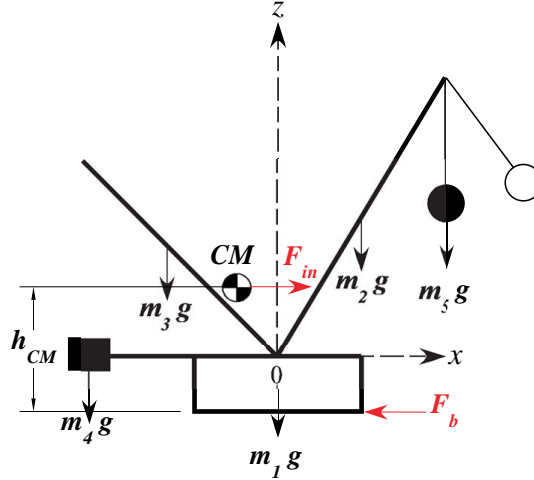


Figure 32: Free Body Diagram of Crawler Crane with Inertial Forces during Deceleration.

For our case study, the crane parameters used for calculations are the same parameters listed in Table 2, except for the hoist length L_5 which is set to 50 m here. Also, the maximum rated linear velocity of the crane base according to the data sheet is 0.6 km/h , so it is assumed that the crane reaches this maximum speed within 1 s to account for the worst case scenario, and this acceleration value is used as the amplitude of the Bang-Coast-Bang command.

For a hoist length of 50 m , the period of oscillation is 14.18 s . Thus, the Bang-Coast-Bang command creating the largest swing angle lasts for twice that period. Changing the width of the acceleration and deceleration pulses, and consequently changing t_{gap} , results in different amplitudes for the payload's residual oscillations.

Figure 33 shows the maximum payload swing with respect to t_{gap} . It can be inferred from the graph that the largest swing angle occurs when t_{gap} is equal to the period of oscillation of the payload; i.e. the acceleration command complies with the vector diagram shown in Figure 31, where $T = 14.18 s$.

The response from the acceleration command creating maximum oscillations is

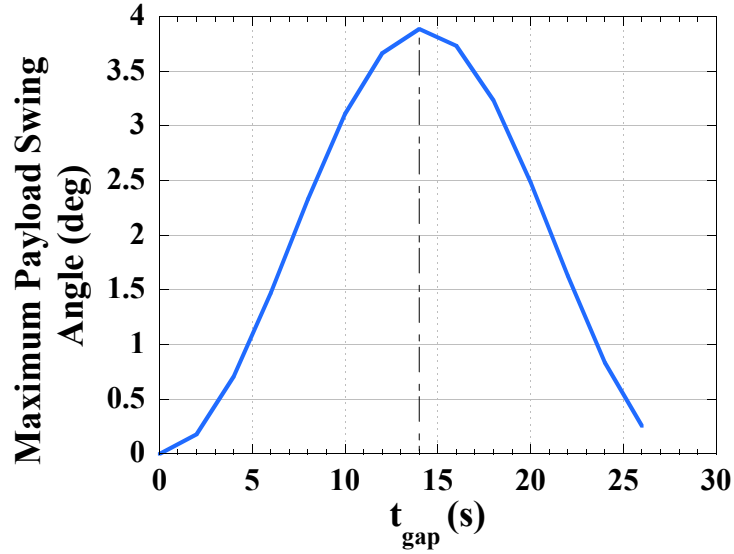


Figure 33: Payload Swing Angle in Bang-Coast-Bang Motion vs. Time with Different Acceleration Durations.

shown in Figure 34. The maximum swing angle in this case is 3.89° , which is the same value obtained if (3.8) is used, and this is the value to be used in the tip-over analysis.

Because both the crane base movement and the payload swinging are slow movements, the payload was assumed to be positioned at the maximum swing angle mentioned before. Also, the inertial force was added to the gravitational forces and a forward tip-over stability analysis was performed again using a counterweight mass of 200 t. The minimum counterweight position to prevent forward tip-over was calculated.

Figure 35 compares the minimum counterweight position to prevent forward tip-over in both the static and dynamic cases. The boom luffing angle was set to 60° , and the counterweight mass was set to 200 t. As the crane base starts to move and then comes to a stop, the acceleration and deceleration pulses create residual swinging, which causes the payload to extend further from the base and causes the crane to be

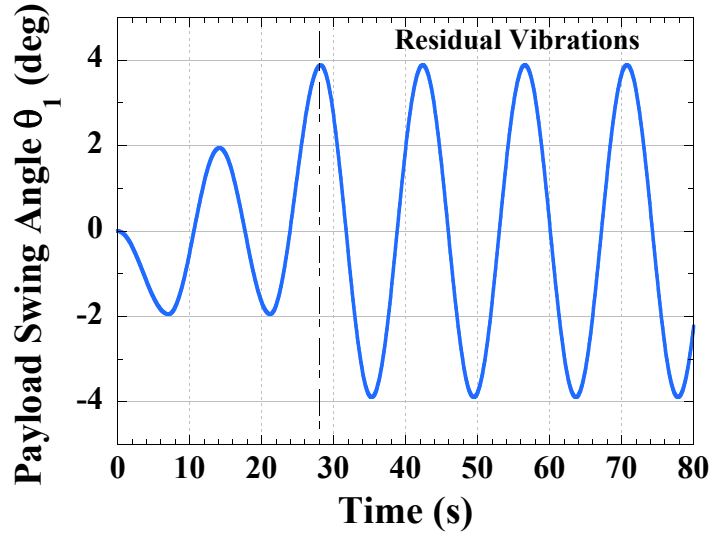


Figure 34: Payload Swing Response to a Bang-Coast-Bang Acceleration Command vs. Time (Maximum Oscillation).

less stable. The effect of the inertial force is added to that, thus the counterweight has to be moved further back.

Analyzing Figure 35, it is clear that dynamic effect is bigger when the boom is directed to the front of the base. The effect is less severe when the boom is directed sideways, and it is minimum when the boom is directed towards the back. Looking closely, it is noticed that the inflection point in the dynamic case is shifted. In the static case, the counterweight is placed at a minimum distance from the center of the crane when the boom is directed towards the corner of the base, i.e. when the slewing angle is 39.1° based on the crane's parameters. However, in the dynamic case the calculations show that the counterweight should be placed at a minimum distance from the center of the crane when the slewing angle is 40.4° .

Thus, to ensure that the results include all possibilities, an investigation was made to determine the potential of the crane tipping forwards about the axis that is always perpendicular to the direction of motion which is the forward tip-over axis, as a result

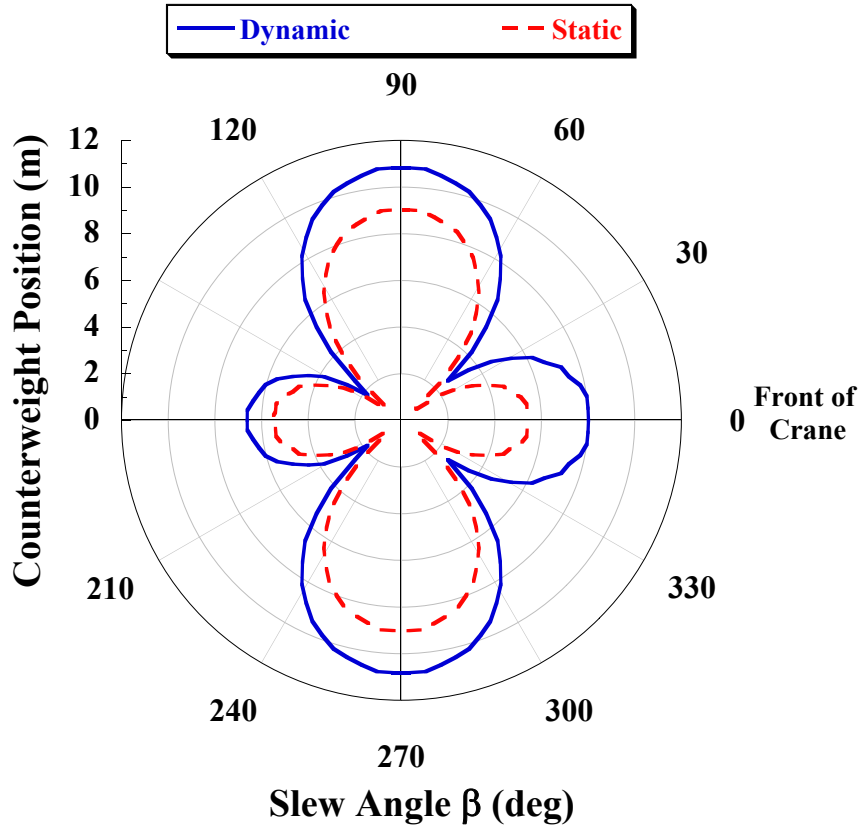


Figure 35: Minimum Counterweight Position to Prevent Forward Tip-Over in the Static and Dynamic Cases with a Payload of 110 t.

of the inertial forces whose direction is always constant regardless of the slewing angle. Results show that for a slewing angle of less than 44.1° the minimum counterweight position calculated and displayed in Figure 35 is larger than or equal to the minimum counterweight position required to prevent tip-over about the forward axis. While, when the slewing angle is larger than 44.1° the moment about the forward axis is never enough to tip the crane over in that direction. This means that the previous study is conclusive. In general, the overall safe counterweight region considering the dynamic effects of the payload swing and inertia forces is smaller, as illustrated in Figure 36.

Another way of representing the data in Figure 36 is by plotting the length of the

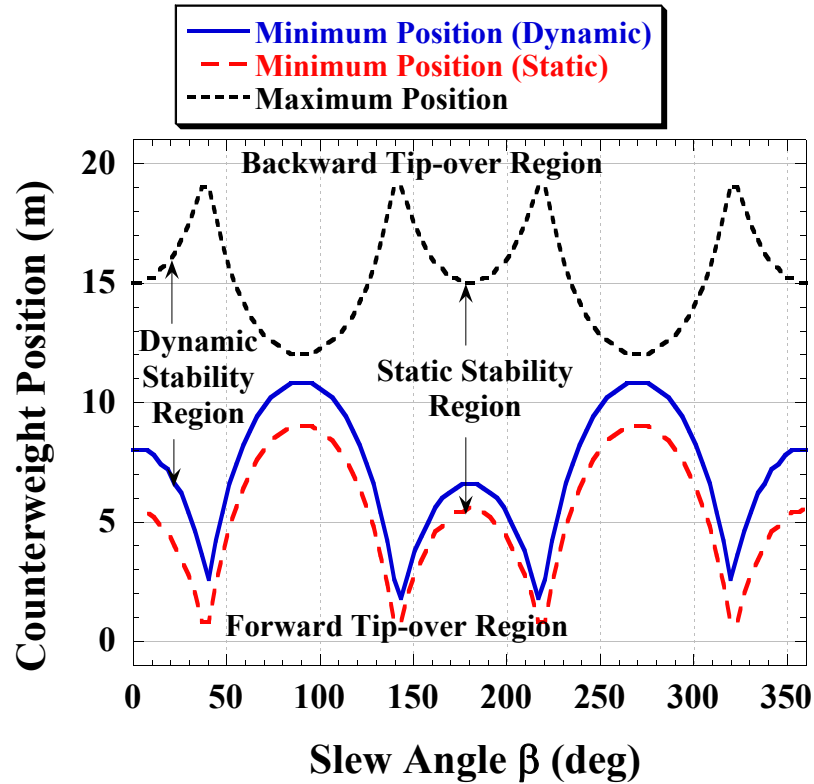


Figure 36: Static and Dynamic Safety Regions for a 200 t Counterweight and Boom Luffing Angle of 60°.

safety region in both the static and dynamic cases with respect to the slew angle. This is shown in Figure 37, which confirms that the stability region when the crane is stationary is bigger than the stability region when the crane is moving. Also, maximum stability is achieved when the slew angle is around 40°; i.e. when the boom is pointing towards the corner of the base, while minimum stability is achieved when the slew angle is 90°; i.e when the boom is pointing sideways.

However, to better understand the curves in Figures 35 and 36, the effect of the payload swing and the inertial forces was studied independently. Then both cases were compared to the static and dynamic results obtained before. The effect decomposition is shown in Figure 38.

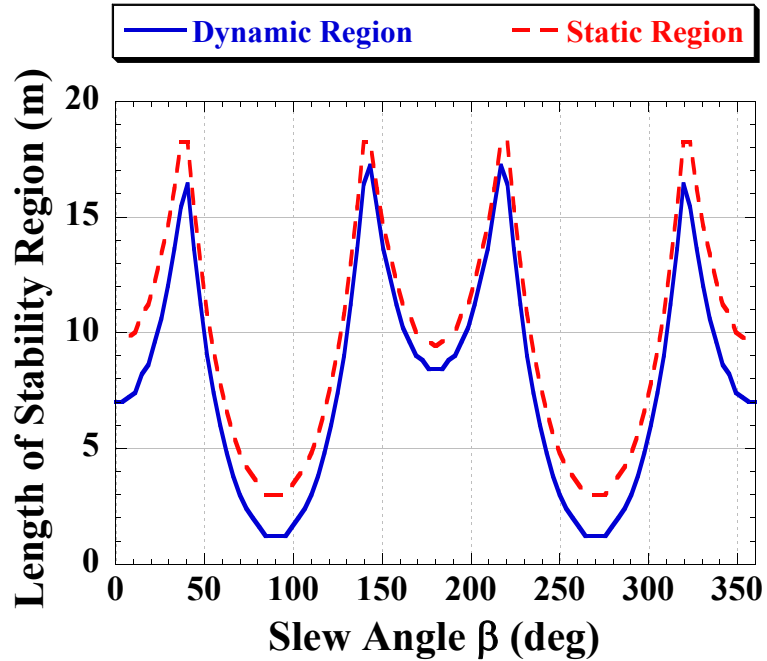


Figure 37: Length of Static and Dynamic Safety Regions for a 200 t Counterweight and Boom Luffing Angle of 60°.

When the boom is directed to the front of the crane base, the inertial force creates a moment in the forward tipping direction, thus it compromises the forward stability of the crane. This requires the counterweight to be moved further backwards. Turning the boom sideways changes the tip-over axis of the crane to the side; while the direction of the moment created by the inertial forces remains the same, because the crane is still moving forward. Thus, because the direction of the moment becomes perpendicular to the tip-over axis in this case, it will not degrade the crane's stability, which explains why the counterweight location here is the same as the static case. Finally, when the boom is facing the back of the crane, the moment created by inertial forces will be working in a direction opposite to that of tipping, towards the boom. This means that it will increase the stability of the crane, which explains why the counterweight can be moved inwards.

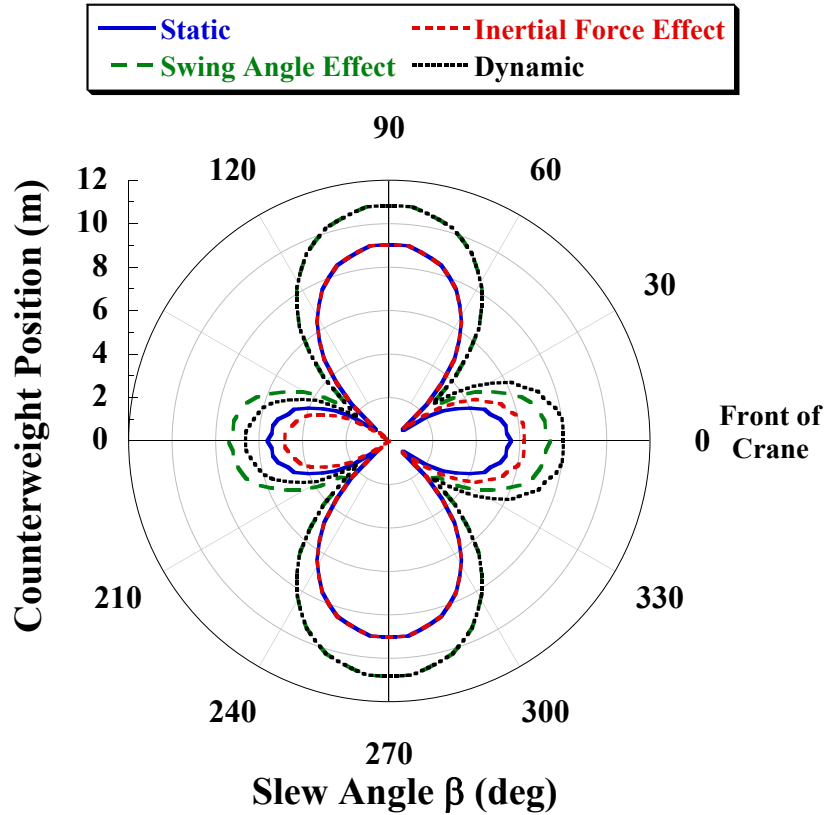


Figure 38: Minimum Counterweight Position to Prevent Forward Tip-over in the Static and Dynamic Case with a Payload of 110 t (Independent Effects of Payload Swing and Inertial Forces).

In all cases, when the payload swings outward it decreases the stability of the crane in the forward direction. This forces the counterweight to be moved further backwards regardless of the boom direction, as illustrated in Figure 38. Combining the two effects discussed above results in the irregular flower shape obtained by the dynamic analysis that was shown in Figure 35.

Figure 39 illustrates the dynamic tip-over stability for various counterweight masses. When the mass of the counterweight increases, the distance it has to be moved in the rearward direction decreases.

The payload mass equivalently has an effect on the dynamic tip-over stability. As the mass of the payload increases, the counterweight has to be moved further

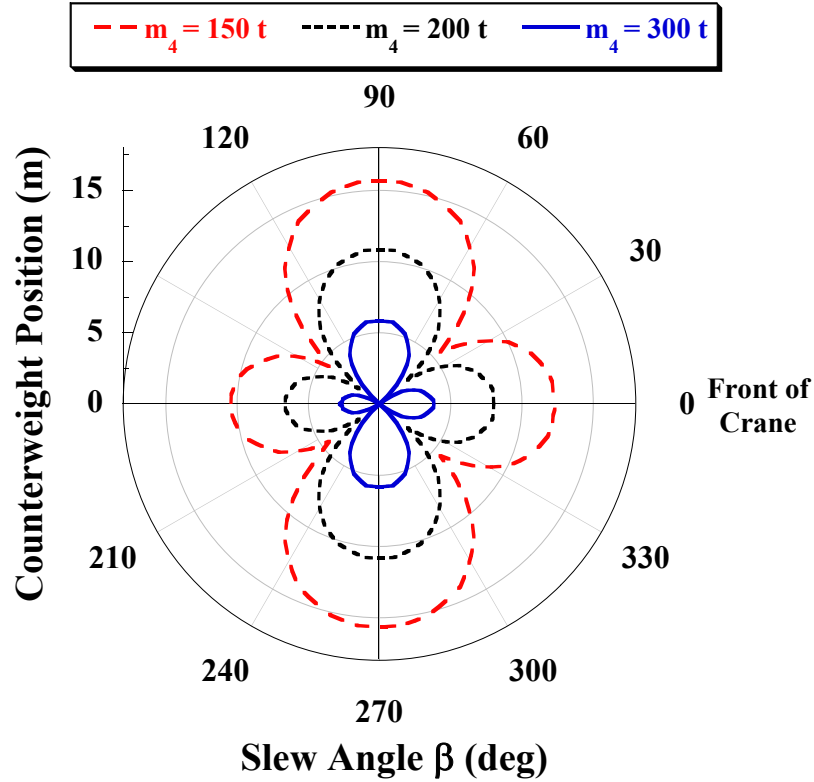


Figure 39: Minimum Counterweight Position to Prevent Forward Tip-over in the Dynamic Case with a Payload of 110 t, (m_4 is the Counterweight Mass).

backwards to counterbalance the effect of the heavier payload. This is clearly shown in Figure 40.

3.2.3 Effect of Hoist Cable Length

For the same bang-coast-bang acceleration command used in the previous calculations, the length of the hoist cable was varied. Each time, the maximum residual payload swing angle was recorded. The result is demonstrated in Figure 41, which shows that the maximum residual payload swing occurs at the length which creates a period of oscillations equal to t_{gap} .

However, the acceleration command can be more easily controlled than the cable length, so a suggested solution to minimize oscillations is to apply the input shaping

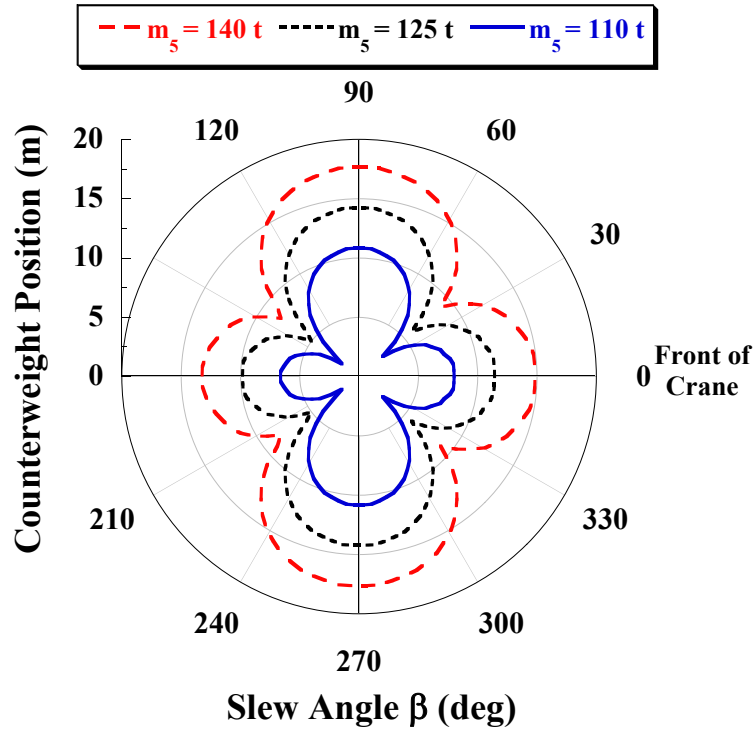


Figure 40: Minimum Counterweight Position to Prevent Forward Tip-Over in the Dynamic Case with a Counterweight of 200 t, (m_5 is the Payload Mass).

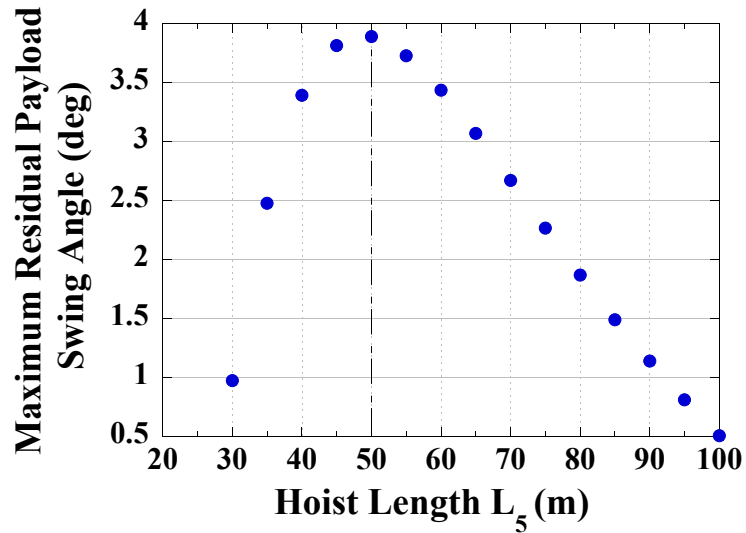
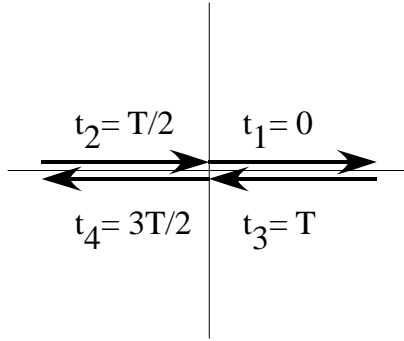


Figure 41: Maximum Residual Payload Swing Angle vs. Hoist Length.



- * Magnitude of each arrow is A.
- * T is the period of oscillation of the payload.

Figure 42: Vector Diagram for the Acceleration Command Resulting in Minimum Residual Vibrations.

to reduce payload swing. If the vectors representing the acceleration command are placed as shown in Figure 42, then they will sum up to zero, thus reducing the residual swing to a minimum.

Therefore, if the previously used acceleration command was modified to have a $t_{gap} = 14$ s, then the response to that command will be the one shown in Figure 43, where it is obvious that the maximum transient swing angle is about 2° , and the maximum residual swing angle is very small. This is one solution, but it is not the only one. However, this shows that controlling the acceleration command while driving the crane has a direct impact on the amount of payload swing, knowing that it will always be less than the maximum value discussed before.

Table 5 provides a general guide that helps choose the acceleration command that will induce minimum vibrations for different hoist lengths.

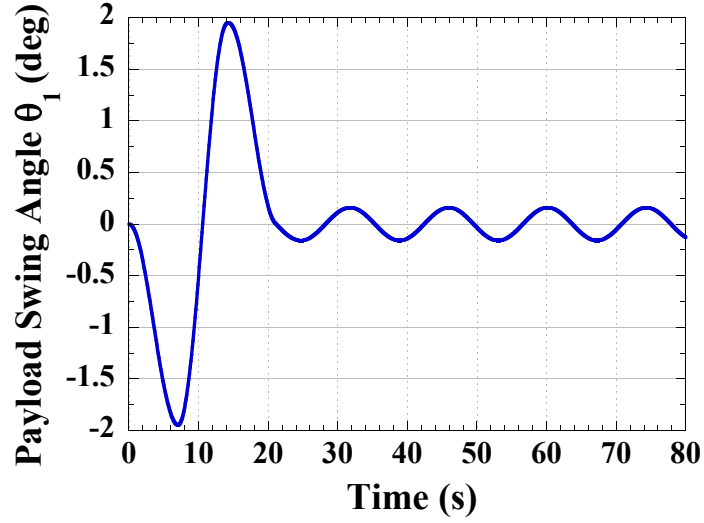


Figure 43: Payload Swing Response to a Bang-Coast-Bang Acceleration Command vs. Time (Minimum Oscillation).

Table 5: Guidelines to Choose the Acceleration Command Generating Minimum Vibrations for Different Hoist Lengths.

Cable Length(m)	t_1 (s)	t_2 (s)	t_3 (s)	t_4 (s)
30	0	5.5	11.0	16.5
35	0	6.0	11.9	17.9
40	0	6.4	12.7	19.1
45	0	6.8	13.5	20.3
50	0	7.1	14.2	21.3
55	0	7.5	14.9	22.4
60	0	7.8	15.5	23.3
65	0	8.1	16.2	24.3
70	0	8.4	16.8	25.2
75	0	8.7	17.4	26.1
80	0	9.0	17.9	26.9
85	0	9.3	18.5	27.8
90	0	9.5	19.0	28.5
95	0	9.8	19.6	29.4
100	0	10.1	20.1	30.2

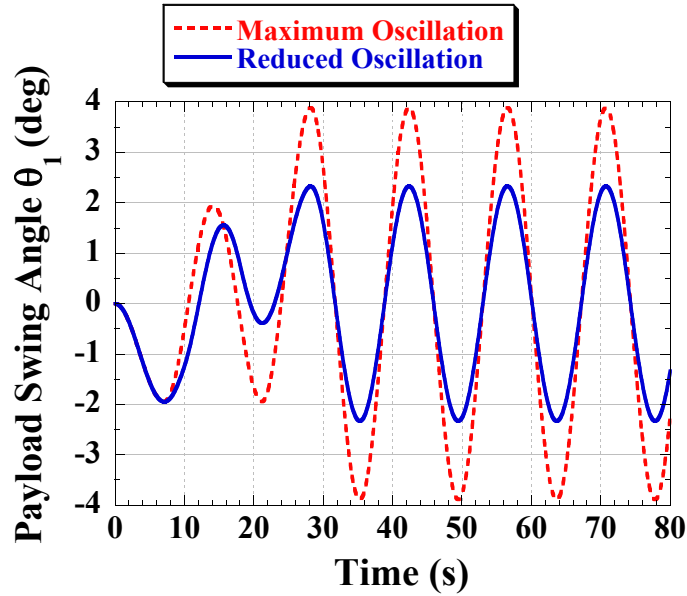


Figure 44: Payload Swing Response to a Bang-Coast-Bang Acceleration Command vs. Time (Reduced Oscillation).

Another solution would be to change the time needed for the crane to reach the maximum velocity. In other words, increase the duration of the two pulses in the bang-coast-bang command. An example of this approach is using the same total period of 28 s, with a duration of 10 s for each of the acceleration and deceleration pulses, and a gap of 8 s. The response for this command is shown in Figure 44, which clearly indicates that the maximum residual swing angle is reduced by almost half the maximum value calculated before. This can be considered another measure to control the swing angle and reduce the severity of its effect.

The stability analysis gets more complicated when the crane is in motion; however the dominant effects can be identified. Methods to account for the motion effects can identify reasonable upper bounds on the additional tip-over moments and add their effects to the static analysis. Parameter values associated with the dynamic effects obviously affect the overall stability of the crane, thus, these parameters should be studied and chosen carefully to avoid catastrophies.

3.3 Boom Luffing Motion

Another important motion for boom crane operation is luffing. Boom luffing motion is defined as raising or lowering the boom, in order to move the payload horizontally. This is achieved by rotating the boom about a pivot located at its lower end. When the boom luffing angle changes, it causes the payload to swing out in the radial direction.

When the payload swing extends outward, away from the mobile base, the tip-over moment will increase, and the crane becomes less stable. Therefore, it is important to take boom-luffing-induced swing angle into consideration when examining tip-over stability. Such considerations create a more reliable tip-over prediction tool.

3.3.1 Mathematical Model and Payload Swing Dynamics

To isolate the effect of the luffing motion on crane tip-over stability, a stationary crane with a single luffing input, as shown in Figure 45, is studied. The slew angle is set to $\beta = 0^\circ$, then the analysis is repeated for different slew angles ranging from 0° to 360° to compare it with the results obtained in Chapter 2. Only the downward motion is considered, because when the boom is luffed downwards it significantly decreases the tip-over stability as the results of Chapter 2 indicated. Luffing the boom upwards will generally make the crane more stable.

It is assumed that the boom rotates with a constant angular velocity $\dot{\phi}_1 = \omega$. The position vector from the boom rotation point to the center of mass of the payload is:

$$\vec{r} = (L_2 \cos \phi_1 + L_5 \sin \theta_1) \vec{i} + (L_2 \sin \phi_1 - L_5 \cos \theta_1) \vec{j} \quad (3.9)$$

By ignoring all inputs other than the boom luffing motion, and assuming that there is no swinging in the tangential direction ($\theta_2 = 0^\circ$), the unconstrained equations of motion of the payload can be derived using the Euler-Lagrangian:

$$\frac{d}{dt} \left(\frac{\partial L}{\partial \dot{q}_k} \right) - \frac{\partial L}{\partial q_k} = Q_k \quad (3.10)$$

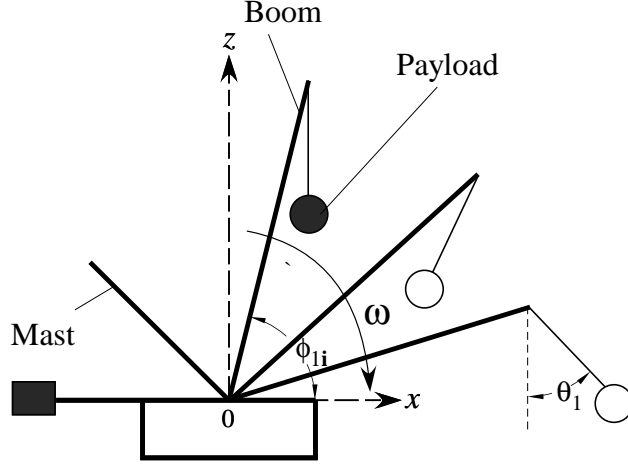


Figure 45: Dynamics in Constant Luffing Down Motion - Side View.

where q_k is the generalized coordinate. In our case $q_k = \theta_1$. L is defined as the difference between kinetic and potential energies: $L = T - V$. The kinetic energy of the payload and the boom T can be expressed by:

$$T = \frac{1}{2}J\dot{\phi}_1^2 + \frac{1}{2}m_5\dot{r}\dot{r}^T \quad (3.11)$$

$$= \frac{1}{2}J\dot{\phi}_1^2 + \frac{1}{2}m_5[(L_2\dot{\phi}_1)^2 + (L_5\dot{\theta}_1)^2 + 2L_2L_5\dot{\phi}_1\dot{\theta}_1\cos\phi_1\sin\theta_1 - 2L_2L_5\dot{\phi}_1\dot{\theta}_1\sin\phi_1\cos\theta_1] \quad (3.12)$$

where J is the moment of inertia of the boom about rotation point O .

V is the potential energy of the payload and the boom, which can be expressed as:

$$V = \frac{1}{2}m_2gL_2\sin\phi_1 + m_5g(L_2\sin\phi_1 - L_5\cos\theta_1) \quad (3.13)$$

Substituting (3.12) and (3.13) into (3.10) yields the nonlinear equation of motion:

$$\begin{aligned} Q_1 = & m_5L_5^2\ddot{\theta}_1 - (m_5L_2L_5\dot{\phi}_1^2\sin\phi_1 - m_5gL_5)\sin\theta_1 \\ & - m_5L_2L_5\dot{\phi}_1^2\cos\phi_1\cos\theta_1 + m_5L_2L_5\ddot{\phi}_1\cos\phi_1\sin\theta_1 \\ & - m_5L_2L_5\ddot{\phi}_1\sin\phi_1\cos\theta_1 \end{aligned} \quad (3.14)$$

where Q_1 is the generalized force acting on the payload, which in our case is zero.

Because the swing angle is usually small, a small angle approximation is used for θ_1 . Thus, (3.14) can be expressed as:

$$\ddot{\theta}_1 + \frac{g}{L_5}\theta_1 - \frac{L_2}{L_5}\dot{\phi}_1^2 \sin \phi_1 \theta_1 + \frac{L_2}{L_5}\ddot{\phi}_1 \cos \phi_1 \theta_1 = \frac{L_2}{L_5}\dot{\phi}_1^2 \cos \phi_1 + \frac{L_2}{L_5}\ddot{\phi}_1 \sin \phi_1 \quad (3.15)$$

This is a linear, homogeneous differential equation with time-varying crane configuration with respect to the boom luffing angle ϕ_1 , where L_2 is the boom length, L_5 is the suspension cable length, $\dot{\phi}_1$ is the boom luffing rotational velocity, and $\ddot{\phi}_1$ is the boom luffing rotational acceleration. The angle θ_1 is the radial swing angle of the payload.

The following state variables were defined:

$$\begin{aligned} x_1 &= \theta_1 \\ x_2 &= \dot{\theta}_1 \\ x_3 &= \phi_1 \\ x_4 &= \dot{\phi}_1 \end{aligned} \quad (3.16)$$

The command used as an input to this system is the rotational boom luffing acceleration:

$$u = \ddot{\phi}_1 \quad (3.17)$$

Based on (3.16) and (3.17), the dynamic system can be described by the following

equations:

$$\begin{aligned}
\dot{x}_1 &= \dot{\theta}_1 = x_2 \\
\dot{x}_2 &= \ddot{\theta}_1 = \frac{L_2}{L_5} x_4^2 \cos x_3 + \frac{L_2}{L_5} u \sin x_3 - \frac{L_2}{L_5} u x_1 \cos x_3 + \frac{L_2}{L_5} x_4^2 x_1 \sin x_3 - \frac{g}{L_5} x_1 \\
\dot{x}_3 &= \dot{\phi}_1 = x_4 \\
\dot{x}_4 &= \ddot{\phi}_1 = u
\end{aligned} \tag{3.18}$$

The time-optimal command with a limited velocity and acceleration is a bang-coast-bang command (trapezoidal velocity profile), similar to the one described in Sections 3.2.1. Here, it will be used to luff the boom downwards in a point-to-point motion by using it as an input command to the system of state equations in (3.18).

Applying a suitable acceleration command, and solving the system of state equations, the residual vibrations of the payload can be predicted. The maximum value in each case is recorded, and then used to perform the stability analysis. This effectively captures the worst case swing-out scenario for a single boom movement.

3.3.2 Tip-over Stability Analysis of Boom Luffing

Figure 46 shows the maximum swing of the payload when the crane boom luffs with an angular velocity of 0.02 rad^1 , with respect to the moving distance. The boom was luffed from an initial boom luffing angle (80° , 70° , and 60°) down to an angle of 30° . It should be mentioned that the crane parameters used for these calculations are the same parameters listed in Table 2, except for the hoist length L_5 which is set to 30 m here. The payload's maximum swing angle generally increases with increasing initial boom angle.

The maximum payload swing was calculated for three different values of initial boom angle with respect to different moving distances. All other crane parameters

¹This value was estimated from the data sheet of the Terex CC 2800-1

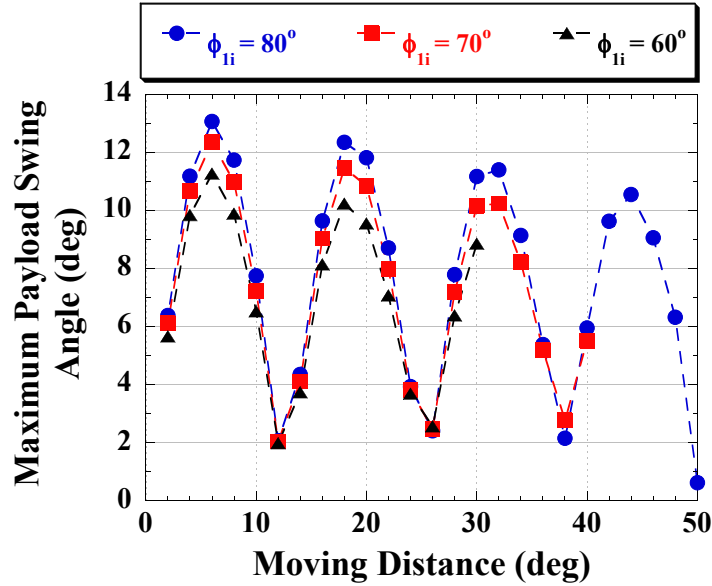


Figure 46: Payload Swing Angle in Constant Luffing Down Motion vs. Time.

were consistent with the parameters used for the static analysis. Because both the boom luffing motion and the payload swing are slow movements, the payload was assumed to be positioned at the maximum swing angle calculated previously, and the forward tip-over stability analysis was performed again using a counterweight mass of 200 t.

Figure 47 shows the minimum counterweight position to prevent forward tip-over. The plot contains similar patterns to those corresponding to the static case where no swinging was considered. The graph indicates that changing the initial boom luffing angle has only a moderate effect on stability. This is explained by the fact that the maximum swing angle induced by various initial boom angles does not vary substantially, as was shown in Figure 46.

Figure 48 compares the minimum counterweight position to prevent forward tip-over in both the static and dynamic boom-luffing cases when the initial boom angle was set to 60° , and the counterweight mass was set to 200 t. The static analysis

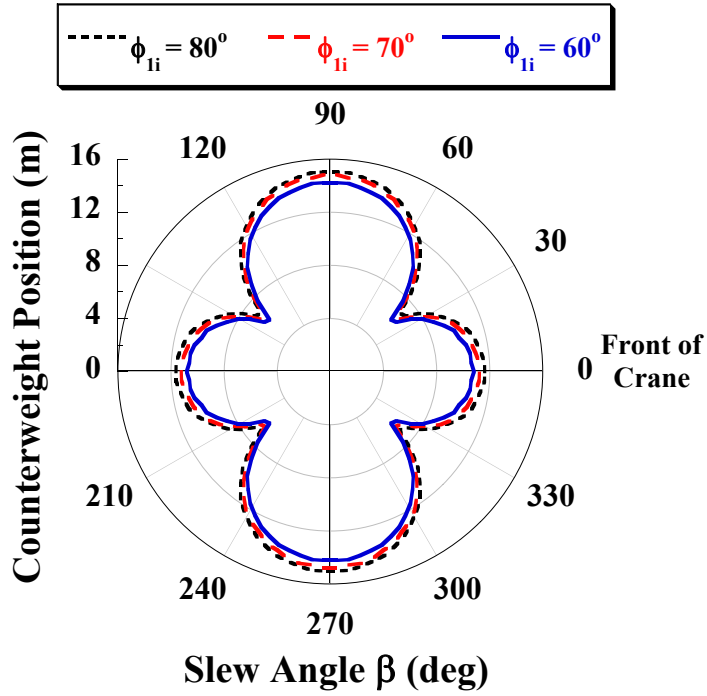


Figure 47: Minimum Counterweight Position to Prevent Forward Tip-over for a Range of Initial Boom Luffing Angles with a Payload of 110 t.

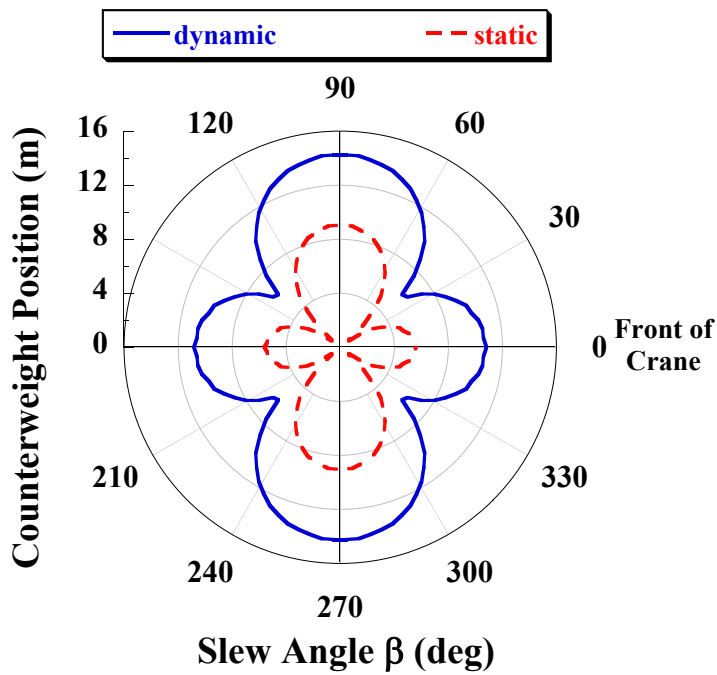


Figure 48: Minimum Counterweight Position to Prevent Forward Tip-over in the Static and Dynamic Boom-Luffing Cases with a Payload of 110 t.

underestimates the minimum position needed to prevent a forward tip over. When the payload swings outward, the crane is less stable, thus the counterweight has to be moved further back. As a result, the overall safe counterweight region considering swing dynamics is smaller than that considered in the static case, as illustrated in Figure 49.

Earlier in Chapter 2, it was mentioned that the boom angle is the most critical parameter, in terms of its effect on tip-over stability. Figures 48 and 49 serve to support that earlier statement. First it is noted that, the counterweight position in the dynamic case, which corresponds to the maximum swing of the payload, and thus covers for all possibilities of swinging, is almost 5 *m* greater than that corresponding to the static case. That is certainly a big difference. This shows that the payload swing resulting from the boom luffing motion significantly compromises the crane's stability.

The minimum safety region of the counterweight position occurs when the slew angle is 90° , while the maximum safety region of the counterweight position occurs when the slew angle is approximately 40° . This is consistent with all the previous results concluding that the crane is least stable when the boom is pointing towards the side. This is also represented by Figure 50, which shows the size of the stability region in both the static and dynamic cases with respect to the slewing angle.

However, Figure 49 shows that, if the slewing angle was close to 90° , i.e. the boom is directed towards the side of the crane, then the minimum counterweight position needed to prevent forward tip-over is greater than the maximum counterweight position needed to prevent backward tip-over. This means that preventing forward tip-over will cause backward tip-over and vice versa. Thus, it is advisable in this case that precautions are taken to prevent the payload from reaching the maximum swing angle by shaping the input command, or applying different solutions, such as using a heavier counterweight, or limiting the payload weight to a smaller value.

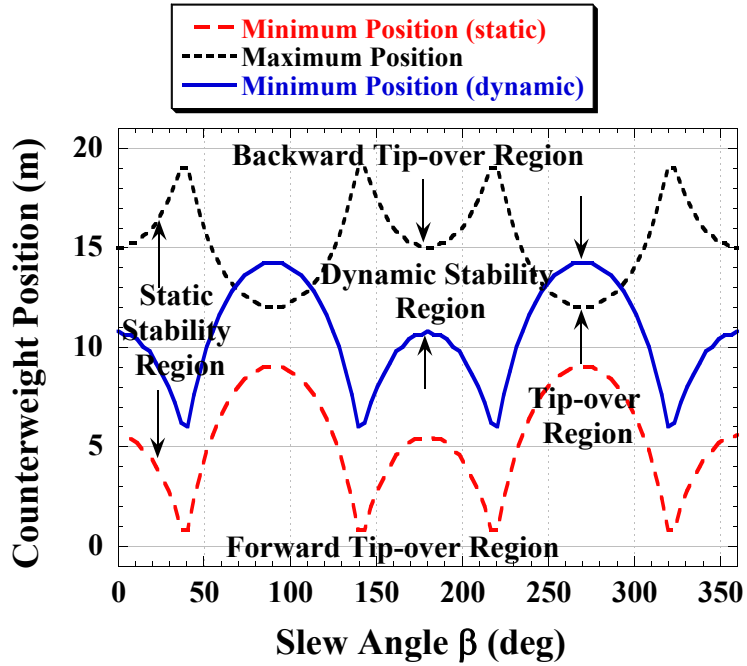


Figure 49: Static and Dynamic Safety Regions for a 200 t Counterweight and an Initial Boom Luffing Angle of 60° .

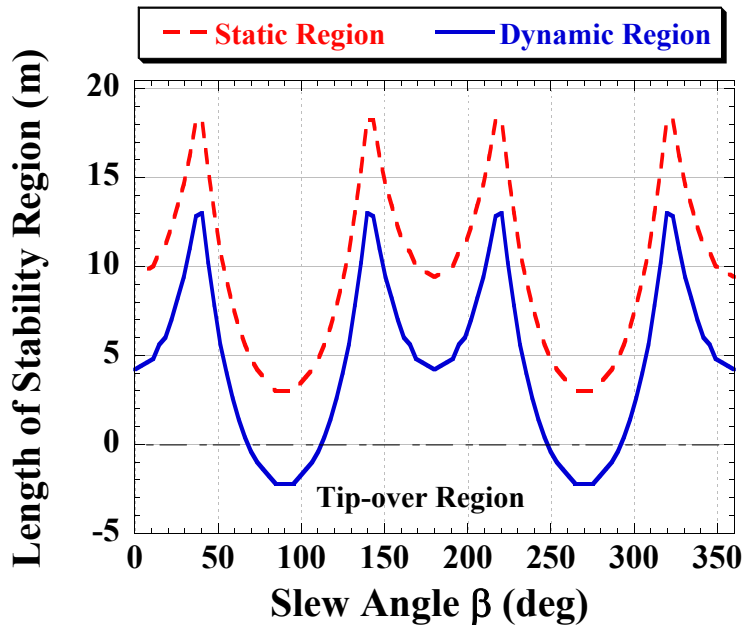


Figure 50: Static and Dynamic Safety Regions for a 200 t Counterweight and an Initial Boom Luffing Angle of 60° .

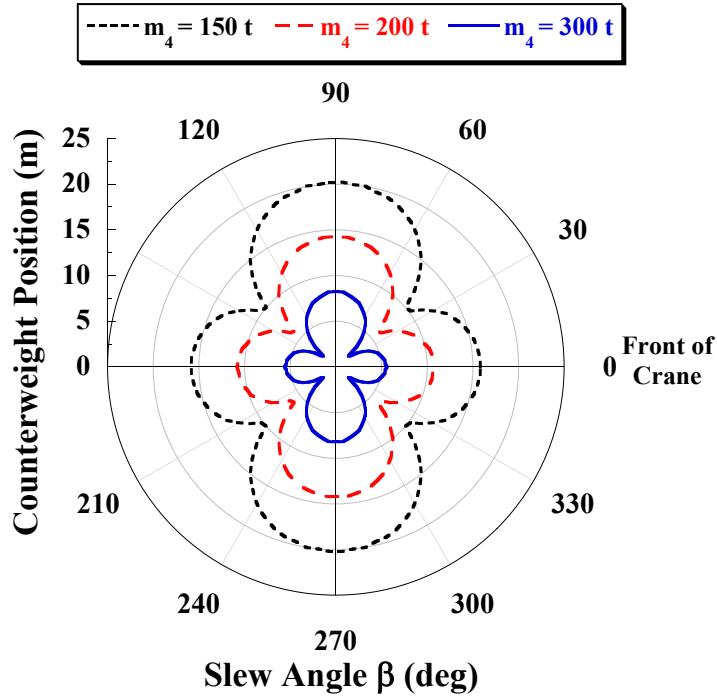


Figure 51: Minimum Counterweight Position to Prevent Forward Tip-over in the Dynamic Case with a Payload of 110 t, (m_4 is the Counterweight Mass).

3.3.3 Effect of Counterweight Mass and Payload Mass

The effect of changing the counterweight mass was studied, and the minimum counterweight position was calculated for different counterweight values using a maximum swing angle. The result is shown in Figure 51 which demonstrates similar trends to those which occurred in the static case. If the counterweight mass increases, then the distance it has to be moved in the rearward direction decreases. This figure also shows that a counterweight of 150 t is not enough to maintain stability in this configuration, because a counterweight that light has to be moved to a distance of 20 m away from the base center which cannot be achieved for this crane configuration.

Finally, Figure 52 illustrates the effect of increasing the payload mass on dynamic stability. It is clear that a 15 t increase in the payload mass requires the counterweight to be positioned at a distance of about 20 m away from the base center, which is

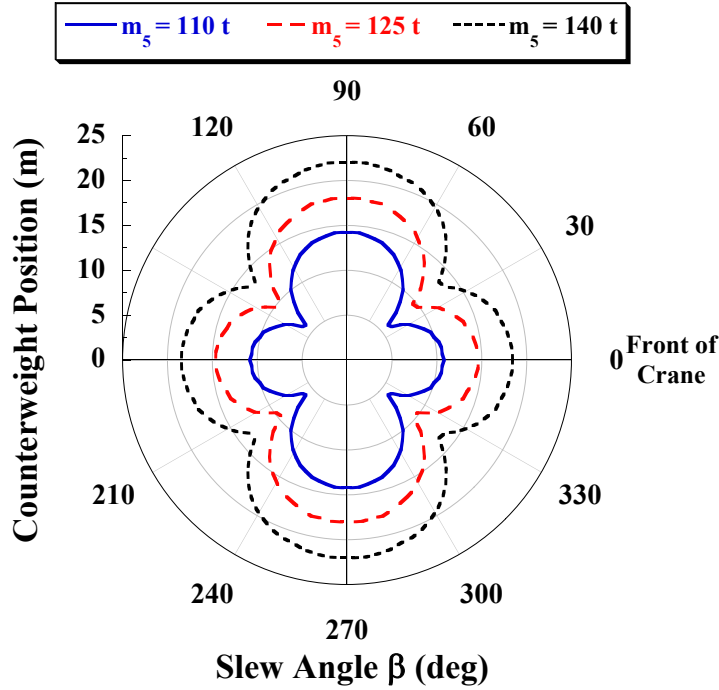


Figure 52: Minimum Counterweight Position to Prevent Forward Tip-over in the Dynamic Case with a Counterweight of 200 t, (m_5 is the Payload Mass).

physically impossible for this crane in this configuration. Thus, it can be concluded that the payload mass is another critical parameter that should be carefully limited to maintain static, as well as dynamic stability.

3.4 Boom Slewing Motion

Slewing is another one of the essential motions that helps move the payload horizontally. However, it induces inertia forces and payload swings that compromise the stability of the crane.

To isolate the influence of slewing motion on the payload swing, the crane is considered to be stationary, except for the boom which slews about the vertical axis with a constant rotational velocity.

In previous research, a pure rotational motion of a tower crane was investigated

[13]. Because the boom slewing motion in the condition described above exhibits analogous dynamics to that of the tower crane, a similar analysis approach is taken to study the dynamics of the crawler crane. An experiment was performed using a tower crane to verify the calculation tool.

3.4.1 Mathematical Model and Payload Swing Dynamics

Figure 53 shows the front, side and top views of the crawler crane experiencing slewing motion. The boom rotates at a constant velocity of ω . This type of motion induces payload swings in two directions; radial (expressed by θ_1) and tangential (expressed by θ_2).

The motion also induces a centrifugal force that acts on the payload, at its center of mass, denoted by F_c . This force points along the horizontal projection of the boom, in other words, its direction is perpendicular to the direction of motion, and always pointing towards the slewing axis of rotation. This means that the direction of this force changes continuously as the boom rotates.

The magnitude of the centrifugal force on a body of mass m moving at a tangential speed v along a path with a radius of curvature R is expressed by:

$$F_c = ma_c = m\frac{v^2}{R} \quad (3.19)$$

where a_c is the centripetal acceleration.

In terms of the angular velocity ω , (3.19) becomes:

$$F_c = mR\omega^2 \quad (3.20)$$

It is noted in (3.20) that the expression for the centrifugal force contains the square of the rotational velocity, which in the case of the crawler crane is a very small value, thus the centrifugal force acting on the payload is considered small and can be ignored for the purpose of this investigation.

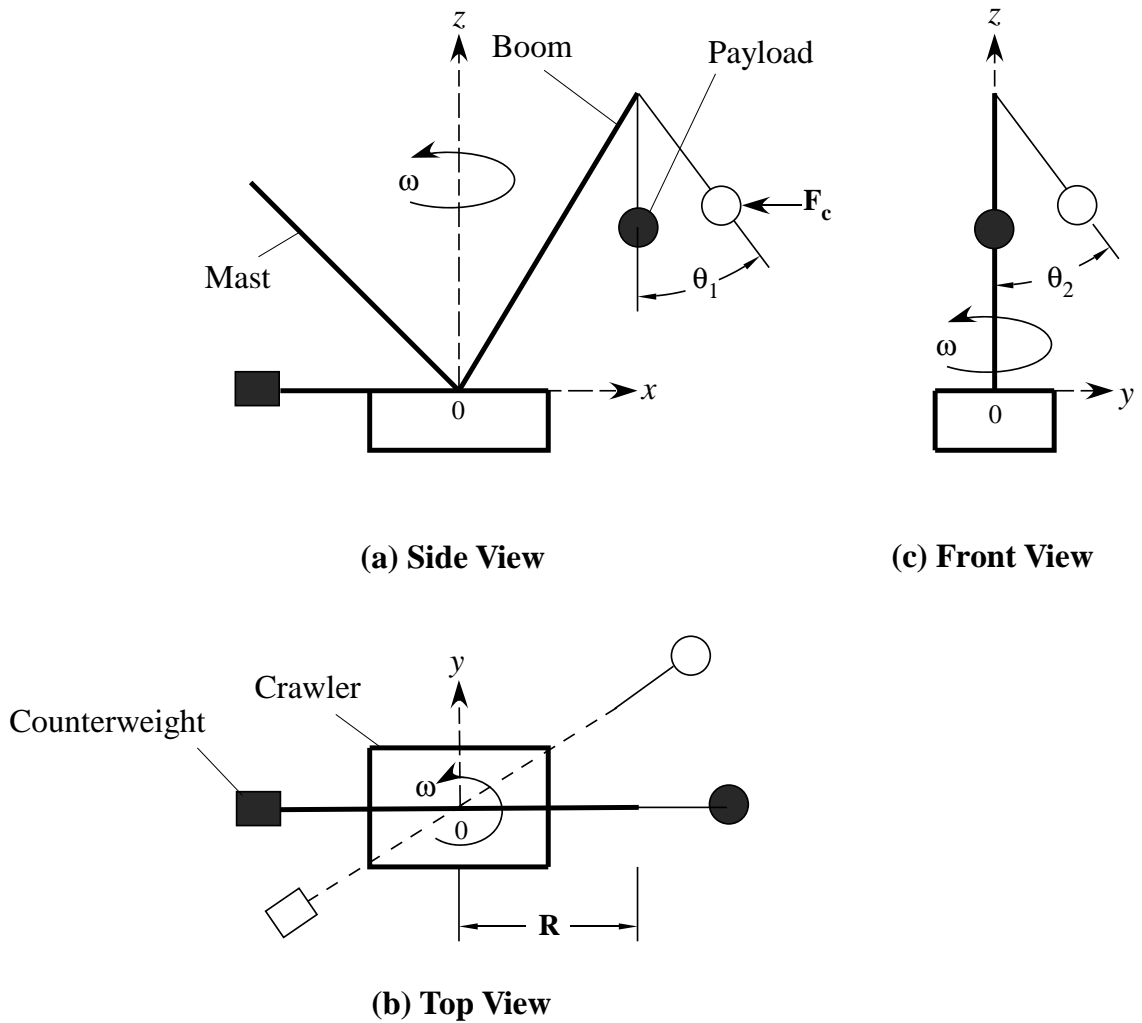


Figure 53: Dynamics in Boom Slewing Motion.

To establish a conservative tip-over prediction that approximates the worst-case scenario, the maximum residual swinging angles of the payload in both directions mentioned earlier is taken into consideration.

The goal now is to establish a mathematical model of the system to calculate these swinging angles, and use them to find the required minimum counterweight position that prevents forward tip-over.

The payload swing angles are computed using the equations of motion derived in

[13]. Assuming a point mass payload and ignoring the payload twisting about the suspension cable, the full dynamic equations of motion describing the swing angles are:

$$\begin{aligned}
L_5\ddot{\theta}_1 + L_5\dot{\theta}_2^2 \cos \theta_1 \sin \theta_1 + g \sin \theta_1 \cos \theta_2 &= -\ddot{R} \cos \theta_1 + R\dot{s}^2 \cos \theta_1 \\
- R\ddot{s} \sin \theta_1 \sin \theta_2 - 2\dot{R}\dot{s} \sin \theta_1 \sin \theta_2 - 2L_5\dot{s}\dot{\theta}_2 \cos^2 \theta_1 \cos \theta_2 \\
- L_5\ddot{s} \sin \theta_2 + L_5\dot{s}^2 \sin \theta_1 \cos^2 \theta_2 \cos \theta_1 & \quad (3.21)
\end{aligned}$$

$$\begin{aligned}
L_5\ddot{\theta}_2 \cos \theta_1 - 2L_5\dot{\theta}_1\dot{\theta}_2 \sin \theta_1 + g \sin \theta_2 &= R\ddot{s} \cos \theta_2 + 2\dot{R}\dot{s} \cos \theta_2 \\
+ 2L_5\dot{s}\dot{\theta}_1 \cos \theta_1 \cos \theta_2 + L_5\ddot{s} \sin \theta_1 \cos \theta_2 + L_5\dot{s}^2 \sin \theta_2 \cos \theta_1 \cos \theta_2 & \quad (3.22)
\end{aligned}$$

where L_5 is the suspension cable length, s is the radial displacement, \dot{s} is the rotational velocity previously denoted by ω , \ddot{s} is the rotational acceleration, and R is the horizontal distance between the boom tip and slewing axis. The angles θ_1 and θ_2 describe the payload swing in the radial and tangential directions with respect to the boom's orientation, respectively.

In a pure slewing rotation motion, the boom configuration remains fixed, which implies that $\dot{R} = \ddot{R} = 0$. Equations(3.21) and (3.22) were not linearized, because experimentation showed that the swing angle is not always small enough to make the linearization assumption valid. The following state variables were defined:

$$\begin{aligned}
x_1 &= \theta_1 \\
x_2 &= \dot{\theta}_1 \\
x_3 &= \theta_2 \\
x_4 &= \dot{\theta}_2 \\
x_5 &= s \\
x_6 &= \dot{s}
\end{aligned} \tag{3.23}$$

The command used as an input to this system is the rotational slewing acceleration:

$$u = \ddot{s} \quad (3.24)$$

Based on (3.23) and (3.24), the dynamic system can be described by the following equations:

$$\begin{aligned}
\dot{x}_1 &= \dot{\theta}_1 = x_2 \\
\dot{x}_2 &= \ddot{\theta}_1 = \frac{R}{L_5} x_6^2 \cos x_1 + \frac{R}{L_5} u \sin x_1 \sin x_3 - 2x_6 x_4 \cos^2 x_1 \cos x_3 - u \sin x_3 \\
&\quad + x_6^2 \sin x_1 \cos^2 x_3 \cos x_1 - \frac{g}{L_5} \sin x_1 \cos x_3 - x_4^2 \cos x_1 \sin x_1 \\
\dot{x}_3 &= \dot{\theta}_2 = x_4 \\
\dot{x}_4 &= \ddot{\theta}_2 = \frac{R}{L_5} u \frac{\cos x_3}{\cos x_1} + 2x_6 x_2 \cos x_1 \cos x_3 + u \cos x_3 \frac{\sin x_1}{\cos x_1} \\
&\quad + x_6^2 \sin x_3 \cos x_1 \cos x_3 + 2x_2 x_4 \frac{\sin x_1}{\cos x_1} - \frac{g}{L_5} \frac{\sin x_3}{\cos x_1} \\
\dot{x}_5 &= \dot{s} = x_6 \\
\dot{x}_6 &= \ddot{s} = u
\end{aligned} \quad (3.25)$$

The time-optimal command with a limited velocity and acceleration again is a bang-coast-bang command, similar to the one described in Sections 3.2.1 and 3.3.1. Here, it will be used to slew the boom in a point-to-point motion about the axis of rotation by using it as an input command to the system of state equations described in (3.25).

Applying a suitable acceleration command, and solving the system of state equations, the residual vibrations of the payload can be predicted, and thus the maximum payload swinging angle, whether radially or tangentially, can be calculated and then used to find the minimum counterweight position that prevents forward tip-over.

3.4.2 Experimental Verification - Tower Crane

Before using the mathematical model derived in the previous section to calculate counterweight position, it was experimentally verified. As mentioned before, the



Figure 54: Tower Crane used in Experiments.

dynamics of the crawler crane in slewing motion are analogous to those of a tower crane. Therefore, an experiment was performed on the tower crane shown in Figure 54.

For a given slewing radius and hoist length, if the crane is actuated by a bang-coast-bang command that has a constant maximum acceleration, and if the slewing velocity has a maximum constant value as well, then the only parameter affecting the swinging angles of the payload is the rotational distance traveled.

The tower crane was driven using a bang-coast-bang command with a varying t_{gap} . For each trial, t_{gap} was chosen such that the crane slewed through angles ranging from 3° to 90° . For each slew distance, the payload swing was recorded in both the radial and tangential directions. Examples of radial and tangential swing are shown in Figures 55 and 56. For each distance, the maximum residual swing angles in the

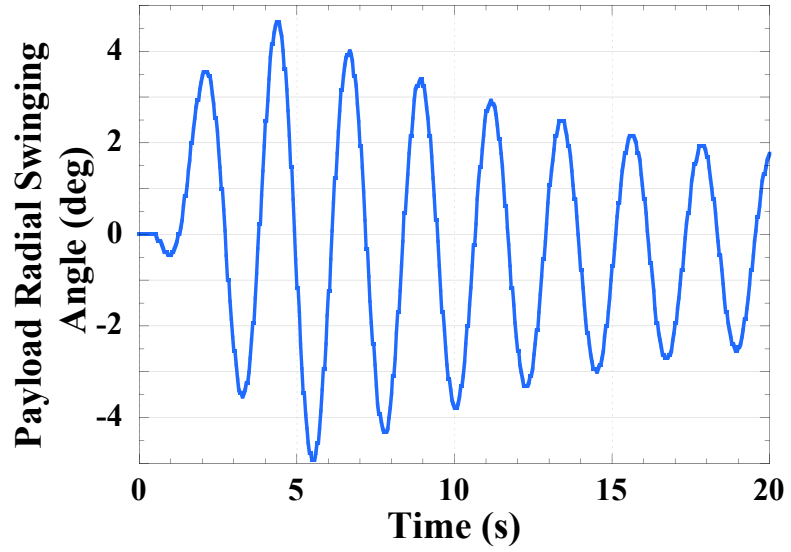


Figure 55: Radial Swing of the Payload when the Tower Crane was Slewed a Distance of 75° .

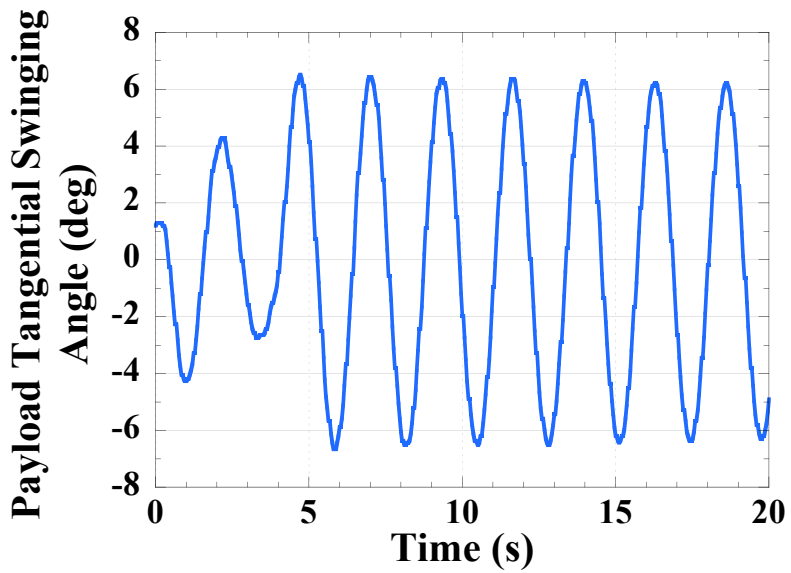


Figure 56: Tangential Swing of the Payload when the Tower Crane was Slewed a Distance of 75° .

Table 6: Parameters of the Tower Crane.

Parameter	Item	Numerical Data
L_5	Hoist Length	0.9 <i>m</i>
R	Slewing Radius	0.908 <i>m</i>
m_h	Mass of the Hook	0.210 <i>kg</i>
m_p	Mass of the Payload	0.500 <i>kg</i>
ω_{max}	Maximum Slewing Velocity	20°/ <i>s</i>
α_{max}	Maximum Slewing Acceleration	27.6°/ <i>s</i> ²
t	Time to Reach Maximum Slewing Velocity	0.728 <i>s</i>

radial and tangential directions were recorded. This set of experiments was repeated four times, and the average of the maximum swinging angles was taken for each corresponding moving distance.

Table 6 displays the numerical data corresponding to the tower crane parameters used in the experiments. These parameters were used in the mathematical model previously derived and a simulation was carried out to calculate the maximum residual swing angles in the radial and tangential directions, so that the simulation results can be compared with the experimental ones. The results are shown in Figures 57 and 58. In both figures, experimental and simulation results follow a similar trend. However, there is an obvious lag in the experimental result as the move distance increases.

Several reasons may have led to this discrepancy, such as nonlinearities that are not taken into account in the mathematical model. Also, the acceleration value used in the simulation was the average of the acceleration values measured in the experiments, thus it is slightly different from the actual values. Another reason is that when the payload travels a longer distance, more disturbances occur during the longer move. Some errors may be due to inaccuracies related to the payload sensor (camera). Moreover, the hook displays some high frequency oscillations that are not taken into consideration in simulation. Finally, the simulation ignores damping, which

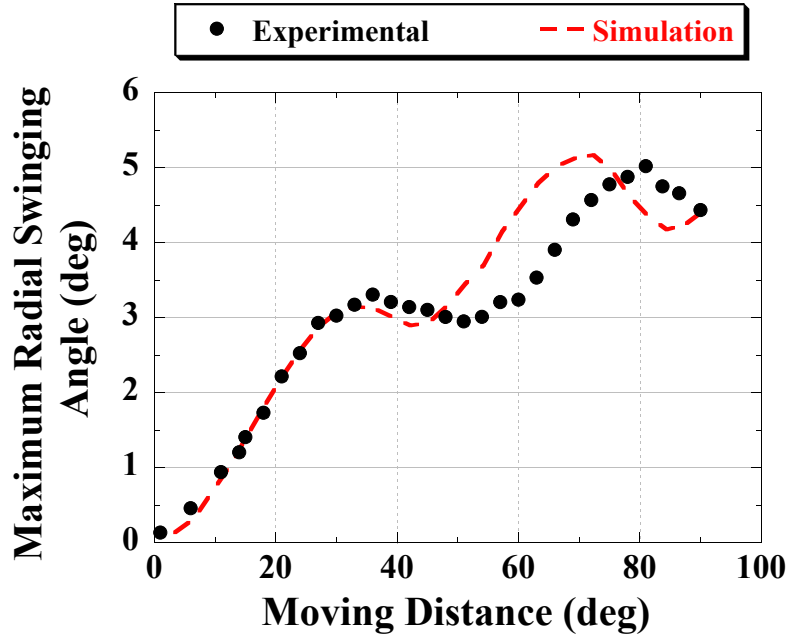


Figure 57: Maximum Radial Swinging Angle of the Payload vs. Slewing Distance (Experimental and Simulation Results).

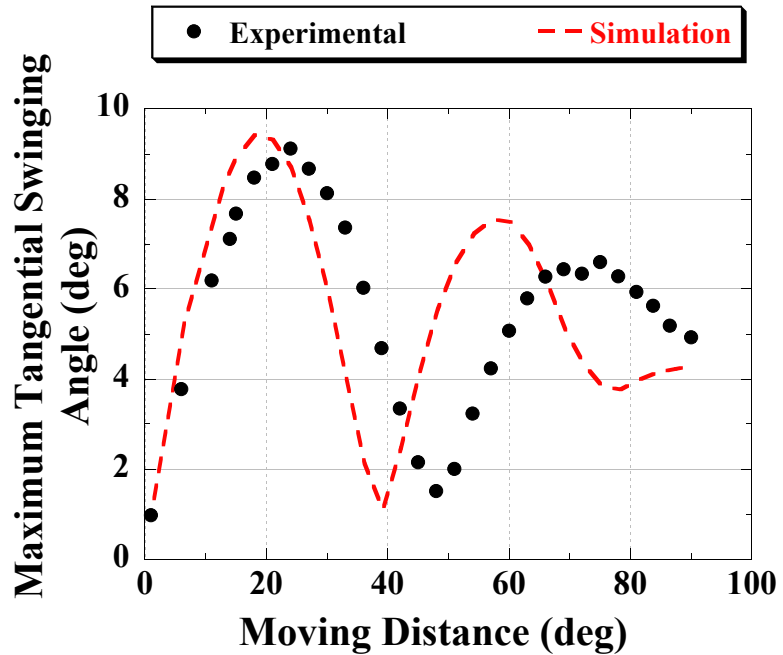


Figure 58: Maximum Tangential Swinging Angle of the Payload vs. Slewing Distance (Experimental and Simulation Results).

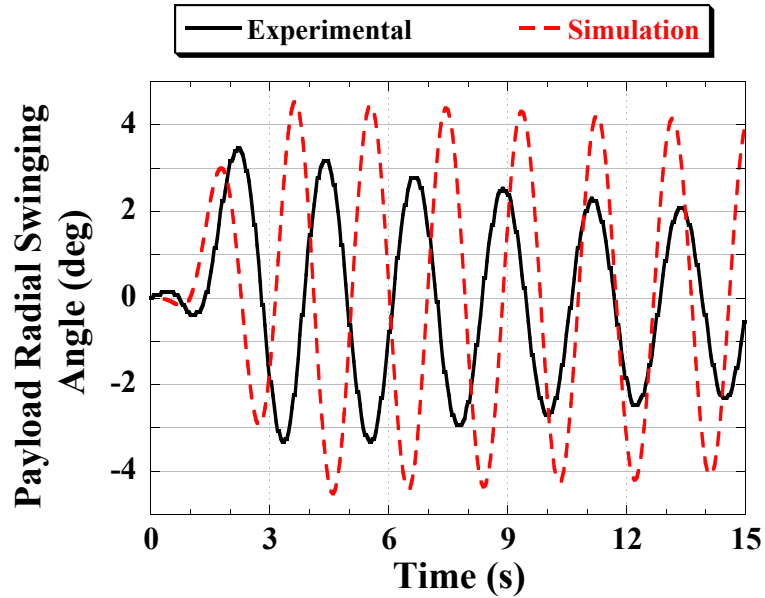


Figure 59: Experimental and Simulated Radial Swinging Angle of the Payload for a Moving Distance of 60° .

is present in the experiment due to air resistance and the hook oscillations mentioned before.

Figure 59 and Figure 60 compare between the experimental and simulated payload radial and tangential swinging angles respectively, for a moving distance of 60° . Figure 59 shows that the experimental payload swinging is slower than the simulation, which is expected due to damping and inertial factors that are not included in simulation. These factors prevent the payload from reaching the expected swing amplitude, which explains the results displayed in Figure 57.

Similarly, Figure 60 displays similar effects in the tangential swing, in addition to an initial value of the swing angle, which is considered zero in the simulation.

Based on the discussion above, the experimental results align reasonably well with the simulation predictions. This indicates that the mathematical model can be used to predict the payload's maximum swing angles (θ_1 and θ_2) under various conditions.

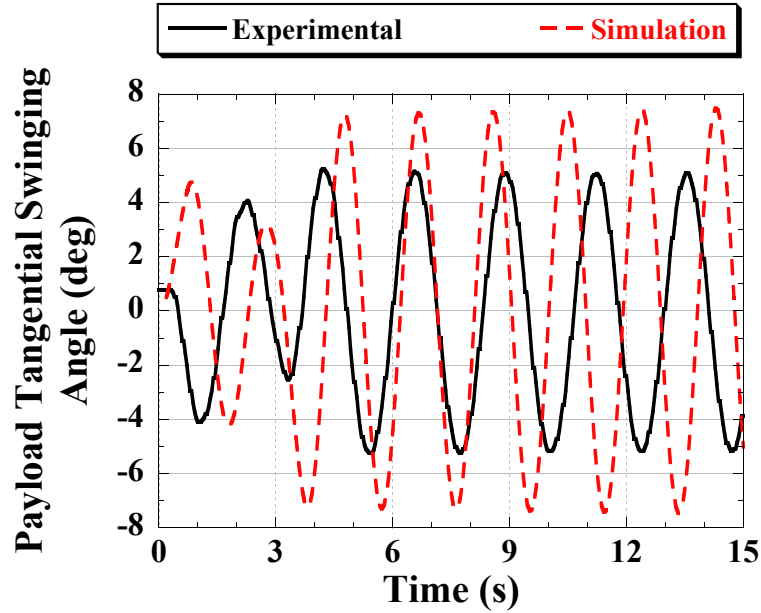


Figure 60: Experimental and Simulated Tangential Swinging Angle of the Payload for a Moving Distance of 60° .

Thus, it will be used to calculate the position of the movable counterweight necessary to avoid tip over in the case of boom slewing motion.

3.4.3 Tip-over Stability Analysis of Boom Slewing

The mathematical model is used to calculate the radial and tangential maximum residual swing angles of the payload carried by the crawler crane whose parameters were listed in Table 2. However, because slewing motion is critical, and it is capable of inducing large swinging angles, especially in the tangential direction, the hoist length will be extended to 70 m , and the boom luffing angle will be increased to 70° . Increasing the boom luffing angle to 70° allows the use of a payload with a mass of 156 t . Based on the data sheet, the maximum slewing velocity of the Terex CC 2800-1 is 0.7 rpm . To approach the worst-case scenario, it is assumed that the crane accelerates to full slewing speed in 1 s .

The maximum residual payload swing angles were calculated with respect to various move distances. The procedure to calculate the minimum position of the movable counterweight to counterbalance the effect of swinging and prevent tip-over is:

1. For each moving distance the location of the payload resulting from the maximum residual and tangential swinging angles is determined.
2. It is assumed that the hoist cable is a rigid body, and the payload is fixed at that location.
3. The sum of moments is calculated about the corresponding tip-over axis depending on the displacement of the payload. Knowing that the slewing of the boom is within the range of 0° to 90° , the potential tip-over axes are the front and side.
4. The calculated sum of moments is used to determine the minimum counterweight position in each case.
5. The minimum counterweight position values are plotted with respect to the moving distances, and the furthest position obtained will be the recommended position to prevent forward tip-over regardless of the move distance for the given configuration.

Figure 61 shows the maximum residual swing angles in both the radial and tangential directions with respect to the move distance. These values are used to determine the location of the payload at each slewing distance.

For each slewing distance the location of the payload was calculated based on maximum swinging angles. Then, the minimum location of the movable counterweight to prevent tip-over about the front axis was calculated. Results are shown in Figure 62. The figure displays minimum counterweight positions for three different masses of the movable counterweight. It should be noted that if the position of the counterweight

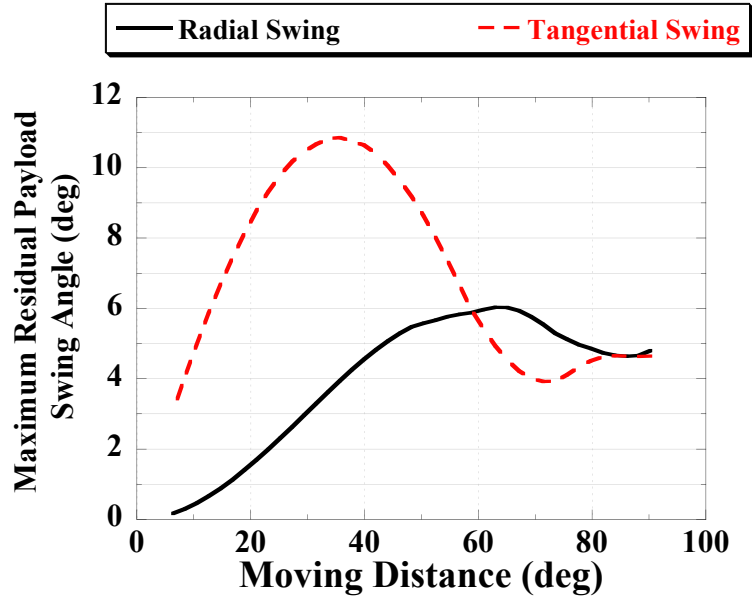


Figure 61: Maximum Swinging Angles of the Payload vs. Slewing Distance.

in the graph is shown as zero, then for that specific slew distance, there is no hazard of tipping over about the front axis. For example, if the boom is slewed for a distance that is larger than 60^0 , there is no longer a potential for the crane to tip-over in the forward direction.

Figure 62 also shows that for a heavier counterweight mass, the minimum counterweight position is less, which is consistent with all the results obtained in this research.

Similarly, Figure 63 illustrates the minimum counterweight position necessary to prevent tipping over to the side. Following the previous discussion, the figure shows that the risk of tipping over sideways begins for slewing distances of more than about 50^0 . Also, the position of the counterweight has a maximum value at a slewing distance of 90^0 , which agrees with the previous results obtained in the static analysis. These results confirm that this location is very dangerous in terms of tip-over stability. Here also, the larger the counterweight, the smaller the distance it needs to be moved

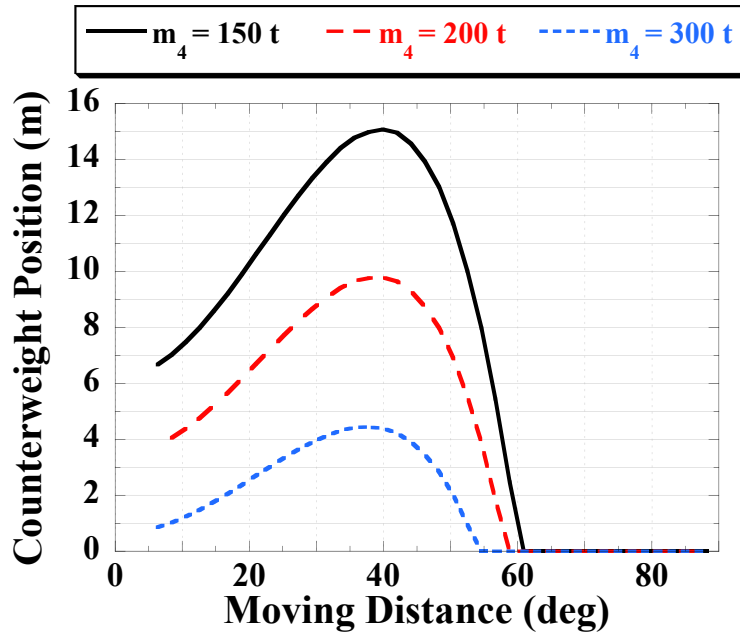


Figure 62: Minimum Counterweight Position to Prevent Forward Tip-over for Different Slewing Distances.

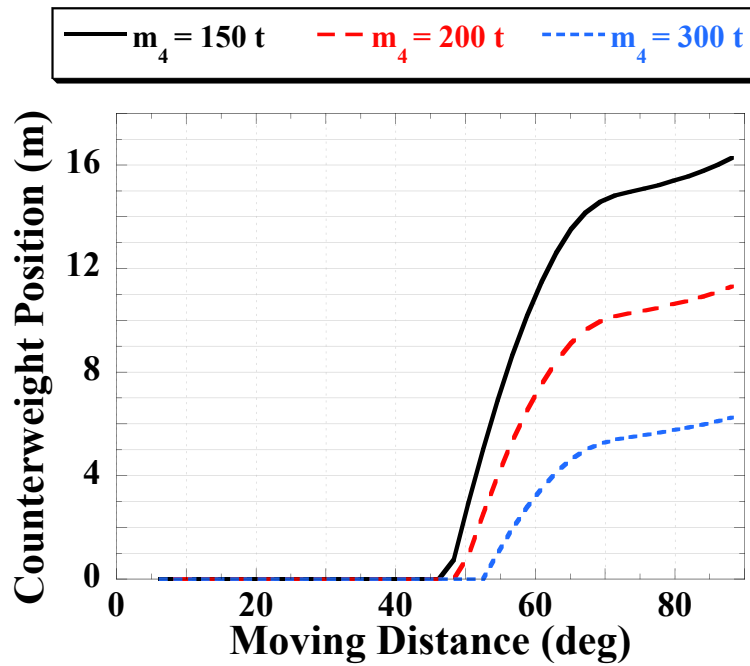


Figure 63: Minimum Counterweight Position to Prevent Sideways Tip-over for Different Slewing Distances.

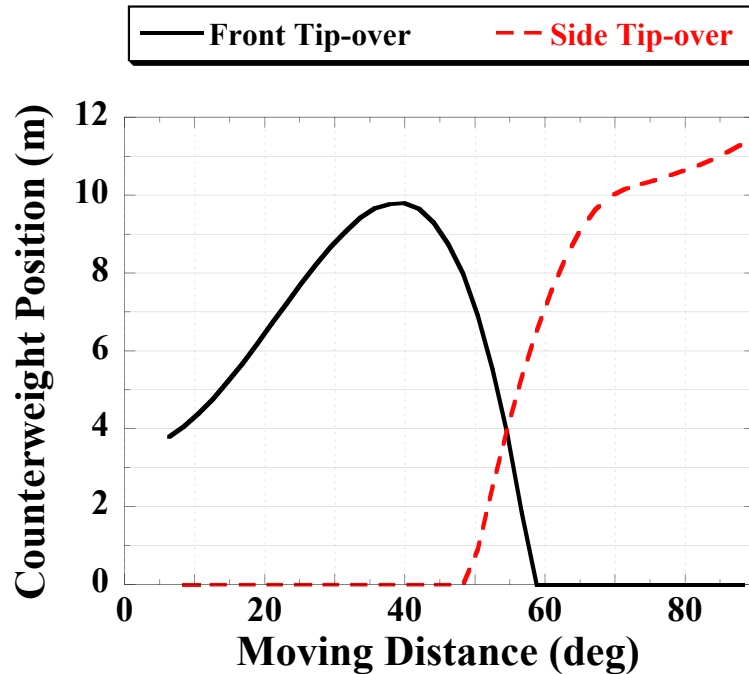


Figure 64: Minimum Counterweight Position to Prevent Front and Sideways Tip-over for Different Slewing Distances for a Counterweight Mass of 200 *t*.

backwards to avoid tipping over.

For a given counterweight mass of 200 *t*, the minimum counterweight position that prevents tipping over in each direction is plotted in Figure 64 with respect to slewing distances. This graph shows that for a slewing distance of 48.3° or less, the crane is likely to tip-over in the front direction, and the minimum counterweight positions to prevent that are displayed by the black solid line in Figure 64. On the other hand, for a slewing distance of 58.8° or more, the crane is in danger of tipping over sideways only, and the minimum counterweight positions to prevent that are displayed by the red dashed line in Figure 64.

This leaves an interval of slewing distances (48.3° - 58.8°), in which the crane can tip over in both directions. Thus, in this interval, the larger of the two counterweight position values that prevent tipping over in either direction should be used.

In general, the global maximum occurs at a slewing distance of 90° as mentioned before. Thus, it is recommended that the counterweight is kept at the minimum position corresponding to that point to ensure a safe operation regardless of the slewing distance. However, if the crane is expected to slew within a smaller range, then the local maximum of that specific interval can be used. Other solutions can be the use of shaped acceleration commands that minimize the oscillations, and therefore the counterweight does not need to be moved as far.

3.5 Summary

Once a crane starts to move, its stability is degraded by additional forces. This chapter discussed various motion scenarios, and studied their effects independently. In each section, the minimum counterweight position to prevent tip-over is calculated and compared to the static case. Due to the fact that any type of motion induces payload swing, the counterweight needs to be moved further backwards than the static case. Future work could expand the scope of these motions, discuss more special and extreme cases, and even examine different types of motions.

CHAPTER IV

EXPERIMENTAL VERIFICATION

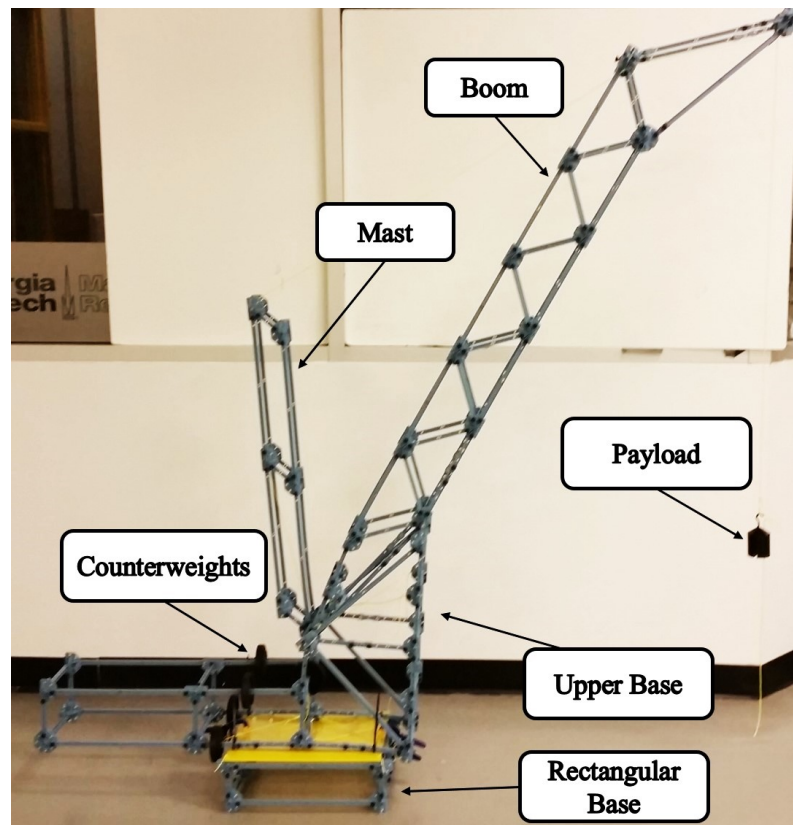


Figure 65: Experimental Scale Crane Model.

The purpose of this chapter is to provide support and verification for some of the key results obtained in Chapters 2 and 3. A small-scale crane model was built and used to achieve these experimental results.

4.1 Introduction

The experimental setup shown in Figure 65 was constructed using the ME-7003 large structure set. This set is one part of the PASCO Structures System [26]. It can be used to build a variety of realistic truss structures. The ME-7003 set has various components that can be used to create different models, such as roller coasters, bridges, tower cranes, skyscrapers, house frames, angle cranes, windmills. The manual provided with this set presented a crane model. This model was modified to suit our application.

4.2 Components

This section lists the components used to create the crane model.

4.2.1 Truss Set Members (ME-6993)

The truss set members consist of five types of I-beams and a half round connector, as shown in Figure 66. The beam lengths are listed in Table 7. Figure 66 also shows the truss set screw, which is a thumbscrew used for attaching I-beams to connectors and other components.

Table 7: Truss Members Set [26].

Member	Length (cm)
#1 Beam	5.5
#2 Beam	8
#3 Beam	11.5
#4 Beam	17
#5 Beam	24

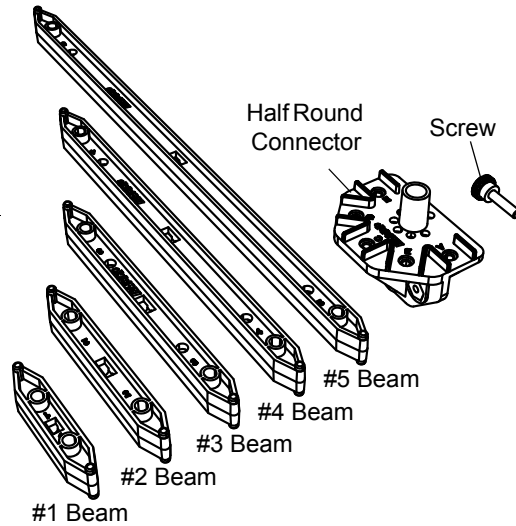


Figure 66: Truss Set Members (ME-6993) [26].

It should be noted that when connected at 180° to form a straight line, two short beams have a combined length equal to one longer beam. For example, two #1 beams connected at 180° to a half round connector have the length of a #3 beam, while two #2 beams create a #4 beam, and two #3 beams have the length of a #5 beam.

4.2.2 #6 I-Beam Spares (ME-7008)

#6 I-beams are similar to the ones in the truss set members, but they have a length of 35 *cm*. Thus they can be used when more length is required.

4.2.3 Flat Structures Members (ME-6987)

This set contains the three types of flat structures shown in Figure 67. These members are: flat 3X4 beams (19 *cm*), flat 2X3 beams (12.5 *cm*), and flat #4 beams which are all used to support structures created by the regular beams. The right side of Figure 67 shows an example of a rectangular structure created by #3 and #4 beams, that are connected at the corners using half round connectors. This rectangular structure is supported by two 3X4 flat beams connecting opposite corners.

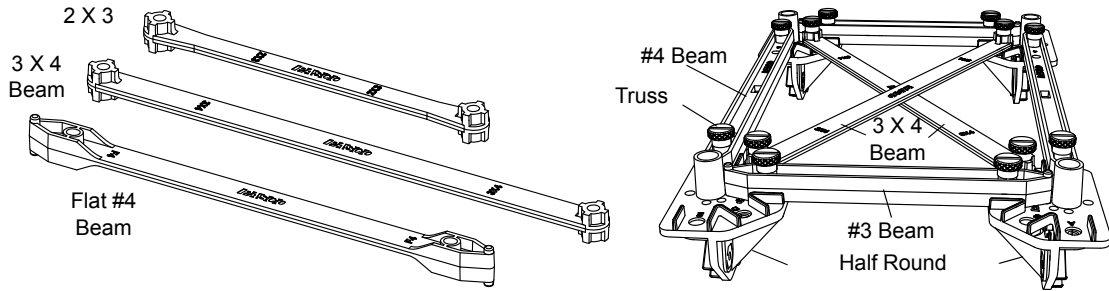


Figure 67: Flat Structures Members (ME-6987) [26].

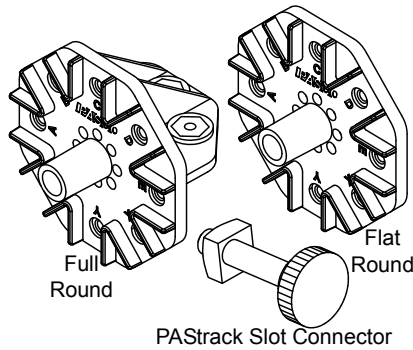


Figure 68: Full Round Connectors Spares (ME-6997) [26].

4.2.4 Full Round Connectors Spares (ME-6997)

Full round connectors have eleven slots for attaching beams, as shown in Figure 68. Eight of these slots are located around the perimeter of the circle, while three are used for connections in a direction perpendicular to that of the circle. Flat round connectors are similar to the full round connectors; however, they only have the eight slots around the perimeter of the circle.

Finally, the PAStack slot connector is a nut and bolt that allows a PAStack to be connected to a structures model. It is shown at the bottom of Figure 68.

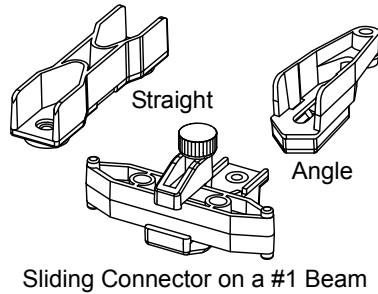


Figure 69: Angle Connectors (ME-6999A) [26].

4.2.5 Angle Connectors (ME-6999A)

Angle connectors include the three types of connectors shown in Figure 69. Straight connectors can connect two beams to make a longer beam. Angle Connectors allow a beam to be connected to a half round connector, full round connector, or flat round connector at an angle other than 0° , 45° , or 90° . They also allow for a small adjustment in the length of the beam. Finally, the sliding connector allows one beam to be connected to another beam at any position along the length of the second beam.

4.2.6 Axle Spares (ME-6998A)

This set consists of steel axles of three different lengths, in addition to pulleys, O-rings, drive wheels, tires, collets, and spacers. Figure 70 shows these components.

4.2.7 Cord Lock Spares (ME-6996)

This set includes cord tensioning clips and a roll of yellow braided cord. When attaching cords for lateral bracing or suspension, cord clips are used to assist in adjusting the tension in the cords. This is illustrated in Figure 71.

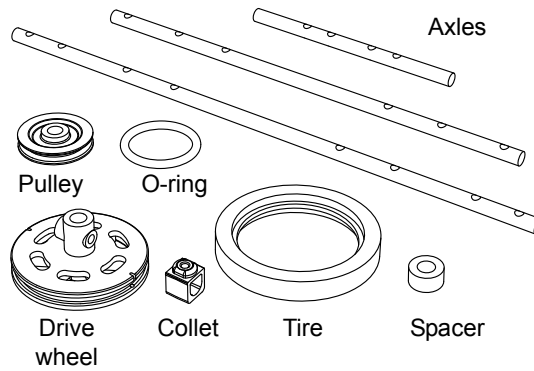


Figure 70: Axle Spares (ME-6998A) [26].

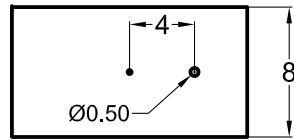


Figure 71: Cord Lock Spares (ME-6996) [26].

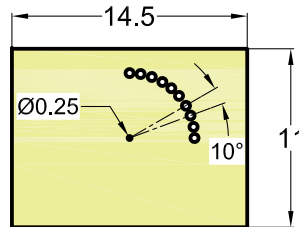
4.3 Crane Model Specifications

The components described in the previous section were used to construct the small-scale experimental crane model that was shown in Figure 65. The design of this model was done in stages. First of all, a small base was created to support the boom and mast. This small base was also connected to an extension on which the movable counterweights are positioned. This whole setup was mounted on top of a rectangular base. This allows the crane upper works to slew around the axis located in the middle of the rectangle.

To facilitate the slewing motion of the upper works on the rectangular lower works,



Transparent, connected to the bottom of the upper base.



Yellow, connected to the top of the rectangular base.

Figure 72: Acrylic Plates Specifications (Units are in inches).

two acrylic rectangular plates were connected to the bottom of the upper base and the top of the rectangular base, respectively. Figure 72 shows a schematic diagram of these two plates. A screw was fastened in the holes located in the middle of each of the plates, to make sure that the crane slewing axis remains fixed, and that the slewing axis is not shifted as the upper works slew on top of the rectangular lower works.

The acrylic plate connected to the rectangular base has ten holes located on the perimeter of a quarter circle with a radius of 4 *in*. The angle between the two lines connecting the center of the rectangle to the centers of two consecutive holes is 10°. Therefore, keeping the two middle holes secured by means of a screw, when the other hole in the transparent rectangular plate attached to the bottom of the upper base matches any of the ten holes in the other yellow plate, this places the upper part of the crane at a specific slewing angle between 0° and 90°. This is illustrated in Figure 73.

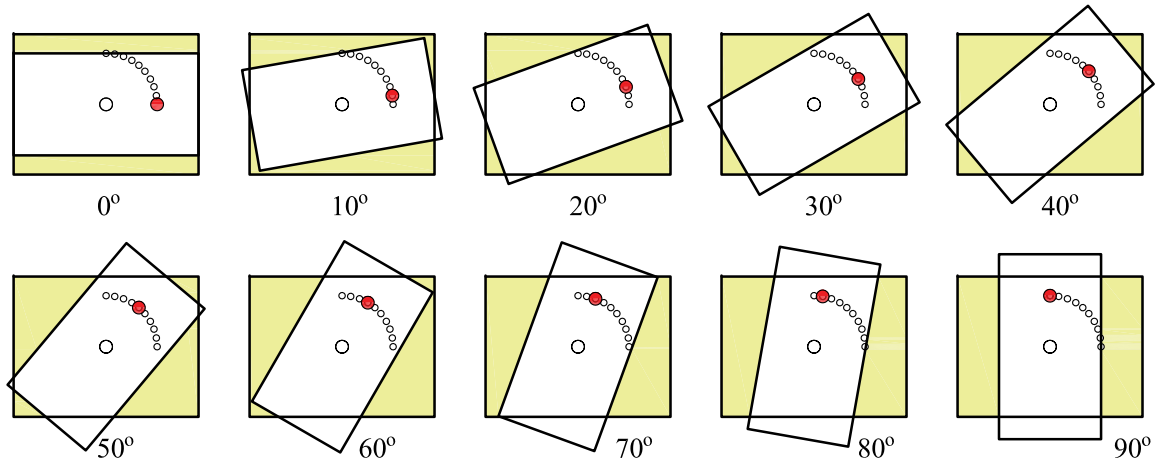


Figure 73: Slewing Mechanism in the Experiment.

The crane's physical parameters are listed in Table 8.

Table 8: Parameters of the Experimental Crane Model.

Parameter	Item	Numerical Data
w	Width of base	24 <i>cm</i>
h	Height of base	8 <i>cm</i>
L_1	Length of base	35 <i>cm</i>
L_2	Length of boom	178 <i>cm</i>
L_3	Length of mast	76 <i>cm</i>
L_{4F}	Length of fixed counterweight	23 <i>cm</i>
L_5	Length of hoist	115 <i>cm</i>
m_1	Mass of rectangular base	2.33 <i>kg</i>
m_2	Mass of boom and upper base	2.55 <i>kg</i>
m_3	Mass of mast	0.51 <i>kg</i>
m_{4F}	Mass of fixed counterweight	2 <i>kg</i>
m_5	Mass of payload	1 <i>kg</i>

4.4 Experimental Procedure

Two experiments were performed using the described setup.

4.4.1 Effect of Crawler Crane Slew Angle on Minimum Counterweight Position Required to Prevent Forward Tip-over

The objective of this experiment is to experimentally construct the graph shown in Figure 19. This serves to verify that the calculation tool used to determine the suitable position of the movable counterweight that prevents tip over gives reasonable results. The same crane configuration was used with two different counterweight masses: 1 *kg* and 1.1 *kg*.

First, the slewing angle was set to 0° , as illustrated in the upper left corner of Figure 73. The payload of 1 *kg* was attached to the hoist cable. The fixed counterweights (1.5 *kg*) were set in place and the movable counterweights (1 *kg*) were pushed to the furthest backward position possible. This position definitely guarantees stability, but our goal is to find the minimum counterweight position that prevents forward tip over. Thus, the procedure followed was to slide the movable counterweights towards the center of the crane gradually, until the crane was on the verge of tipping over. At this location, the counterweight position was measured and recorded.

Then, a payload of 100 *g* was added to the original payload and the same procedure was repeated to find the minimum counterweight position to prevent tip over. Once the required readings were obtained, the slewing angle was changed to 10° and so on, until the slewing angle became 90° . Figure 74 and Figure 75 show the crane with a slewing angle of 30° and 90° , respectively.

In the calculations performed in Chapter 2, the slewing angle was varied between 0° and 360° . Due to the advantage of symmetry in the crane model, it was enough to record measurements from 0° to 90° and then using that to predict the rest of the graph for a full 360° revolution, taking into consideration that the slewing axis is located in the middle of the rectangular base and passes through the bottom end of

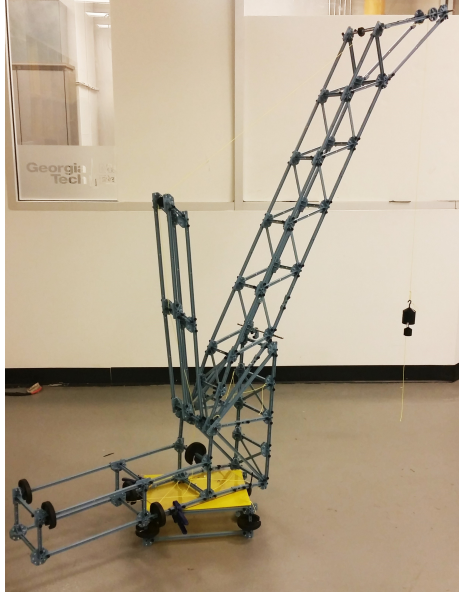


Figure 74: Experimental Crane Setup - Slew Angle is 30° .

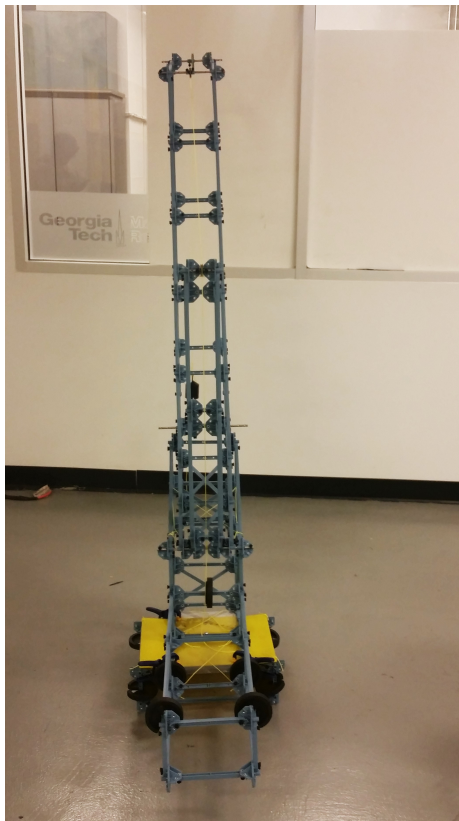


Figure 75: Experimental Crane Setup - Slew Angle is 90° .

the boom all the time.

4.4.2 Effect of Payload Swing

In Chapter 3, the payload swing induced by three different motions of the crane was investigated. The larger the payload swing, the further the counterweight needed to be moved backwards to prevent forward tip-over. The objective of this experiment is to verify this relationship.

First, the slew angle was fixed at 0° , and the counterweight was pushed backwards to the furthest position away from the slewing axis. On the experimental setup, this distance is 23 *in*. The boom luffing angle was fixed at 66° and the payload mass was set to 1 *kg*. The payload was pulled inward toward the slewing axis to create an initial swing angle of 1° . It was then released and left to swing freely. The crane was observed. Then, the initial payload swing angle was increased gradually, each time by 1° , until the swing angle that caused the crane to buck forward and almost tip-over was reached. This swing angle value was recorded.

This procedure was repeated, and each time the counterweight was moved inward 1 *in* towards the slewing axis. The corresponding payload swing angles that caused the crane to almost tip-over were recorded for each position of the counterweight.

4.5 Results

4.5.1 Effect of Crawler Crane Slew Angle on Minimum Counterweight Position Required to Prevent Forward Tip-over

Figure 76 shows the minimum counterweight position required to prevent forward tip-over of the small-scale crane model for a range of slewing angles. The payload mass was set to 1 *kg*, and the movable counterweight mass was also set to 1 *kg*. The boom angle was fixed at 66° .

It is obvious that the experimental data follows the same general trends as those predicted in Chapter 2 for the full-scale Terex crane. The graph emulates the previous

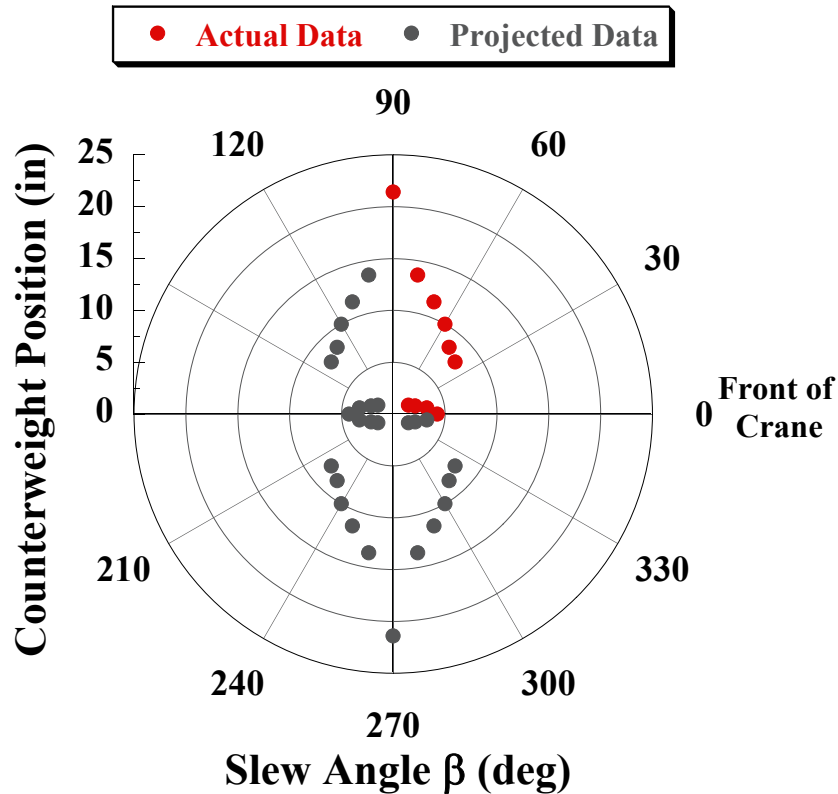


Figure 76: Minimum Counterweight Position to Prevent Forward Tip-over [Boom Luffing Angle of 66° , Payload Mass of 1 kg , and Counterweight Mass of 1 kg].

results by showing that the crane is most stable when the boom is pointing to the corner of the crane base of support, while it is least stable when the boom is pointing towards the side.

The large jump in the counterweight position values as the slewing angle is changed from 30° to 40° can be explained using Figure 73. The figure shows that, there are areas of the upper base that are not directly supported by the lower base. These areas get larger with increasing slewing angle, requiring the counterweight to be moved further back. The large unsupported areas induced bending of the upper works. This structural deflection affected the results obtained. This also explains the very large value of the counterweight position when the slew angle was 90° . Therefore, the

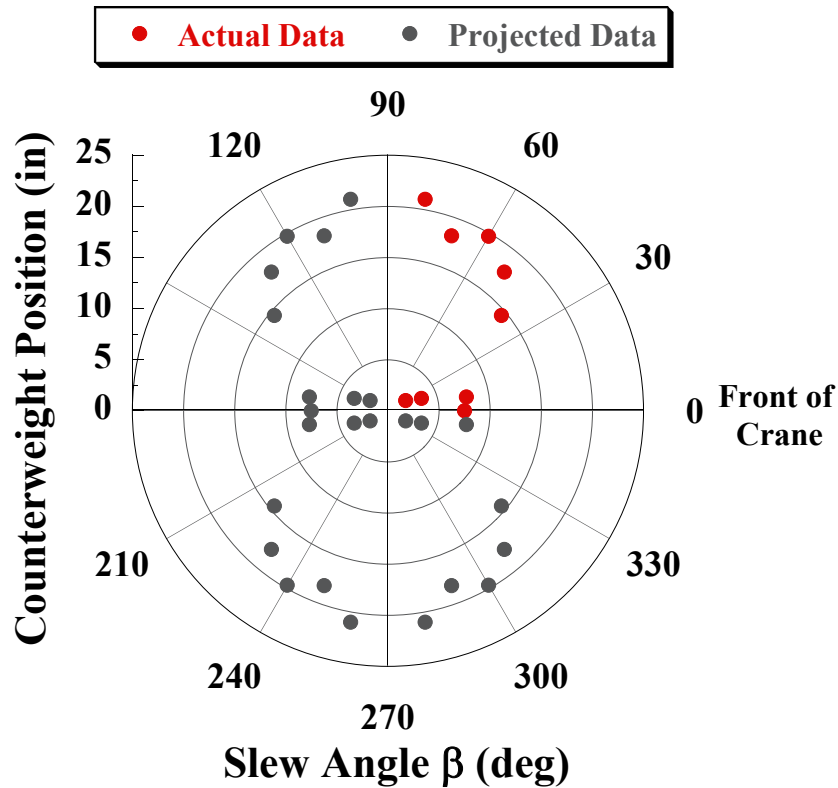


Figure 77: Minimum Counterweight Position to Prevent Forward Tip-over [Boom Angle of 66° , Payload Mass of 1.1 kg , and Counterweight Mass of 1 kg].

experimental results for slew angles beyond 30° are larger than would be predicted by theory, the reason is that theory assumes a fairly rigid upper work structure.

Figure 77 shows the minimum counterweight position to prevent forward tip-over when the payload mass was increased 10% to 1.1 kg . The first observation is that the counterweight needs to be moved further backwards when the payload mass increases, a result clearly documented in Chapter 2. The graph displays similar characteristics as the graph in Figure 76. However, when the slew angle was set to 90° , the maximum possible counterweight position in the experimental setup was not enough to counterbalance the moment creating forward tip-over. Thus, the crane could not be stabilized by the counterweight when the boom was directed 90° to the

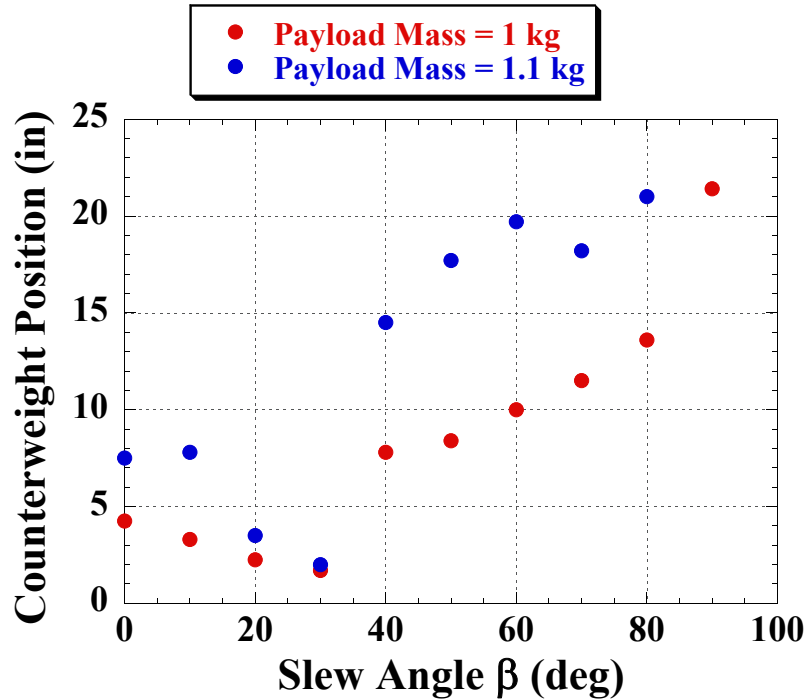


Figure 78: Minimum Counterweight Position to Prevent Forward Tip-over for Both Payload Masses.

side.

To understand the effect of increasing the payload mass on the minimum counterweight position to prevent forward tip-over, the results for both the 1 and 1.1 kg payload masses were plotted on the same graph for slew angles between 0° and 90° . Figure 78 clearly shows that increasing the payload mass requires the counterweight to be moved further backwards.

4.5.2 Effect of Payload Swing

As expected, the closer the counterweight position is to the slewing axis, the smaller the payload swing angle that causes forward tip-over. This effect is shown in Figure 79. Another way to interpret the results in this graph is that for a certain counterweight position, the payload swing needs to be limited to a value less than that shown in

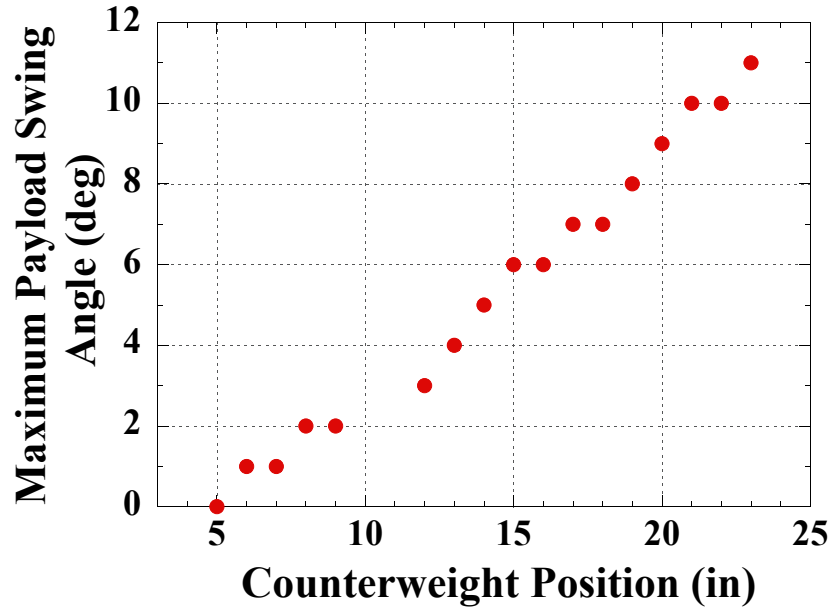


Figure 79: Maximum Payload Swing Angle to Prevent Forward Tip-over.

the graph. This can be accomplished by applying suitable acceleration profiles that do not induce significant swing, as discussed in Chapter 3. However, uncontrollable forces such as wind loads, can induce additional swing. Therefore, the counterweight needs to be moved backwards by a reasonable safety factor to avoid forward tip-over.

An important verification was provided by this experiment. Figure 79 indicates that for a counterweight position of 5 *in* any non-zero payload swing will cause a tip-over. Referring back to Figure 76, for a slew angle of 0° , the minimum counterweight position that prevents forward tip-over is almost 5 *in*. Recall that data was generated with a non-swinging payload. Once the payload starts to swing, the counterweight has to be moved further backwards. This agrees with the results obtained in Chapter 3, stating that the dynamic stability region is always smaller than the static stability region. It also shows that both the static and dynamic experiments converge to the same results as the swing angle approaches zero.

A gap near 10 *in* appears in the data shown in Figure 79. This gap occurs because

there is a half round connector at that position in the experimental setup. Therefore, the round slotted counterweights cannot be positioned in that location.

4.6 Limitations and Challenges

The components used to create the experimental crane model are not designed to perform in extreme loading conditions that create large bending forces on the components. Therefore, the experiment was limited to relatively light-weight payloads and counterweights. The effects of the structural limitations that prevented us from expanding the experiment to include all aspects discussed in Chapters 2 and 3 include:

1. The beams used in the structure have a degree of flexibility that caused them to bend excessively in certain locations, thus violating the concept of rigidity of the crane components.
2. The counterweight mass could not be changed significantly, since we were using 500 *g* on each side. Smaller adjustable weights were not available, and adding another two 500 *g* required the payload to be very large. This created a large tension force that the whole structure was not able to support without significant deflection.
3. The experimental boom luffing angle was created by letting the boom lie on the triangular part of the upper base. The effect of decreasing that angle was difficult to study, because decreasing the angle created a large bending in the boom, due to its weight and length which are supported only at one pivot point.
4. When the upper works were slewed, there were some angles at which the corners of the upper part were not fully supported, thus it caused the structure to bend.

These limitations of the experimental setup restricted the procedure and resulted in some skewing of the results. Nevertheless, the experiment was conclusive, and it

proved that our calculation tool is successful in predicting the counterweight position boundaries that prevent crawler crane tip over.

4.7 Summary

Experimentation is an important element of research, that can validate that the theory presented is representative of practical applications. In this chapter, an experiment helped verify the calculation tool presented earlier, and provided a deeper understanding of the concept of a movable counterweight. It also helped demonstrating the difference a counterweight imposes on the system when it moves relative to the crane body. And finally, it showed how sensitive the crane's stability is to slight changes in the counterweight position, which complies with our previous results that indicate that the counterweight position to prevent tip over is a complex function of the crane's parameters.

CHAPTER V

CRAWLER CRANES IN TANDEM LIFTING

5.1 Overview

Moving heavy and over-sized loads poses significant challenges. A single crawler crane may prove deficient for such lifting tasks if the payload exceeds the capacity, or the payload size and shape make it impossible to secure it to a single crane hook. In view of these problems, it may be necessary to manipulate such items by tandem lifting with two cranes [7]. An example tandem lifting operation is shown in Figure 80.

Tandem lifts present greater safety risks than single lifts. One safety risk involves synchronizing the movement of both cranes. Lateral forces acting on the crane boom has to be prevented, in addition to overloads, side loads, unequal load sharing, and overturning moments. Hoisting at unequal speeds, for example, can result in unequal load distribution. This scenario can lead to an overload on one of the cranes. The two cranes involved in tandem lifting are operated by two crane drivers; therefore, synchronizing human operator actions comes into play. It should be noted that even if the operators perform flawlessly, it is still impossible to synchronize the cranes' movement perfectly. Therefore, additional safety measures should be utilized [7].

To mitigate hazards, ISO standard 12480-1 suggests that all lateral forces on the crane boom have to be avoided, the crane movements have to be synchronous, and a crane is allowed to lift 100% of the load suggested in its load chart, only if all relevant factors can be monitored. If one or more of the factors cannot be evaluated, then the load weight must be down-rated by 25% or more, depending on the situation. Thus, it should be understood that for almost every advantage gained by using tandem lifting cranes, there is a disadvantage to consider [7].



Figure 80: Tandem Lifting Cranes [36].

Because perfect synchronization during a tandem lift is not possible, lateral forces are always present in these lifting scenarios. This chapter investigates the impact of these forces as they pertain to tip-over stability. More specifically, this chapter investigates the following:

1. The relationship between boom luffing angle and cable swing angle.
2. The relationship between the payload mass and cable swing angle.
3. The relationship between hoist length and cable swing angle.
4. The relationship between the separation distance and cable swing angle, when one crane or both of them are moving.

The analysis shows that the stability properties are a complex function of both the crane and payload parameters.

5.2 Tip-over Stability Based on the Sum of Moments About the Forward Tip-over Axis

In this section, static tip-over stability is investigated; therefore the moment created by each gravitational force about a corresponding tip-over axis is calculated. In order to maintain crane stability, the sum of these moments should be less than or equal to zero.

Figure 81 shows the general geometry of the possible tip-over axes of a crawler crane. The possible tip-over axes run along the front and rear edges, as well as the outside edges of the crawler tracks. Vectors \vec{a}_1 and \vec{a}_3 represent the forward and backward tip-over axes respectively, while \vec{a}_2 and \vec{a}_4 represent the sideways tip-over axes.

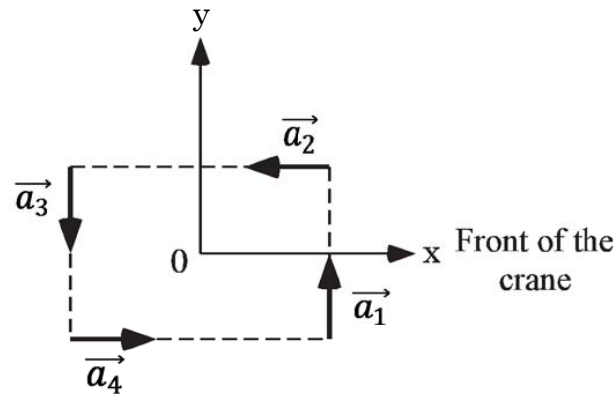


Figure 81: Top View of the Horizontal Plane Formed by the Possible Tip-over Axes.

Figure 82 illustrates two tandem crawler cranes, where the payload is swinging. For simplicity and minimum computational cost to predict the tip-over stability of the two cranes in this case, it is assumed that when the suspension cable is deflected

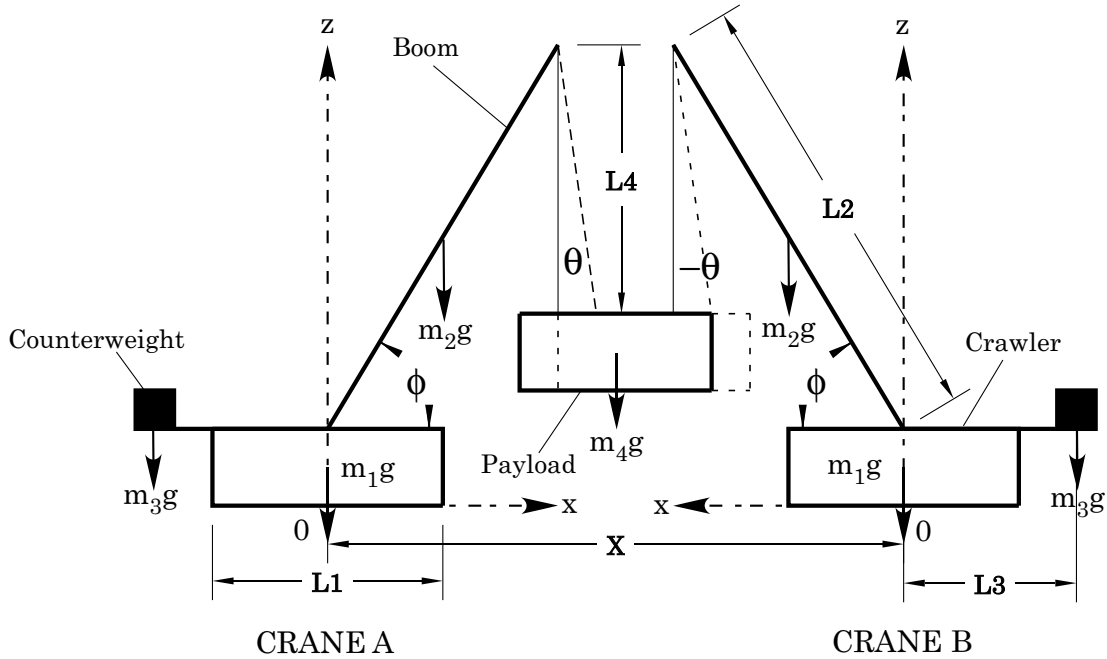


Figure 82: Schematic Diagram for Tandem Crawler Cranes (load is swinging)

by the swinging payload, it remains fixed in the maximum deflected position, thus the static equations apply. Figure 83 illustrates a representative case wherein the cranes are too far apart, thereby causing the payload to be swung outward from both cranes. Each case is composed of two crawler cranes, each of them consisting of a mobile base, m_1 , a rotational boom, m_2 , a counterweight, m_3 , and a suspension cable with a payload mass, m_4 that is shared between both cranes. The base is modeled as a thin plate and has a center of gravity at the center of the base. The boom has a length of L_2 . Its center of mass is located in the middle of the boom. The boom is elevated at an angle ϕ relative to the horizontal plane. This angle is known as the luffing, or boom, angle. The position of the counterweight is measured by a distance, L_3 , from the central axis. The payload swinging angle, measured from the vertical is θ . To calculate the moment generated by each of the gravitational forces about a given axis we use:

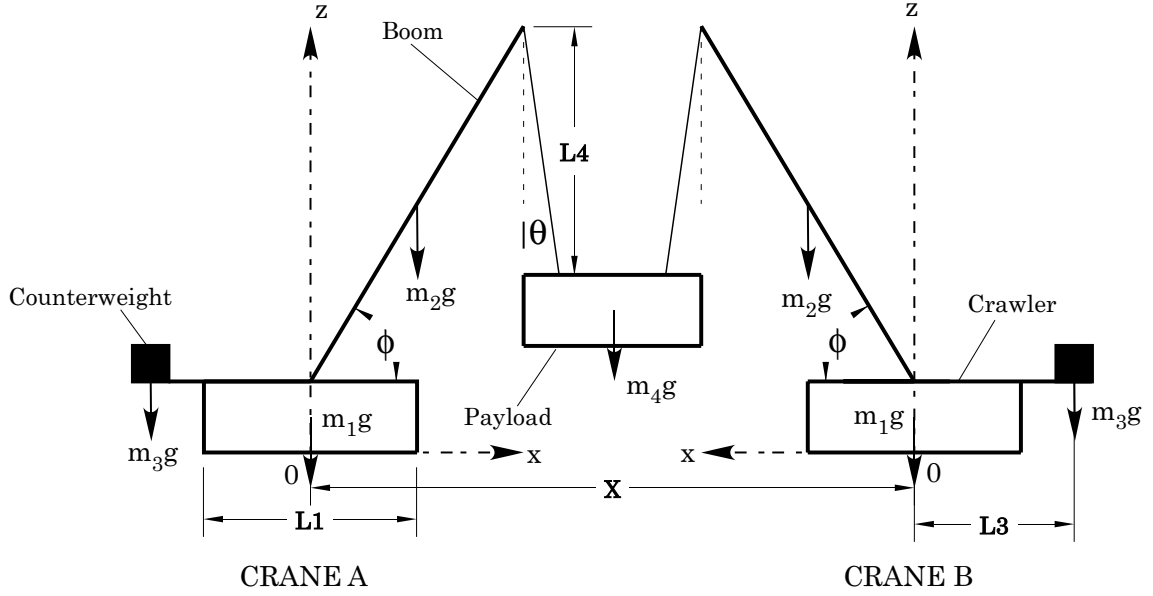


Figure 83: Schematic Diagram for Tandem Crawler Cranes (load is pulled)

$$\vec{M}_{ij} = \vec{a}_j \cdot (\vec{r}_i \times \vec{f}_i) \quad (5.1)$$

where:

$i = 1, \dots, 5$ and $j = 1, \dots, 4$.

\vec{M}_{ij} is the moment generated by the force \vec{f}_i about the axis \vec{a}_j [Nm].

\vec{f}_i is the gravitational force acting on body i at its gravitational center [N].

\vec{a}_j is a unit vector along the j^{th} tip-over axis.

\vec{r}_i is a position vector pointing from any point on the tip-over axis to any point on the line of action of the force [m].

The individual moments found using (5.1) are combined to get the total moment about each tip-over axis:

$$\vec{M}_j = \sum_{i=1}^5 \vec{M}_{ij} = \sum_{i=1}^5 \vec{a}_j \cdot (\vec{r}_i \times \vec{f}_i) \quad (5.2)$$

It is important to study the free body diagram of the payload in order to derive

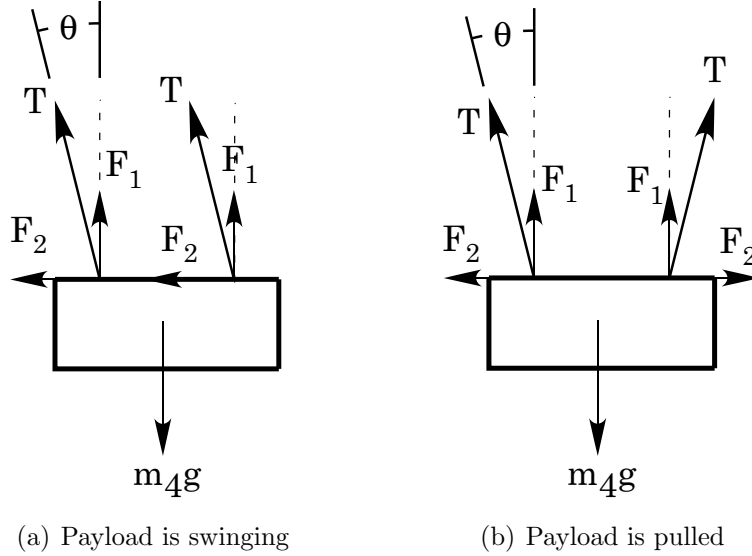


Figure 84: Free Body Diagram of Payload.

the moment equations correctly. Figure 84 shows the forces acting on the payload in both the free swinging and outwardly pulling positions. The reactions of these forces act on Cranes A and B and should be used in the moment equation in addition to the gravitational forces. Where:

$$\vec{F}_1 = \frac{m_4}{2}g \quad (5.3)$$

$$\vec{F}_2 = \frac{m_4}{2}g \tan \theta \quad (5.4)$$

Therefore, the moment creating a forward tip-over for Crane A when the load is swinging is:

$$\begin{aligned} \vec{M}_{fA} = & m_2g\left(\frac{L_2}{2} \cos \phi - \frac{L_1}{2}\right) - m_1g\frac{L_1}{2} - m_3g\left(L_3 + \frac{L_1}{2}\right) \\ & + \frac{m_4}{2}g\left(L_2 \cos \phi - \frac{L_1}{2}\right) + \frac{m_4}{2}g \tan \theta(L_2 \sin \phi + h) \end{aligned} \quad (5.5)$$

And the moment creating a forward tip-over for Crane B when the load is swinging

is:

$$\begin{aligned}
 \vec{M}_{fB} = m_2g\left(\frac{L_2}{2} \cos \phi - \frac{L_1}{2}\right) - m_1g\frac{L_1}{2} - m_3g\left(L_3 + \frac{L_1}{2}\right) \\
 + \frac{m_4}{2}g\left(L_2 \cos \phi + \frac{L_1}{2}\right) - \frac{m_4}{2}g \tan \theta(L_2 \sin \phi + h) \quad (5.6)
 \end{aligned}$$

Equations (5.5) and (5.6) assume that the payload is swung outward from crane A and inward toward crane B. Therefore, if the payload is in the outward pulling position, then (5.5) holds for both cranes.

5.3 Case Study - Terex CC 2800-1

The tipping-moment equations were examined using the Terex CC 2800-1. Two identical Terex cranes are assumed to be lifting a shared payload. The configuration used has no mast and a fixed-position counterweight was used for simplicity.

The parameters of the Terex crane in this configuration are listed in Table 9.

Table 9: Parameters of the Terex CC 2800-1.

Parameter	Item	Numerical Data
w	Width of base	8.4 m
h	Height of base	2.45 m
L_1	Length of base	10.33 m
L_2	Length of boom	102 m
L_3	Length of counterweight	7 m
L_4	Length of hoist	80 m
m_1	Mass of base	125 t
m_2	Mass of boom	60 t
m_3	Mass of counterweight	160 t
m_4	Mass of payload	220 t

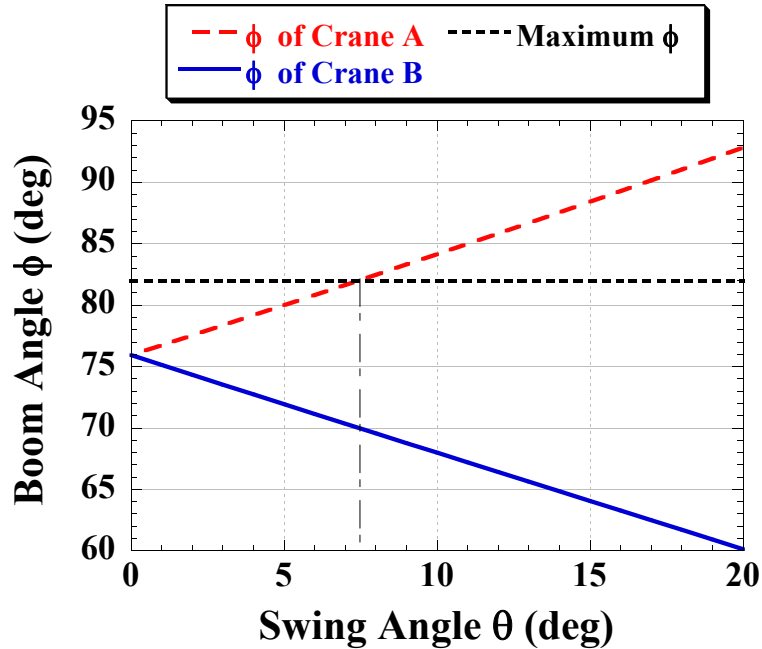


Figure 85: Minimum Boom Angle to Prevent Forward Tip-over vs. Swing Angle for a Payload Mass of 220 t.

5.3.1 Boom Luffing Angle vs. Swing Angle

Assuming the payload swing angle varies between 0° and 20° , the minimum boom angle to prevent forward tip-over of both cranes was calculated.

Figure 85 shows that, for Crane A, as the swing angle gets larger, the minimum boom angle increases almost linearly to counterbalance the effect of the tension forces acting on the tip of the boom due to the payload swing-out angle. On the other hand, for Crane B, the value of the minimum boom angle decreases, and is much less than that of Crane A. This is due to the fact that the horizontal component of the tension forces act in the opposite direction of forward tip-over.

Note that the maximum allowable boom angle for this crane configuration is 82° (higher boom angles introduce a danger of backward tip over). This 82° angle is the required value when the swing-out angle is 8° . This means that a swing angle of more

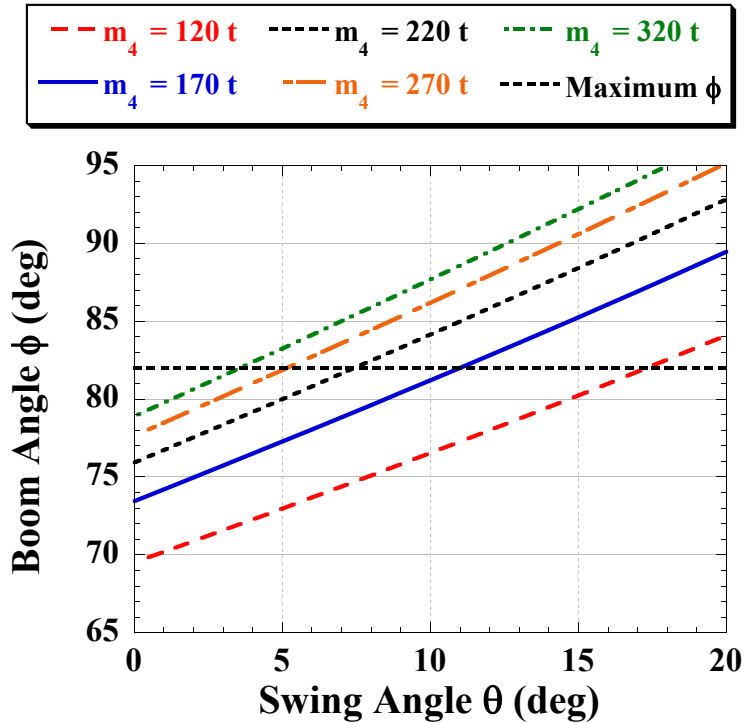


Figure 86: Minimum Boom Angle to Prevent Forward Tip-over vs. Swing Angle for Different Payload Masses for Crane A, (m_4 is the Payload Mass).

than 8° will cause Crane A to tip over. Thus, the whole system will collapse.

Another important observation is that the boom angle value is critical for Crane A, but Crane B is more stable. Thus if both cranes have perfectly matching configurations, then observing the boom angle of the crane with the outwardly-swinging payload would be sufficient to maintain stability. However, if the payload was pulled between the two cranes, or if it was swinging back and forth, then both cranes will experience similar tip-over moments.

As the payload mass increases, the minimum boom angle increases. This effect for Crane A is shown in Figure 86.

It is obvious that as the payload mass increases, the critical value of the swing angle decreases. This means that less swinging is allowed to maintain stability. It

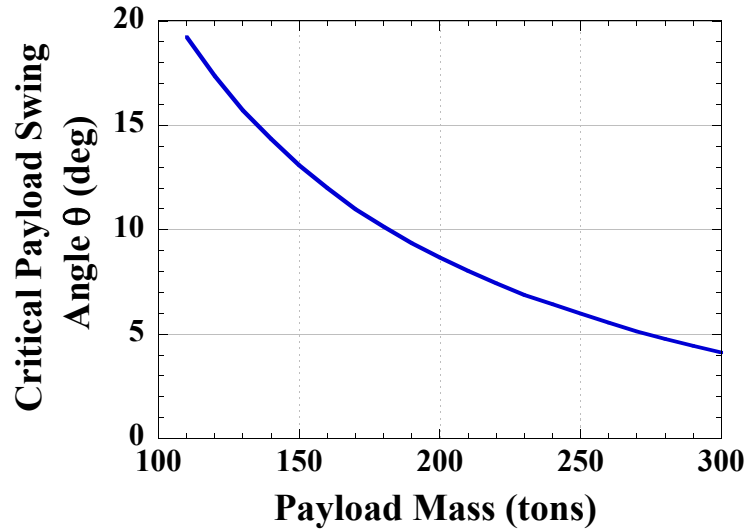


Figure 87: Critical Payload Swing Angle vs. Payload Mass for a Boom Angle of 82° .

can also be inferred that increasing the payload mass above the rated mass causes the system's stability to become more critically affected by payload swing. This is demonstrated by Figure 87, which shows how the critical payload swing angle decreases as the payload mass increases.

5.3.1.1 *The Effect of a Triangular-shaped Payload*

If a right triangular payload is attached to the two cranes as shown in Figure 88, then Crane B bears one third of the load while Crane A bears two thirds. Assuming the payload swings outwards away from both cranes, then the minimum boom luffing angle necessary to prevent forward tip-over with respect to the payload swing angle is plotted in Figure 89.

This figure shows that the minimum boom angle required to prevent forward tip-over of Crane B, which in this case bears one third of the load, is about 8° less than that of Crane A. Thus, assuming the performance of both cranes is synchronized, then only considering Crane B will indicate that the critical payload swing angle is

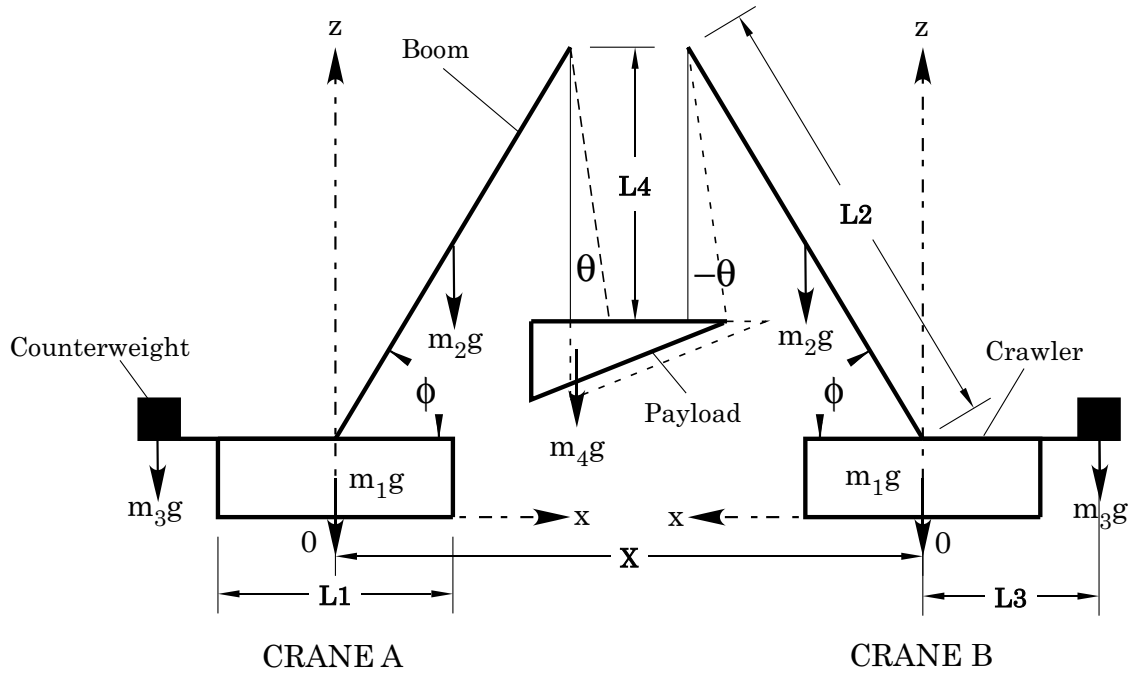


Figure 88: Schematic Diagram for Tandem Crawler Cranes (Triangular Payload).

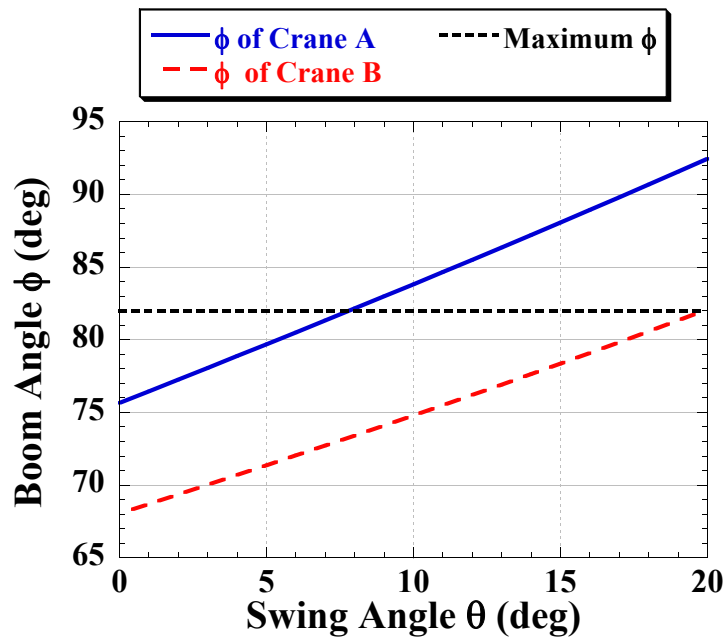


Figure 89: Minimum Boom Angle to Prevent Forward Tip-over vs. Swing Angle for a Triangular Payload with a Mass of 220 t.

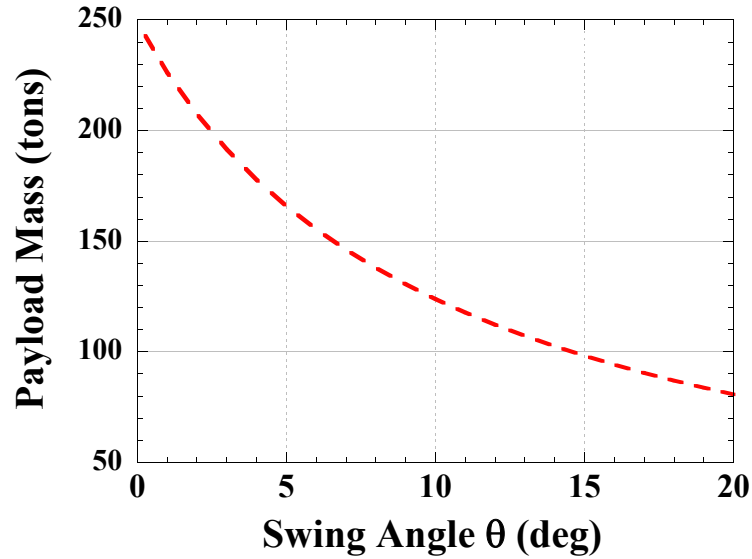


Figure 90: Maximum Payload Mass to Prevent Forward Tip-over vs. Swing Angle for a Boom Angle of 77° .

20° . However, Figure 89 shows that if the payload swing angle increases above 8° , then the minimum boom angle required to prevent forward tip-over of Crane A has to be increased above 82° , which is physically impossible for this configuration. Such a swing angle will lead to the destruction of the whole system regardless of the fact that Crane B was “safe”. This case illustrates the complexity of such systems.

Thus, in some cases like irregular payloads, it is very critical to observe and analyze the performance of both cranes and closely monitor the crane with more dangerous conditions in order to avoid tip-overs.

5.3.2 Payload Mass vs. Swing Angle

Assuming the payload is swinging with an angle that varies between 0° and 20° , the maximum payload mass to prevent forward tip-over of Crane A was calculated. The boom angle was fixed to 77° . The result is shown in Figure 90.

The data shows that as the swing angle increases, the maximum allowable payload

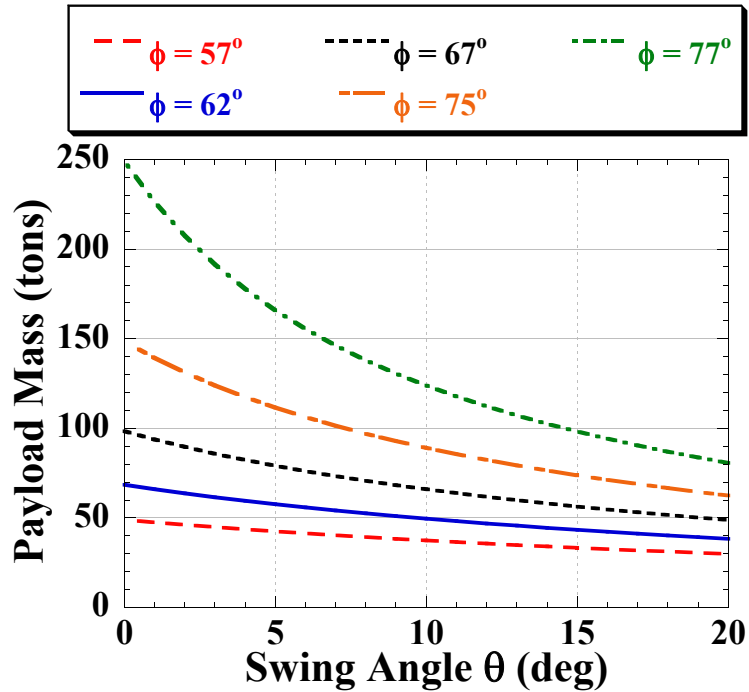


Figure 91: Maximum Payload Mass to Prevent Forward Tip-over vs. Swing Angle for Different Boom Angles.

mass to prevent forward tip-over decreases, which is logically expected. On the other hand, this parameter does not affect the stability of Crane B in this case. So, again, Crane A can be sufficient to ensure stability, excluding the case of the payload being pulled, where both cranes' parameters are crucial. Note that half a period later, as the payload swings, Crane B becomes Crane A and so on.

Figure 91 shows the maximum allowable payload mass that prevents tip-over with respect to the swing angle, for multiple values of the boom angle. It can be inferred that, as the boom angle decreases, the allowable payload masses decrease dramatically. For low values of ϕ , the graph shows that the payload mass does not change significantly as the swing angle increases, thus proving that the crane, at low boom angles, can handle a range of payload swing angles. In other words, for small boom angles, the payload swing angle is no longer the most critical parameter

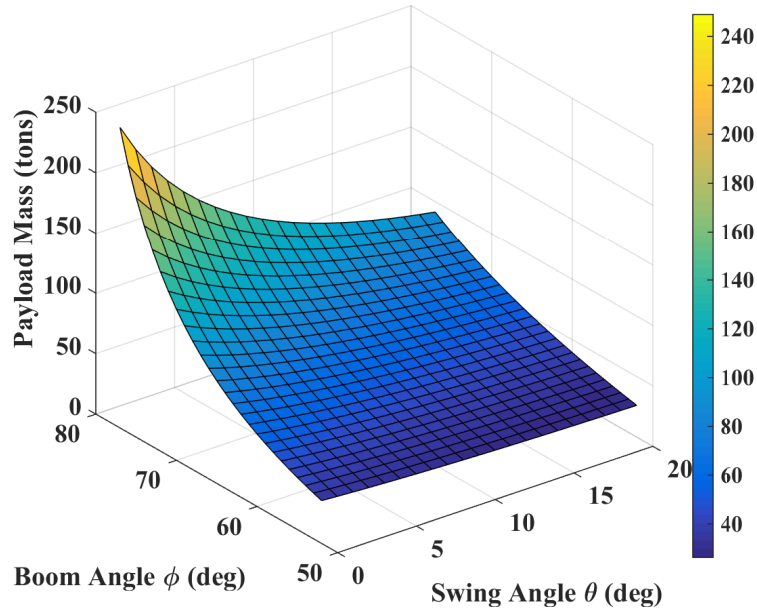


Figure 92: Minimum Boom Angle and Maximum Payload Mass to Prevent Forward Tip-over vs. Swing Angle.

affecting the crane’s stability, it is rather the boom angle itself. It can also be seen that a decrease of 5° in the boom angle reduced the allowable payload mass by almost 50%. This indicates again that the boom luffing angle is the most critical parameter when it comes to the crane’s stability.

The effects of boom angle and payload mass are combined in Figure 92. This data represents the minimum boom angle and maximum payload mass required to maintain stability for various payload swing angles. It shows that the larger the payload mass and the larger the boom angle, the less payload swing is allowed.

5.3.3 Separation Distance vs. Swing Angle

Assuming that one or both cranes move linearly, thereby increasing the separation distance between them, then for a moving distance of x , the swing-out angle can be

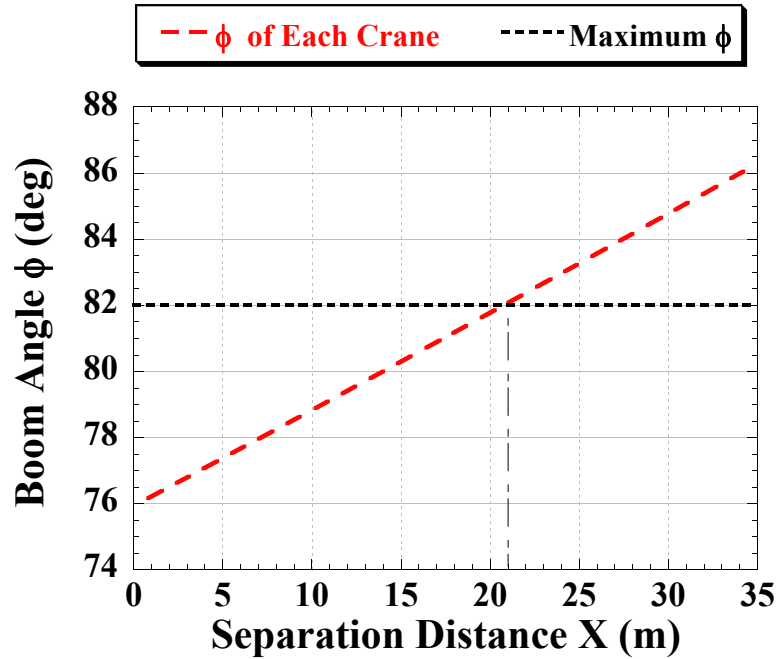


Figure 93: Minimum Boom Angle to Prevent Forward Tip-over vs. Separation Distance for a Payload Mass of 220 *t*.

calculated as follows:

$$\theta = \sin^{-1}\left(\frac{0.5x}{L_4}\right) \quad (5.7)$$

where x is measured relative to the position of the cranes where the swing angles of the payload were zero.

For small values of the swing-out angle θ , the relationship between x and θ can be considered linear, thus the relationships discussed before will follow the same trend with a different range of x values instead of the 0 to 20° swing angle.

Figure 93 shows that the maximum distance one of the cranes can move away from the other, or the summation of the distances both cranes can move away from each other, without tipping over is approximately 21 *m*. This corresponds to a swing angle of 8°, as shown previously.

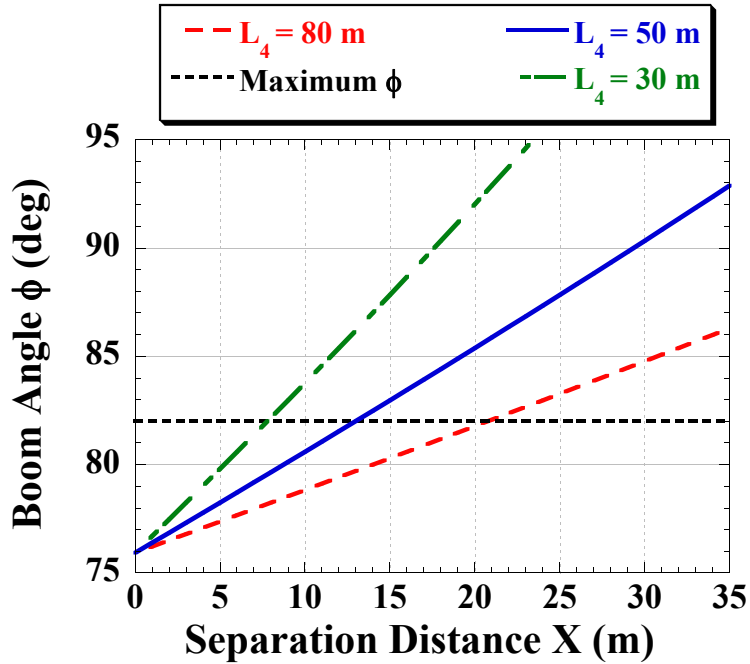


Figure 94: Minimum Boom Angle to Prevent Forward Tip-over vs. Separation Distance for a Payload Mass of 220 t and Different Hoist Cable Lengths L_4 .

5.3.4 Effect of Hoist Length

Hoist length L_4 is a parameter that does not generally affect the tip-over moment. This is because the force due to the payload weight is transmitted to the boom tip through the cable. Using a fixed cable angle, the force will have the same magnitude and direction regardless of the hoist length. This was established in (5.5) and (5.6); L_4 was not part of the equations. However, the hoist cable length affects the relationship between the swing angle and the separation distance as shown in (5.7), thus changing the cable length will result in a different allowable separation distance corresponding to the same swing angle.

Figure 94 illustrates the effect of the hoist cable length on the minimum boom luffing angle required to prevent forward tip-over with respect to the separation distance. It is clear in this figure that the critical separation distance is larger when a

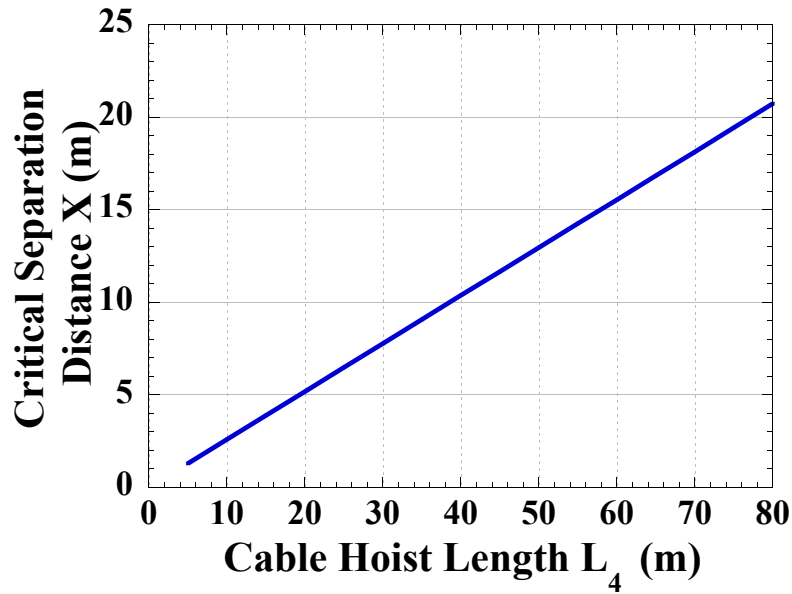


Figure 95: Critical Separation Distance vs. Different Hoist Cable Lengths for a Boom Angle of 82° .

longer cable length is used. The relationship between the critical separation distance and the cable length is shown in Figure 95.

In general, it is advisable to keep the payload as close to the ground as possible, so that if a forward tip-over occurs, the payload would hit the ground quickly and minimize damage to both cranes.

5.4 Summary

Tandem lifting cranes are useful when it comes to moving heavy and bulky payloads; however having two cranes connected by a shared payload makes the system more complicated and subject to greater tip-over hazard. The configuration and motions of the first crane directly affects the second crane. This complication provides more factors that can cause tip-over accidents. The analysis shows that the crane and payload states must be carefully selected and monitored throughout the lift in order

to avoid tipping over. In fact, the complexity of the tip-over stability conditions make it apparent that the crane operators cannot reasonably be expected to monitor and control all of the important parameters. Additional sensors and monitoring devices should be employed to ensure safe operating conditions throughout the lift.

CHAPTER VI

CONCLUSIONS AND FUTURE WORK

6.1 Conclusions

Preventing tip-over accidents of cranes, is an important factor for protecting the lives of operators and reducing the risks of damage. At the same time, high productivity must be maintained for efficient crane operations. One way to achieve these somewhat conflicting requirements, is to develop a monitoring system that can predict the potential for tip-over and send a warning signal to the operator.

This thesis investigated the tip-over stability of crawler cranes because of their huge size and their susceptibility to tip-over in catastrophic accidents. The thesis discussed two lifting alternatives that can be used in case of heavy lifting payloads: (i) using a movable counterweight, and (ii) tandem lifting. When using a movable counterweight, this thesis presented a method to anticipate the stability region in which the movable counterweight should be placed in order to prevent forward and backward tip-overs. The detailed stability analysis revealed the effects of the crane parameters and configuration on the general characteristics of the crane's tip-over stability when a movable counterweight is utilized.

When crawler cranes move their base and boom while carrying a payload, the motions greatly enhance the workspace, and thus the productivity. However, these motions can induce large amounts of payload swing, which compromises the crane's tip-over stability. After studying the influence of the crane's parameters and configuration on the static stability, a pseudo-dynamic stability analysis was performed to investigate the crane's tip-over stability. The analysis discussed three fundamental and common crane motions. In each case, the effect of the acceleration commands,

moving distances, and other crane parameters was studied in order to find the reasonable worst-case scenario inducing the largest payload swing. Then, this maximum payload swing was introduced to the stability analysis.

An experimental setup was used to support the results obtained in both the static and pseudo-dynamic tip-over stability analyses. The theoretical approach and the experimental results showed that the calculation tool provides reliable predictions that can help guide the lifting operation and prevent tip-over accidents.

The final chapter of this thesis discussed tandem lifting using two cranes. This is a final resolution when the payload to be lifted is over-sized or has an irregular shape. This thesis analyzed the static tip-over stability of two identical crawler cranes lifting a shared payload. The effects of different parameters and configurations of the two cranes on the static tip-over stability were discussed. Finally, some guidelines were provided on how to make tandem lifting safer and less susceptible to tip-over accidents.

6.2 Future Work

The results and insights gained in this thesis build a foundation for further work in the area of crawler crane tip-over stability analysis. There are several directions in which future investigations can extend the analysis.

First, the current pseudo-dynamic stability analysis presented in this thesis can be improved to include more motion scenarios than those discussed. Combinations of these motions can also be introduced. In this thesis, whenever a portion of a crane was moving, all the other parts were considered stationary. Also, more complex payload swing can be considered, such as combinations of tangential and radial swinging, large nonlinear swinging angles, and double-pendulum effects.

Another avenue of research is applying input-shaping methods and trajectory planning. This can guarantee optimum operation time and minimum payload swing, and will improve the quality of the lifting operation. If these points were addressed,

then the pseudo-dynamic stability analysis becomes more accurate and reliable.

In the area of tandem lifting, what is presented in this thesis is a strong foundation on which further analysis can build upon. First, the analysis presented here only considers statics, thus it can be further extended to include a fuller pseudo-dynamic tip-over stability analysis. This analysis can cover different motion scenarios and acceleration commands. Also, this thesis only covered the analysis related to two identical cranes with identical parameters. In real applications, this is not usually the case. When two different cranes are used, the analysis needs to account for their differences. More than two cranes lifting a common load can also be considered.

In general, wind effects were ignored in the analysis. However, in real applications it is always present, and can be treated as a force acting on the crane components and payload. Thus, this analysis can become more thorough by taking into consideration wind effects.

Finally, follow-on research can consider crawler cranes in tandem lifting with movable counterweights. This will introduce interesting static and dynamic characteristics, that can improve the area of tip-over stability analysis of crawler cranes.

APPENDIX A

MATLAB SOURCE CODES

Listing A.1: Forward Tip-over Analysis (m_4 is the variable)

```
1 % This code calculates the counterweight displacement with ...
    respect to
2 % different slew angles in order to prevent forward tip-over, ...
    this is done
3 % for three values of moveable counterweight mass
4
5 clear
6
7 %% Defining all parameters
8 g=9.8;                % Gravitational acceleration [m/s^2]
9 % Defining Lengths of different components
10 L1 = 10.33;          % Length of Base Body [m]
11 L2 = 102;           % Length of boom [m]
12 L3 = 30;            % Length of mast [m]
13 L4_fixed = 7;       % Position of fixed counterweight [m]
14 L5 = 10;            % Length of payload hoist [m]
15 L4_min = 0;         % Minimum position of moveable ...
    counterweight [m]
16 L4_max = 100;       % Maximum position of moveable ...
    counterweight [m]
17 % Range of allowed locations for counterweight [m]
18 L4_range = linspace(L4_min,L4_max,500);
19 % Other dimensions
20 w = 8.4;            % Width of base [m]
```



```

21 h = 2.45; % Height of base [m]
22 % Mass parameters
23 m1 = 125; % Mass of Car Body [tons]
24 m2 = 60; % Mass of boom [tons]
25 m3 = 12.5; % Mass of mast [tons]
26 m4i = [150 200 300]; % Different masses of moveable ...
    counterweight [tons]
27 m4_fixed = 240; % Mass of fixed counterweight [tons]
28 m5 = 110 ; % Mass of Payload [tons]
29 % Angles
30 p1 = 62*pi/180; % Boom Luffing Angle [rad]
31 B = linspace(0,pi,50); % Slewing Angle [rad]
32
33 %% Calculating minimum location of counterweight to ensure safety
34
35 for k=1:length(m4i) % Loop repeats for each value of m4
36     m4 = m4i(k);
37     for i=1:length(B) % Loop repeats for every slew angle
38         for j = length(L4_range):-1:1 % Loop repeats for every ...
            value of L4
39             L4 = L4_range(j);
40             p2 = acos(L4/L3); % Mast angle
41 % Set up coordinate systems for mass centers
42 c1 = [0 0 h/2]'; % Car Body mass center
43 c2 = [L2*cos(p1)*cos(B(i))/2,...
44     L2*cos(p1)*sin(B(i))/2,...
45     (L2*sin(p1)/2)+h]'; % Boom mass center
46 c3 = [-L3*cos(p2)*cos(B(i))/2,...
47     -L3*cos(p2)*sin(B(i))/2,...
48     (L3*sin(p2)/2)+h]'; % Mast mass center
49 c4 = [-L4*cos(B(i)),...
50     -L4*sin(B(i)), h]'; % Moving counterweight mass center

```

```

51 c4.fixed = [-7*cos(B(i)),...
52             -7*sin(B(i)), 3]'; % Fixed counterweight mass center
53 c5 = [L2*cos(p1)*cos(B(i)),...
54       L2*cos(p1)*sin(B(i)),...
55       L2*sin(p1)+h-L5]'; % Payload mass center
56
57 % Forces:
58 G = [0 0 -1]'; % Direction of gravitational force
59 f1 = m1*g*G; % Weight of car body
60 f2 = m2*g*G; % Weight of boom
61 f3 = m3*g*G; % Weight of mast
62 f4 = m4*g*G; % Weight of moveable counterweight
63 f4.fixed = m4.fixed*g*G; % Weight of fixed counterweight
64 f5 = m5*g*G; % Weight of payload
65
66 % Instantaneous inertial location of the ith ground contact point
67 p01 = [-L1/2 w/2 0]';
68 p02 = [L1/2 w/2 0]';
69 p03 = [L1/2 -w/2 0]';
70 p04 = [-L1/2 -w/2 0]';
71
72 % ith tip-over mode axis
73 a1 = p02-p01;
74 a2 = p03-p02;
75 a3 = p04-p03;
76 a4 = p01-p04;
77
78 % Expressing each ith tip-over mode axis as a unit vector
79 a11 = -a1/norm(a1);
80 a22 = -a2/norm(a2);
81 a33 = a3/norm(a3);
82 a44 = -a4/norm(a4);

```

```

83
84 % Deciding which is the tip-over axis based on the value of the ...
      slew angle
85 theta1 = atan((w/2)/(L1/2));
86 theta2 = pi-theta1;
87 %-----
88 if B(i)<theta1 % Tip over axis is a2
89     pa2 = [L1/2 0 0]';           % Location of a point on axis a2
90     % Vectors pointing from mass centers to the point on a2
91     r1a = c1-pa2;
92     r2a = c2-pa2;
93     r3a = c3-pa2;
94     r4a = c4-pa2;
95     r4a.fixed = c4.fixed-pa2;
96     r5a = c5-pa2;
97
98     % Calculating sum of moments about axis a2:
99     M2(i) = dot(a22,cross(r1a,f1))+dot(a22,cross(r2a,f2))+...
100            dot(a22,cross(r3a,f3))+dot(a22,cross(r4a,f4))+...
101            dot(a22,cross(r4a.fixed,f4.fixed))+dot(a22,cross(r5a,f5));
102
103     if M2(i)>0 % Loop chooses value of L4 to prevent tip-over
104         L4.long(k,i)=L4;
105         break
106     end
107 end
108 %-----
109 if B(i)>=theta1 && B(i)<=theta2 % Tip over axis is a1
110     pa1 = [0 w/2 0]';           % Location of a point on axis a1
111     % Vectors pointing from mass centers to the point on a1
112     r1a = c1-pa1;
113     r2a = c2-pa1;

```

```

114   r3a = c3-pa1;
115   r4a = c4-pa1;
116   r4a.fixed = c4.fixed-pa1;
117   r5a = c5-pa1;
118
119   % Calculating sum of moments about axis a1:
120   M1(i) = dot(a11,cross(r1a,f1))+dot(a11,cross(r2a,f2))+...
121           dot(a11,cross(r3a,f3))+dot(a11,cross(r4a,f4))+...
122           dot(a11,cross(r4a.fixed,f4.fixed))+dot(a11,cross(r5a,f5));
123
124       if M1(i)>0 % Loop chooses value of L4 to prevent tip-over
125           L4.long(k,i)=L4;
126           break
127       end
128   end
129   %-----
130   if B(i)>theta2 % Tip over axis is a4
131       pa4 = [-L1/2 0 0]';           % Location of a point on axis a4
132       % Vectors pointing from mass centers to the point on a4
133       r1a = c1-pa4;
134       r2a = c2-pa4;
135       r3a = c3-pa4;
136       r4a = c4-pa4;
137       r4a.fixed = c4.fixed-pa4;
138       r5a = c5-pa4;
139
140
141       % Calculating sum of moments about axis a4:
142       M4(i) = dot(a44,cross(r1a,f1))+dot(a44,cross(r2a,f2))+...
143              dot(a44,cross(r3a,f3))+dot(a44,cross(r4a,f4))+...
144              dot(a44,cross(r4a.fixed,f4.fixed))+dot(a44,cross(r5a,f5));
145

```

```

146         if M4(i)>0
147             L4_long(k,i)=L4;
148             break
149         end
150     end
151         end
152     end
153 end
154
155 %% Plotting
156 figure
157 for k = 1:length(m4i)
158     x = [B,B];
159     y = [L4_long(k,:),-fliplr(L4_long(k,:))];
160     polar(x,y)
161     xlabel('Slew Angle \beta [deg]')
162     ylabel('Counterweight Position [m]')
163     legend('m_4 = 150 t','m_4 = 200 t','m_4 = 300 t')
164     hold on
165 end

```

Listing A.2: Backward Tip-over Analysis (m_4 is the variable)

```

1 % This code calculates the counterweight displacement with ...
   respect to
2 % different slew angles in order to prevent backward tip-over, ...
   this is done
3 % for three values of moveable counterweight mass
4
5 clear
6
7 %% Defining all parameters

```

```

8 g=9.8; % Gravitational acceleration [m/s^2]
9 % Defining Lengths of different components
10 L1 = 10.33; % Length of Base Body [m]
11 L2 = 102; % Length of boom [m]
12 L3 = 30; % Length of mast [m]
13 L4_fixed = 7; % Position of fixed counterweight [m]
14 L5 = 10; % Length of payload hoist [m]
15 L4_min = 0; % Minimum position of moveable ...
    counterweight [m]
16 L4_max = 100; % Maximum position of moveable ...
    counterweight [m]
17 % Range of allowed locations for counterwieght [m]
18 L4_range = linspace(L4_min,L4_max,500);
19 % Other dimensions
20 w = 8.4; % Width of base [m]
21 h = 2.45; % Height of base [m]
22 % Mass parameters
23 m1 = 125; % Mass of Car Body [tons]
24 m2 = 60; % Mass of boom [tons]
25 m3 = 0;%12.5; % Mass of mast [tons]
26 m4i = [150 200 300]; % Different masses of moveable ...
    counterweight [tons]
27 m4_fixed = 240; % Mass of fixed counterweight [tons]
28 m5 = 0 ; % Mass of Payload [tons]
29 % Angles
30 p1 = 62*pi/180; % Boom Luffing Angle [rad]
31 B = linspace(0,pi,50); % Slewing Angle [rad]
32
33 %% Calculating maximum location for counterweight to ensure safety
34
35 for k=1:length(m4i) % Loop repeats for each value of m4
36     m4 = m4i(k);

```

```

37     for i=1:length(B) % Loop repeats for every slew angle
38         for j = 1:length(L4_range) % Loop repeats for every value ...
39             of L4
40                 L4 = L4_range(j);
41                 p2 = acos(L4/L3); % Mast angle
42 %Set up coordinate systems for mass centers
43 c1 = [0 0 h/2]'; % Car Body mass center
44 c2 = [L2*cos(p1)*cos(B(i))/2,...
45       L2*cos(p1)*sin(B(i))/2,...
46       (L2*sin(p1)/2)+h]'; % Boom mass center
47 c3 = [-L3*cos(p2)*cos(B(i))/2,...
48       -L3*cos(p2)*sin(B(i))/2,...
49       (L3*sin(p2)/2)+h]'; % Mast mass center
50 c4 = [-L4*cos(B(i)),...
51       -L4*sin(B(i)), h]'; % Moving counterweight mass center
52 c4.fixed = [-7*cos(B(i)),...
53            -7*sin(B(i)), 3]'; % Fixed counterweight mass center
54 c5 = [L2*cos(p1)*cos(B(i)),...
55       L2*cos(p1)*sin(B(i)),...
56       L2*sin(p1)+h-L5]'; % Payload mass center
57 % Forces:
58 G = [0 0 -1]'; % Direction of gravitational force
59 f1 = m1*g*G; % Weight of car body
60 f2 = m2*g*G; % Weight of boom
61 f3 = m3*g*G; % Weight of mast
62 f4 = m4*g*G; % Weight of moveable counterweight
63 f4.fixed = m4.fixed*g*G; % Weight of fixed counterweight
64 f5 = m5*g*G; % Weight of payload
65
66 % Instantaneous inertial location of the ith ground contact point
67 p01 = [-L1/2 w/2 0]';

```

```

68 p02 = [L1/2 w/2 0]';
69 p03 = [L1/2 -w/2 0]';
70 p04 = [-L1/2 -w/2 0]';
71
72 % ith tip-over mode axis
73 a1 = p02-p01;
74 a2 = p03-p02;
75 a3 = p04-p03;
76 a4 = p01-p04;
77
78 % Expressing each ith tip-over mode axis as a unit vector
79 a11 = -a1/norm(a1);
80 a22 = -a2/norm(a2);
81 a33 = -a3/norm(a3);
82 a44 = -a4/norm(a4);
83
84 % Deciding which is the tip-over axis based on the value of the ...
      slew angle
85 theta1 = atan((w/2)/(L1/2));
86 theta2 = pi-theta1;
87 %-----
88 if B(i)<theta1 % Tip over axis is a4
89     pa4 = [-L1/2 0 0]'; % Location of a point on axis a4
90     % Vectors pointing from mass centers to the point on a4
91     r1a = c1-pa4;
92     r2a = c2-pa4;
93     r3a = c3-pa4;
94     r4a = c4-pa4;
95     r4a.fixed = c4.fixed-pa4;
96     r5a = c5-pa4;
97
98     % Calculating sum of moments about axis a4:

```



```

99     M4(i) = dot(a44,cross(r1a,f1))+dot(a44,cross(r2a,f2))+...
100           dot(a44,cross(r3a,f3))+dot(a44,cross(r4a,f4))+...
101           dot(a44,cross(r4a_fixed,f4_fixed))+dot(a44,cross(r5a,f5));
102
103     if M4(i)>0 % Loop chooses value of L4 to prevent tip-over
104         L4_short(k,i)=L4;
105         break
106     end
107 end
108 %-----
109 if B(i)>=theta1 && B(i)<=theta2 % Tip over axis is a3
110     pa3 = [0 -w/2 0]'; % Location of a point on axis a3
111     % Vectors pointing from mass centers to the point on a3
112     r1a = c1-pa3;
113     r2a = c2-pa3;
114     r3a = c3-pa3;
115     r4a = c4-pa3;
116     r4a_fixed = c4_fixed-pa3;
117     r5a = c5-pa3;
118
119     % Calculating sum of moments about axis a3:
120     M3(i) = dot(a33,cross(r1a,f1))+dot(a33,cross(r2a,f2))+...
121           dot(a33,cross(r3a,f3))+dot(a33,cross(r4a,f4))+...
122           dot(a33,cross(r4a_fixed,f4_fixed))+dot(a33,cross(r5a,f5));
123
124     if M3(i)>0 % Loop chooses value of L4 to prevent tip-over
125         L4_short(k,i)=L4;
126         break
127     end
128 end
129 %-----
130 if B(i)>theta2 % Tip over axis is a2

```

```

131 pa2 = [L1/2 0 0]'; % Location of a point on axis a2
132 % Vectors pointing from mass centers to the point on a2
133 r1a = c1-pa2;
134 r2a = c2-pa2;
135 r3a = c3-pa2;
136 r4a = c4-pa2;
137 r4a.fixed = c4.fixed-pa2;
138 r5a = c5-pa2;
139
140 % Calculating sum of moments about axis a2:
141 M2(i) = dot(a22,cross(r1a,f1))+dot(a22,cross(r2a,f2))+...
142         dot(a22,cross(r3a,f3))+dot(a22,cross(r4a,f4))+...
143         dot(a22,cross(r4a.fixed,f4.fixed))+dot(a22,cross(r5a,f5));
144
145     if M2(i)>0 % Loop chooses value of L4 to prevent tip-over
146         L4_short(k,i)=L4;
147         break
148     end
149 end
150     end
151 end
152 end
153
154 %% Plotting
155 figure
156 for k = 1:length(m4i)
157     x = [B,B];
158     y = [L4_short(k,:),-fliplr(L4_short(k,:))];
159     polar(x,y)
160     xlabel('Slew Angle \beta [deg]')
161     ylabel('Counterweight Position [m]')
162     legend('m_4 = 150 t','m_4 = 200 t','m_4 = 300 t')

```

```
163     hold on
164 end
```

Listing A.3: Forward and Backward Tip-Over Limits

```
1 % This code calculates the counterweight displacement with ...
   respect to
2 % different slew angles in order to prevent forward and backward ...
   tip-overs
3
4 clear
5
6 %% Defining all parameters
7 g=9.8;                % Gravitational acceleration [m/s^2]
8 % Defining Lengths of different components
9 L1 = 10.33;           % Length of Base Body [m]
10 L2 = 102;            % Length of boom [m]
11 L3 = 30;             % Length of mast [m]
12 L4_fixed = 7;        % Position of fixed counterweight [m]
13 L5 = 10;             % Length of payload hoist [m]
14 L4_min = 0;          % Minimum position of moveable ...
   counterweight [m]
15 L4_max = 100;        % Maximum position of moveable ...
   counterweight [m]
16 % Range of allowed locations for counterweight [m]
17 L4_range = linspace(L4_min,L4_max,500);
18 % Other dimensions
19 w = 8.4;             % Width of base [m]
20 h = 2.45;           % Height of base [m]
21 % Mass parameters
22 m1 = 125;            % Mass of Car Body [tons]
23 m2 = 60;            % Mass of boom [tons]
```

```

24 m3 = 12.5;           % Mass of mast [tons]
25 m4 = 200;           % Masses of moveable counterweight [tons]
26 m4.fixed = 240;     % Mass of fixed counterweight [tons]
27 m5 = 110 ;          % Mass of Payload [tons]
28 % Angles
29 p1 = 62*pi/180;     % Boom Luffing Angle [rad]
30 B = linspace(0,pi,50); % Slewing Angle [rad]
31
32 %% Calculating minimum location of counterweight to ensure safety
33
34
35     for i=1:length(B) % Loop repeats for every slew angle
36         for j = length(L4_range):-1:1 % Loop repeats for every ...
37             value of L4
38                 L4 = L4_range(j);
39                 p2 = acos(L4/L3); % Mast angle
40 % Set up coordinate systems for mass centers
41 c1 = [0 0 h/2]';      % Car Body mass center
42 c2 = [L2*cos(p1)*cos(B(i))/2,...
43       L2*cos(p1)*sin(B(i))/2,...
44       (L2*sin(p1)/2)+h]'; % Boom mass center
45 c3 = [-L3*cos(p2)*cos(B(i))/2,...
46       -L3*cos(p2)*sin(B(i))/2,...
47       (L3*sin(p2)/2)+h]'; % Mast mass center
48 c4 = [-L4*cos(B(i)),...
49       -L4*sin(B(i)), h]'; % Moving counterweight mass center
50 c4.fixed = [-7*cos(B(i)),...
51            -7*sin(B(i)), 3]'; % Fixed counterweight mass center
52 c5 = [L2*cos(p1)*cos(B(i)),...
53       L2*cos(p1)*sin(B(i)),...
54       L2*sin(p1)+h-L5]'; % Payload mass center

```

```

55 % Forces:
56 G = [0 0 -1]'; % Direction of gravitational force
57 f1 = m1*g*G; % Weight of car body
58 f2 = m2*g*G; % Weight of boom
59 f3 = m3*g*G; % Weight of mast
60 f4 = m4*g*G; % Weight of moveable counterweight
61 f4.fixed = m4.fixed*g*G; % Weight of fixed counterweight
62 f5 = m5*g*G; % Weight of payload
63
64 % Instantaneous inertial location of the ith ground contact point
65 p01 = [-L1/2 w/2 0]';
66 p02 = [L1/2 w/2 0]';
67 p03 = [L1/2 -w/2 0]';
68 p04 = [-L1/2 -w/2 0]';
69
70 % ith tip-over mode axis
71 a1 = p02-p01;
72 a2 = p03-p02;
73 a3 = p04-p03;
74 a4 = p01-p04;
75
76 % Expressing each ith tip-over mode axis as a unit vector
77 a11 = -a1/norm(a1);
78 a22 = -a2/norm(a2);
79 a33 = a3/norm(a3);
80 a44 = -a4/norm(a4);
81
82 % Deciding which is the tip-over axis based on the value of the ...
    slew angle
83 theta1 = atan((w/2)/(L1/2));
84 theta2 = pi-theta1;
85 %-----

```

```

86 if B(i)<theta1 % Tip over axis is a2
87     pa2 = [L1/2 0 0]'; % Location of a point on axis a2
88     % Vectors pointing from mass centers to the point on a2
89     r1a = c1-pa2;
90     r2a = c2-pa2;
91     r3a = c3-pa2;
92     r4a = c4-pa2;
93     r4a.fixed = c4.fixed-pa2;
94     r5a = c5-pa2;
95
96     % Calculating sum of moments about axis a2:
97     M2(i) = dot(a22,cross(r1a,f1))+dot(a22,cross(r2a,f2))+...
98             dot(a22,cross(r3a,f3))+dot(a22,cross(r4a,f4))+...
99             dot(a22,cross(r4a.fixed,f4.fixed))+dot(a22,cross(r5a,f5));
100
101     if M2(i)>0 % Loop chooses value of L4 to prevent tip-over
102         L4.long(i)=L4;
103         break
104     end
105 end
106 %-----
107 if B(i)>theta1 && B(i)<=theta2 % Tip over axis is a1
108     pa1 = [0 w/2 0]'; % Location of a point on axis a1
109     % Vectors pointing from mass centers to the point on a1
110     r1a = c1-pa1;
111     r2a = c2-pa1;
112     r3a = c3-pa1;
113     r4a = c4-pa1;
114     r4a.fixed = c4.fixed-pa1;
115     r5a = c5-pa1;
116
117     % Calculating sum of moments about axis a1:

```

```

118 M1(i) = dot(a11,cross(r1a,f1))+dot(a11,cross(r2a,f2))+...
119         dot(a11,cross(r3a,f3))+dot(a11,cross(r4a,f4))+...
120         dot(a11,cross(r4a_fixed,f4_fixed))+dot(a11,cross(r5a,f5));
121
122     if M1(i)>0 % Loop chooses value of L4 to prevent tip-over
123         L4_long(i)=L4;
124         break
125     end
126 end
127 %-----
128 if B(i)>theta2 % Tip over axis is a4
129     pa4 = [-L1/2 0 0]'; % Location of a point on axis a4
130     % Vectors pointing from mass centers to the point on a4
131     r1a = c1-pa4;
132     r2a = c2-pa4;
133     r3a = c3-pa4;
134     r4a = c4-pa4;
135     r4a_fixed = c4_fixed-pa4;
136     r5a = c5-pa4;
137
138     % Calculating sum of moments about axis a4:
139     M4(i) = dot(a44,cross(r1a,f1))+dot(a44,cross(r2a,f2))+...
140            dot(a44,cross(r3a,f3))+dot(a44,cross(r4a,f4))+...
141            dot(a44,cross(r4a_fixed,f4_fixed))+dot(a44,cross(r5a,f5));
142
143     if M4(i)>0
144         L4_long(i)=L4;
145         break
146     end
147 end
148     end
149 end

```

```

150
151 %% Calculating maximum location for counterweight to ensure safety
152
153 m5 = 0; % Assuming Payload fell off
154 for i=1:length(B) % Loop repeats for every slew angle
155     for j = 1:length(L4_range) % Loop repeats for every value ...
156         of L4
157             L4 = L4_range(j);
158             p2 = acos(L4/L3); % Mast angle
159 %Set up coordinate systems for mass centers
160 c1 = [0 0 h/2]'; % Car Body mass center
161 c2 = [L2*cos(p1)*cos(B(i))/2,...
162       L2*cos(p1)*sin(B(i))/2,...
163       (L2*sin(p1)/2)+h]'; % Boom mass center
164 c3 = [-L3*cos(p2)*cos(B(i))/2,...
165       -L3*cos(p2)*sin(B(i))/2,...
166       (L3*sin(p2)/2)+h]'; % Mast mass center
167 c4 = [-L4*cos(B(i)),...
168       -L4*sin(B(i)), h]'; % Moving counterweight mass center
169 c4.fixed = [-7*cos(B(i)),...
170            -7*sin(B(i)), 3]'; % Fixed counterweight mass center
171 c5 = [L2*cos(p1)*cos(B(i)),...
172       L2*cos(p1)*sin(B(i)),...
173       L2*sin(p1)+h-L5]'; % Payload mass center
174
175 % Forces:
176 G = [0 0 -1]'; % Direction of gravitational force
177 f1 = m1*g*G; % Weight of car body
178 f2 = m2*g*G; % Weight of boom
179 f3 = m3*g*G; % Weight of mast
180 f4 = m4*g*G; % Weight of moveable counterweight
181 f4.fixed = m4.fixed*g*G; % Weight of fixed counterweight

```



```

181 f5 = m5*g*G; % Weight of payload
182
183 % Instantaneous inertial location of the ith ground contact point
184 p01 = [-L1/2 w/2 0]';
185 p02 = [L1/2 w/2 0]';
186 p03 = [L1/2 -w/2 0]';
187 p04 = [-L1/2 -w/2 0]';
188
189 % ith tip-over mode axis
190 a1 = p02-p01;
191 a2 = p03-p02;
192 a3 = p04-p03;
193 a4 = p01-p04;
194
195 % Expressing each ith tip-over mode axis as a unit vector
196 a11 = -a1/norm(a1);
197 a22 = -a2/norm(a2);
198 a33 = -a3/norm(a3);
199 a44 = -a4/norm(a4);
200
201 % Deciding which is the tip-over axis based on the value of the ...
    slew angle
202 theta1 = atan((w/2)/(L1/2));
203 theta2 = pi-theta1;
204 %-----
205 if B(i)<theta1 % Tip over axis is a4
206     pa4 = [-L1/2 0 0]'; % Location of a point on axis a4
207     % Vectors pointing from mass centers to the point on a4
208     r1a = c1-pa4;
209     r2a = c2-pa4;
210     r3a = c3-pa4;
211     r4a = c4-pa4;

```

```

212 r4a_fixed = c4_fixed-pa4;
213 r5a = c5-pa4;
214
215 % Calculating sum of moments about axis a4:
216 M4(i) = dot(a44,cross(r1a,f1))+dot(a44,cross(r2a,f2))+...
217         dot(a44,cross(r3a,f3))+dot(a44,cross(r4a,f4))+...
218         dot(a44,cross(r4a_fixed,f4_fixed))+dot(a44,cross(r5a,f5));
219
220     if M4(i)>0 % Loop chooses value of L4 to prevent tip-over
221         L4_short(i)=L4;
222         break
223     end
224 end
225 %-----
226 if B(i)>theta1 && B(i)<theta2 % Tip over axis is a3
227     pa3 = [0 -w/2 0]'; % Location of a point on axis a3
228     % Vectors pointing from mass centers to the point on a3
229     r1a = c1-pa3;
230     r2a = c2-pa3;
231     r3a = c3-pa3;
232     r4a = c4-pa3;
233     r4a_fixed = c4_fixed-pa3;
234     r5a = c5-pa3;
235
236 % Calculating sum of moments about axis a3:
237 M3(i) = dot(a33,cross(r1a,f1))+dot(a33,cross(r2a,f2))+...
238         dot(a33,cross(r3a,f3))+dot(a33,cross(r4a,f4))+...
239         dot(a33,cross(r4a_fixed,f4_fixed))+dot(a33,cross(r5a,f5));
240
241     if M3(i)>0 % Loop chooses value of L4 to prevent tip-over
242         L4_short(i)=L4;
243         break

```

```

244         end
245     end
246     %-----
247     if B(i)>theta2 % Tip over axis is a2
248         pa2 = [L1/2 0 0]'; % Location of a point on axis a2
249         % Vectors pointing from mass centers to the point on a2
250         r1a = c1-pa2;
251         r2a = c2-pa2;
252         r3a = c3-pa2;
253         r4a = c4-pa2;
254         r4a.fixed = c4.fixed-pa2;
255         r5a = c5-pa2;
256
257         % Calculating sum of moments about axis a2:
258         M2(i) = dot(a22,cross(r1a,f1))+dot(a22,cross(r2a,f2))+...
259                 dot(a22,cross(r3a,f3))+dot(a22,cross(r4a,f4))+...
260                 dot(a22,cross(r4a.fixed,f4.fixed))+dot(a22,cross(r5a,f5));
261
262         if M2(i)>0 % Loop chooses value of L4 to prevent tip-over
263             L4_short(i)=L4;
264             break
265         end
266     end
267         end
268     end
269
270     %% Plotting
271     figure
272
273     x = [B,B];
274     yb = [L4_short(:);-fliplr(L4_short(:))]' ;
275     yf = [L4_long(:);-fliplr(L4_long(:))]' ;

```

```

276     polar(x,yb)
277     hold on
278     polar(x,yf)
279     xlabel('Slew Angle \beta [deg]')
280     ylabel('Counterweight Position [m]')
281     legend('Maximum','Minimum')

```

Listing A.4: Forward Tip-over Analysis (m_5 is the variable)

```

1 % This code calculates the counterweight displacement with ...
   respect to
2 % different slew angles in order to prevent forward tip-over, ...
   this is done
3 % for three values of payload mass
4
5 clear
6
7 %% Defining all parameters
8 g=9.8;           % Gravitational acceleration [m/s^2]
9 % Defining Lengths of different components
10 L1 = 10.33;     % Length of Base Body [m]
11 L2 = 102;      % Length of boom [m]
12 L3 = 30;       % Length of mast [m]
13 L4_fixed = 7;  % Position of fixed counterweight [m]
14 L5 = 10;       % Length of payload hoist [m]
15 L4_min = 0;    % Minimum position of moveable ...
   counterweight [m]
16 L4_max = 100;  % Maximum position of moveable ...
   counterweight [m]
17 % Range of allowed locations for counterwieght [m]
18 L4_range = linspace(L4_min,L4_max,500);
19 % Other dimensions

```

```

20 w = 8.4; % Width of base [m]
21 h = 2.45; % Height of base [m]
22 % Mass parameters
23 m1 = 125; % Mass of Car Body [tons]
24 m2 = 60; % Mass of boom [tons]
25 m3 = 12.5; % Mass of mast [tons]
26 m5i = [110 160 210]; % Different masses of payloads [tons]
27 m4_fixed = 240; % Mass of fixed counterweight [tons]
28 m4 = 200 ; % Mass of moveable counterweight [tons]
29 % Angles
30 p1 = 62*pi/180; % Boom Luffing Angle [rad]
31 B = linspace(0,pi,50); % Slewing Angle [rad]
32
33 %% Calculating minimum location of counterweight to ensure safety
34
35 for k=1:length(m5i) % Loop repeats for each value of m5
36     m5 = m5i(k);
37     for i=1:length(B) % Loop repeats for every slew angle
38         for j = length(L4_range):-1:1 % Loop repeats for every ...
39             value of L4
40                 L4 = L4_range(j);
41                 p2 = acos(L4/L3); % Mast angle
42 % Set up coordinate systems for mass centers
43 c1 = [0 0 h/2]'; % Car Body mass center
44 c2 = [L2*cos(p1)*cos(B(i))/2,...
45       L2*cos(p1)*sin(B(i))/2,...
46       (L2*sin(p1)/2)+h]'; % Boom mass center
47 c3 = [-L3*cos(p2)*cos(B(i))/2,...
48       -L3*cos(p2)*sin(B(i))/2,...
49       (L3*sin(p2)/2)+h]'; % Mast mass center
50 c4 = [-L4*cos(B(i)),...
51       -L4*sin(B(i)), h]'; % Moving counterweight mass center

```

```

51 c4.fixed = [-7*cos(B(i)),...
52           -7*sin(B(i)), 3]'; % Fixed counterweight mass center
53 c5 = [L2*cos(p1)*cos(B(i)),...
54       L2*cos(p1)*sin(B(i)),...
55       L2*sin(p1)+h-L5]'; % Payload mass center
56
57 % Forces:
58 G = [0 0 -1]'; % Direction of gravitational force
59 f1 = m1*g*G; % Weight of car body
60 f2 = m2*g*G; % Weight of boom
61 f3 = m3*g*G; % Weight of mast
62 f4 = m4*g*G; % Weight of moveable counterweight
63 f4.fixed = m4.fixed*g*G; % Weight of fixed counterweight
64 f5 = m5*g*G; % Weight of payload
65
66 % Instantaneous inertial location of the ith ground contact point
67 p01 = [-L1/2 w/2 0]';
68 p02 = [L1/2 w/2 0]';
69 p03 = [L1/2 -w/2 0]';
70 p04 = [-L1/2 -w/2 0]';
71
72 % ith tip-over mode axis
73 a1 = p02-p01;
74 a2 = p03-p02;
75 a3 = p04-p03;
76 a4 = p01-p04;
77
78 % Expressing each ith tip-over mode axis as a unit vector
79 a11 = -a1/norm(a1);
80 a22 = -a2/norm(a2);
81 a33 = a3/norm(a3);
82 a44 = -a4/norm(a4);

```

```

83
84 % Deciding which is the tip-over axis based on the value of the ...
      slew angle
85 theta1 = atan((w/2)/(L1/2));
86 theta2 = pi-theta1;
87 %-----
88 if B(i)<theta1 % Tip over axis is a2
89     pa2 = [L1/2 0 0]';           % Location of a point on axis a2
90     % Vectors pointing from mass centers to the point on a2
91     r1a = c1-pa2;
92     r2a = c2-pa2;
93     r3a = c3-pa2;
94     r4a = c4-pa2;
95     r4a.fixed = c4.fixed-pa2;
96     r5a = c5-pa2;
97
98     % Calculating sum of moments about axis a2:
99     M2(i) = dot(a22,cross(r1a,f1))+dot(a22,cross(r2a,f2))+...
100           dot(a22,cross(r3a,f3))+dot(a22,cross(r4a,f4))+...
101           dot(a22,cross(r4a.fixed,f4.fixed))+dot(a22,cross(r5a,f5));
102
103     if M2(i)>0 % Loop chooses value of L4 to prevent tip-over
104         L4.long(k,i)=L4;
105         break
106     end
107 end
108 %-----
109 if B(i)>=theta1 && B(i)<=theta2 % Tip over axis is a1
110     pa1 = [0 w/2 0]';           % Location of a point on axis a1
111     % Vectors pointing from mass centers to the point on a1
112     r1a = c1-pa1;
113     r2a = c2-pa1;

```

```

114   r3a = c3-pa1;
115   r4a = c4-pa1;
116   r4a.fixed = c4.fixed-pa1;
117   r5a = c5-pa1;
118
119   % Calculating sum of moments about axis a1:
120   M1(i) = dot(a11,cross(r1a,f1))+dot(a11,cross(r2a,f2))+...
121           dot(a11,cross(r3a,f3))+dot(a11,cross(r4a,f4))+...
122           dot(a11,cross(r4a.fixed,f4.fixed))+dot(a11,cross(r5a,f5));
123
124       if M1(i)>0 % Loop chooses value of L4 to prevent tip-over
125           L4.long(k,i)=L4;
126           break
127       end
128   end
129   %-----
130   if B(i)>theta2 % Tip over axis is a4
131       pa4 = [-L1/2 0 0]'; % Location of a point on axis a4
132       % Vectors pointing from mass centers to the point on a4
133       r1a = c1-pa4;
134       r2a = c2-pa4;
135       r3a = c3-pa4;
136       r4a = c4-pa4;
137       r4a.fixed = c4.fixed-pa4;
138       r5a = c5-pa4;
139
140       % Calculating sum of moments about axis a4:
141       M4(i) = dot(a44,cross(r1a,f1))+dot(a44,cross(r2a,f2))+...
142             dot(a44,cross(r3a,f3))+dot(a44,cross(r4a,f4))+...
143             dot(a44,cross(r4a.fixed,f4.fixed))+dot(a44,cross(r5a,f5));
144
145       if M4(i)>0

```



```

146         L4.long(k,i)=L4;
147         break
148     end
149 end
150     end
151 end
152 end
153
154 %% Plotting
155 figure
156 for k = length(m5i):-1:1
157     x = [B,B];
158     y = [L4.long(k,:),-fliplr(L4.long(k,:))];
159     polar(x,y)
160     xlabel('Slew Angle \beta [deg]')
161     ylabel('Counterweight Position [m]')
162     legend('m_5 = 210 t','m_5 = 160 t','m_5 = 110 t')
163     hold on
164 end

```

Listing A.5: Forward Tip-over Analysis (ϕ_1 is the variable)

```

1 % This code calculates the counterweight displacement with ...
   respect to
2 % different slew angles in order to prevent forward tip-over, ...
   this is done
3 % for three values of luffing angle
4
5 clear
6
7 %% Defining all parameters
8 g=9.8;           % Gravitational acceleration [m/s^2]

```

```

9 % Defining Lengths of different components
10 L1 = 10.33;           % Length of Base Body [m]
11 L2 = 102;           % Length of boom [m]
12 L3 = 30;           % Length of mast [m]
13 L4_fixed = 7;       % Position of fixed counterweight [m]
14 L5 = 10;           % Length of payload hoist [m]
15 L4_min = 0;         % Minimum position of moveable ...
    counterweight [m]
16 L4_max = 100;       % Maximum position of moveable ...
    counterweight [m]
17 % Range of allowed locations for counterweight [m]
18 L4_range = linspace(L4_min,L4_max,500);
19 % Other dimensions
20 w = 8.4;           % Width of base [m]
21 h = 2.45;         % Height of base [m]
22 % Mass parameters
23 m1 = 125;          % Mass of Car Body [tons]
24 m2 = 60;           % Mass of boom [tons]
25 m3 = 12.5;         % Mass of mast [tons]
26 m4 = 200;          % Mass of moveable counterweight [tons]
27 m4_fixed = 240;    % Mass of fixed counterweight [tons]
28 m5 = 110 ;         % Mass of Payload [tons]
29 % Angles
30 pli = [30 45 60]*pi/180; % Different values of boom luffing ...
    angles [rad]
31 B = linspace(0,pi,50); % Slewing Angle [rad]
32
33 %% Calculating minimum location of counterweight to ensure safety
34
35 for k=1:length(pli) % Loop repeats for each value of pl
36     pl = pli(k);
37     for i=1:length(B) % Loop repeats for every slew angle

```

```

38     for j = length(L4_range):-1:1 % Loop repeats for every ...
        value of L4
39         L4 = L4_range(j);
40         p2 = acos(L4/L3); % Mast angle
41 % Set up coordinate systems for mass centers
42 c1 = [0 0 h/2]'; % Car Body mass center
43 c2 = [L2*cos(p1)*cos(B(i))/2,...
44       L2*cos(p1)*sin(B(i))/2,...
45       (L2*sin(p1)/2)+h]'; % Boom mass center
46 c3 = [-L3*cos(p2)*cos(B(i))/2,...
47       -L3*cos(p2)*sin(B(i))/2,...
48       (L3*sin(p2)/2)+h]'; % Mast mass center
49 c4 = [-L4*cos(B(i)),...
50       -L4*sin(B(i)), h]'; % Moving counterweight mass center
51 c4_fixed = [-7*cos(B(i)),...
52            -7*sin(B(i)), 3]'; % Fixed counterweight mass center
53 c5 = [L2*cos(p1)*cos(B(i)),...
54       L2*cos(p1)*sin(B(i)),...
55       L2*sin(p1)+h-L5]'; % Payload mass center
56
57 % Forces:
58 G = [0 0 -1]'; % Direction of gravitational force
59 f1 = m1*g*G; % Weight of car body
60 f2 = m2*g*G; % Weight of boom
61 f3 = m3*g*G; % Weight of mast
62 f4 = m4*g*G; % Weight of moveable counterweight
63 f4_fixed = m4_fixed*g*G; % Weight of fixed counterweight
64 f5 = m5*g*G; % Weight of payload
65
66 % Instantaneous inertial location of the ith ground contact point
67 p01 = [-L1/2 w/2 0]';
68 p02 = [L1/2 w/2 0]';

```

```

69 p03 = [L1/2 -w/2 0]';
70 p04 = [-L1/2 -w/2 0]';
71
72 % ith tip-over mode axis
73 a1 = p02-p01;
74 a2 = p03-p02;
75 a3 = p04-p03;
76 a4 = p01-p04;
77
78 % Expressing each ith tip-over mode axis as a unit vector
79 a11 = -a1/norm(a1);
80 a22 = -a2/norm(a2);
81 a33 = a3/norm(a3);
82 a44 = -a4/norm(a4);
83
84 % Deciding which is the tip-over axis based on the value of the ...
      slew angle
85 theta1 = atan((w/2)/(L1/2));
86 theta2 = pi-theta1;
87 %-----
88 if B(i)<theta1 % Tip over axis is a2
89     pa2 = [L1/2 0 0]'; % Location of a point on axis a2
90     % Vectors pointing from mass centers to the point on a2
91     r1a = c1-pa2;
92     r2a = c2-pa2;
93     r3a = c3-pa2;
94     r4a = c4-pa2;
95     r4a.fixed = c4.fixed-pa2;
96     r5a = c5-pa2;
97
98     % Calculating sum of moments about axis a2:
99     M2(i) = dot(a22,cross(r1a,f1))+dot(a22,cross(r2a,f2))+...

```

```

100         dot(a22,cross(r3a,f3))+dot(a22,cross(r4a,f4))+...
101         dot(a22,cross(r4a.fixed,f4.fixed))+dot(a22,cross(r5a,f5));
102
103     if M2(i)>0 % Loop chooses value of L4 to prevent tip-over
104         L4.long(k,i)=L4;
105         break
106     end
107 end
108 %-----
109 if B(i)>theta1 && B(i)<=theta2 % Tip over axis is a1
110     pa1 = [0 w/2 0]'; % Location of a point on axis a1
111     % Vectors pointing from mass centers to the point on a1
112     r1a = c1-pa1;
113     r2a = c2-pa1;
114     r3a = c3-pa1;
115     r4a = c4-pa1;
116     r4a.fixed = c4.fixed-pa1;
117     r5a = c5-pa1;
118
119     % Calculating sum of moments about axis a1:
120     M1(i) = dot(a11,cross(r1a,f1))+dot(a11,cross(r2a,f2))+...
121             dot(a11,cross(r3a,f3))+dot(a11,cross(r4a,f4))+...
122             dot(a11,cross(r4a.fixed,f4.fixed))+dot(a11,cross(r5a,f5));
123
124     if M1(i)>0 % Loop chooses value of L4 to prevent tip-over
125         L4.long(k,i)=L4;
126         break
127     end
128 end
129 %-----
130 if B(i)>theta2 % Tip over axis is a4
131     pa4 = [-L1/2 0 0]'; % Location of a point on axis a4

```

```

132 % Vectors pointing from mass centers to the point on a4
133 r1a = c1-pa4;
134 r2a = c2-pa4;
135 r3a = c3-pa4;
136 r4a = c4-pa4;
137 r4a_fixed = c4_fixed-pa4;
138 r5a = c5-pa4;
139
140 % Calculating sum of moments about axis a4:
141 M4(i) = dot(a44,cross(r1a,f1))+dot(a44,cross(r2a,f2))+...
142         dot(a44,cross(r3a,f3))+dot(a44,cross(r4a,f4))+...
143         dot(a44,cross(r4a_fixed,f4_fixed))+dot(a44,cross(r5a,f5));
144
145     if M4(i)>0
146         L4_long(k,i)=L4;
147         break
148     end
149 end
150     end
151 end
152 end
153
154 %% Plotting
155 figure
156 for k = 1:length(pli)
157     x = [B,B];
158     y = [L4_long(k,:),-fliplr(L4_long(k,:))];
159     polar(x,y)
160     xlabel('Slew Angle \beta [deg]')
161     ylabel('Counterweight Position [m]')
162     legend('\phi_1 = 30', '\phi_1 = 45', '\phi_1 = 60')
163     hold on

```

Listing A.6: Backward Tip-over Analysis (ϕ_1 is the variable)

```

1 % This code calculates the counterweight displacement with ...
    respect to
2 % different slew angles in order to prevent backward tip-over, ...
    this is done
3 % for three values of luffing angle
4
5 clear
6
7 %% Defining all parameters
8 g=9.8;                % Gravitational acceleration [m/s^2]
9 % Defining Lengths of different components
10 L1 = 10.33;          % Length of Base Body [m]
11 L2 = 102;           % Length of boom [m]
12 L3 = 30;            % Length of mast [m]
13 L4_fixed = 7;       % Position of fixed counterweight [m]
14 L5 = 10;            % Length of payload hoist [m]
15 L4_min = 0;         % Minimum position of moveable ...
    counterweight [m]
16 L4_max = 100;       % Maximum position of moveable ...
    counterweight [m]
17 % Range of allowed locations for counterweight [m]
18 L4_range = linspace(L4_min,L4_max,500);
19 % Other dimensions
20 w = 8.4;            % Width of base [m]
21 h = 2.45;          % Height of base [m]
22 % Mass parameters
23 m1 = 125;           % Mass of Car Body [tons]
24 m2 = 60;            % Mass of boom [tons]

```

```

25 m3 = 12.5; % Mass of mast [tons]
26 m4 = 200; % Mass of moveable counterweight [tons]
27 m4.fixed = 240; % Mass of fixed counterweight [tons]
28 m5 = 0; % Mass of Payload [tons]
29 % Angles
30 pli = [30 45 60]*pi/180; % Different values of boom luffing ...
    angles [rad]
31 B = linspace(0,pi,50); % Slewing Angle [rad]
32
33 %% Calculating maximum location for counterweight to ensure safety
34
35 for k=1:length(pli) % Loop repeats for each value of pl
36     p1 = pli(k);
37     for i=1:length(B) % Loop repeats for every slew angle
38         for j = 1:length(L4_range) % Loop repeats for every value ...
39             of L4
40                 L4 = L4_range(j);
41                 p2 = acos(L4/L3); % Mast angle
42 %Set up coordinate systems for mass centers
43 c1 = [0 0 h/2]'; % Car Body mass center
44 c2 = [L2*cos(p1)*cos(B(i))/2,...
45       L2*cos(p1)*sin(B(i))/2,...
46       (L2*sin(p1)/2)+h]'; % Boom mass center
47 c3 = [-L3*cos(p2)*cos(B(i))/2,...
48       -L3*cos(p2)*sin(B(i))/2,...
49       (L3*sin(p2)/2)+h]'; % Mast mass center
50 c4 = [-L4*cos(B(i)),...
51       -L4*sin(B(i)), h]'; % Moving counterweight mass center
52 c4.fixed = [-7*cos(B(i)),...
53            -7*sin(B(i)), 3]'; % Fixed counterweight mass center
54 c5 = [L2*cos(p1)*cos(B(i)),...
55       L2*cos(p1)*sin(B(i)),...

```



```

55     L2*sin(p1)+h-L5]';           % Payload mass center
56
57 % Forces:
58 G = [0 0 -1]';               % Direction of gravitational force
59 f1 = m1*g*G;                 % Weight of car body
60 f2 = m2*g*G;                 % Weight of boom
61 f3 = m3*g*G;                 % Weight of mast
62 f4 = m4*g*G;                 % Weight of moveable counterweight
63 f4_fixed = m4_fixed*g*G;     % Weight of fixed counterweight
64 f5 = m5*g*G;                 % Weight of payload
65
66 % Instantaneous inertial location of the ith ground contact point
67 p01 = [-L1/2 w/2 0]';
68 p02 = [L1/2 w/2 0]';
69 p03 = [L1/2 -w/2 0]';
70 p04 = [-L1/2 -w/2 0]';
71
72 % ith tip-over mode axis
73 a1 = p02-p01;
74 a2 = p03-p02;
75 a3 = p04-p03;
76 a4 = p01-p04;
77
78 % Expressing each ith tip-over mode axis as a unit vector
79 a11 = -a1/norm(a1);
80 a22 = -a2/norm(a2);
81 a33 = -a3/norm(a3);
82 a44 = -a4/norm(a4);
83
84 % Deciding which is the tip-over axis based on the value of the ...
      slew angle
85 theta1 = atan((w/2)/(L1/2));

```

```

86 theta2 = pi-theta1;
87 %-----
88 if B(i)<theta1 % Tip over axis is a4
89     pa4 = [-L1/2 0 0]'; % Location of a point on axis a4
90     % Vectors pointing from mass centers to the point on a4
91     r1a = c1-pa4;
92     r2a = c2-pa4;
93     r3a = c3-pa4;
94     r4a = c4-pa4;
95     r4a.fixed = c4.fixed-pa4;
96     r5a = c5-pa4;
97
98     % Calculating sum of moments about axis a4:
99     M4(i) = dot(a44,cross(r1a,f1))+dot(a44,cross(r2a,f2))+...
100            dot(a44,cross(r3a,f3))+dot(a44,cross(r4a,f4))+...
101            dot(a44,cross(r4a.fixed,f4.fixed))+dot(a44,cross(r5a,f5));
102
103     if M4(i)>0 % Loop chooses value of L4 to prevent tip-over
104         L4.short(k,i)=L4;
105         break
106     end
107 end
108 %-----
109 if B(i)>theta1 && B(i)<=theta2 % Tip over axis is a3
110     pa3 = [0 -w/2 0]'; % Location of a point on axis a3
111     % Vectors pointing from mass centers to the point on a3
112     r1a = c1-pa3;
113     r2a = c2-pa3;
114     r3a = c3-pa3;
115     r4a = c4-pa3;
116     r4a.fixed = c4.fixed-pa3;
117     r5a = c5-pa3;

```

```

118
119 % Calculating sum of moments about axis a3:
120 M3(i) = dot(a33,cross(r1a,f1))+dot(a33,cross(r2a,f2))+...
121         dot(a33,cross(r3a,f3))+dot(a33,cross(r4a,f4))+...
122         dot(a33,cross(r4a_fixed,f4_fixed))+dot(a33,cross(r5a,f5));
123
124     if M3(i)>0 % Loop chooses value of L4 to prevent tip-over
125         L4_short(k,i)=L4;
126         break
127     end
128 end
129 %-----
130 if B(i)>theta2 % Tip over axis is a2
131     pa2 = [L1/2 0 0]'; % Location of a point on axis a2
132     % Vectors pointing from mass centers to the point on a2
133     r1a = c1-pa2;
134     r2a = c2-pa2;
135     r3a = c3-pa2;
136     r4a = c4-pa2;
137     r4a_fixed = c4_fixed-pa2;
138     r5a = c5-pa2;
139
140 % Calculating sum of moments about axis a2:
141 M2(i) = dot(a22,cross(r1a,f1))+dot(a22,cross(r2a,f2))+...
142         dot(a22,cross(r3a,f3))+dot(a22,cross(r4a,f4))+...
143         dot(a22,cross(r4a_fixed,f4_fixed))+dot(a22,cross(r5a,f5));
144
145     if M2(i)>0 % Loop chooses value of L4 to prevent tip-over
146         L4_short(k,i)=L4;
147         break
148     end
149 end

```

```

150         end
151     end
152 end
153
154 %% Plotting
155 figure
156 for k = 1:length(phi)
157     x = [B,B];
158     y = [L4_short(k,:),-fliplr(L4_short(k,:))];
159     polar(x,y)
160     xlabel('Slew Angle \beta [deg]')
161     ylabel('Counterweight Position [m]')
162     legend('\phi_1 = 30', '\phi_1 = 45', '\phi_1 = 60')
163     hold on
164 end

```

Listing A.7: Forward Tip-over Analysis for the jib configuration (m_4 is the variable)

```

1 % This code calculates the counterweight displacement with ...
   respect to
2 % different slew angles in order to prevent forward tip-over, ...
   this is done
3 % for three values of moveable counterweight mass (jib configuration)
4
5 clear
6
7 %% Defining all parameters
8 g=9.8;           % Gravitational acceleration [m/s^2]
9 % Defining Lengths of different components
10 L1 = 10.33;     % Length of Base Body [m]
11 L2 = 96;       % Length of boom [m]
12 L3 = 30;       % Length of mast [m]

```

```

13 L4.fixed = 7;           % Position of fixed counterweight [m]
14 L5 = 50;               % Length of payload hoist [m]
15 L6 = 96;               % Length of jib [m]
16 L4_min = 0;           % Minimum position of moveable ...
    counterweight [m]
17 L4_max = 100;         % Maximum position of moveable ...
    counterweight [m]
18 % Range of allowed locations for counterweight [m]
19 L4_range = linspace(L4_min,L4_max,500);
20 % Other dimensions
21 w = 8.4;               % Width of base [m]
22 h = 2.45;             % Height of base [m]
23 % Mass parameters
24 m1 = 125;              % Mass of Car Body [tons]
25 m2 = 56;               % Mass of boom [tons]
26 m3 = 12.5;            % Mass of mast [tons]
27 m4i = [150 200 300]; % Different masses of moveable ...
    counterweight [tons]
28 m4.fixed = 240;       % Mass of fixed counterweight [tons]
29 m5 = 65;               % Mass of Payload [tons]
30 m6 = 40;               % Mass of jib [tons]
31 % Angles
32 p1 = 65*pi/180;       % Boom Luffing Angle [rad]
33 p3 = p1-15*pi/180;    % Jib angle wrt x-axis [rad]
34 B = linspace(0,pi,50); % Slewing Angle [rad]
35
36 %% Calculating minimum location of counterweight to ensure safety
37
38 for k=1:length(m4i) % Loop repeats for each value of m4
39     m4 = m4i(k);
40     for i=1:length(B) % Loop repeats for every slew angle

```

```

41     for j = length(L4_range):-1:1 % Loop repeats for every ...
        value of L4
42         L4 = L4_range(j);
43         p2 = acos(L4/L3); % Mast angle
44 % Set up coordinate systems for mass centers
45 c1 = [0 0 h/2]'; % Car Body mass center
46 c2 = [L2*cos(p1)*cos(B(i))/2,...
47       L2*cos(p1)*sin(B(i))/2,...
48       (L2*sin(p1)/2)+h]'; % Boom mass center
49 c3 = [-L3*cos(p2)*cos(B(i))/2,...
50       -L3*cos(p2)*sin(B(i))/2,...
51       (L3*sin(p2)/2)+h]'; % Mast mass center
52 c4 = [-L4*cos(B(i)),...
53       -L4*sin(B(i)), h]'; % Moving counterweight mass center
54 c4_fixed = [-7*cos(B(i)),...
55             -7*sin(B(i)), 3]'; % Fixed counterweight mass center
56 c5 = [L2*cos(p1)*cos(B(i)),...
57       L2*cos(p1)*sin(B(i)),...
58       L2*sin(p1)+h-L5]'; % Payload mass center
59 c6 = [(L2*cos(p1)+0.5*L6*cos(p3))*cos(B(i)),...
60       (L2*cos(p1)+.5*L6*cos(p3))*sin(B(i)),...
61       L2*sin(p1)+.5*L6*sin(p3)+h]'; % Jib mass center
62
63 % Forces:
64 G = [0 0 -1]'; % Direction of gravitational force
65 f1 = m1*g*G; % Weight of car body
66 f2 = m2*g*G; % Weight of boom
67 f3 = m3*g*G; % Weight of mast
68 f4 = m4*g*G; % Weight of moveable counterweight
69 f4_fixed = m4_fixed*g*G; % Weight of fixed counterweight
70 f5 = m5*g*G; % Weight of payload
71 f6 = m6*g*G; % Weight of jib

```

```

72
73 % Instantaneous inertial location of the ith ground contact point
74 p01 = [-L1/2 w/2 0]';
75 p02 = [L1/2 w/2 0]';
76 p03 = [L1/2 -w/2 0]';
77 p04 = [-L1/2 -w/2 0]';
78
79 % ith tip-over mode axis
80 a1 = p02-p01;
81 a2 = p03-p02;
82 a3 = p04-p03;
83 a4 = p01-p04;
84
85 % Expressing each ith tip-over mode axis as a unit vector
86 a11 = -a1/norm(a1);
87 a22 = -a2/norm(a2);
88 a33 = a3/norm(a3);
89 a44 = -a4/norm(a4);
90
91 % Deciding which is the tip-over axis based on the value of the ...
    slew angle
92 theta1 = atan((w/2)/(L1/2));
93 theta2 = pi-theta1;
94 %-----
95 if B(i)<theta1 % Tip over axis is a2
96     pa2 = [L1/2 0 0]'; % Location of a point on axis a2
97     % Vectors pointing from mass centers to the point on a2
98     r1a = c1-pa2;
99     r2a = c2-pa2;
100    r3a = c3-pa2;
101    r4a = c4-pa2;
102    r4a.fixed = c4.fixed-pa2;

```

```

103   r5a = c5-pa2;
104   r6a = c6-pa2;
105
106   % Calculating sum of moments about axis a2:
107   M2(i) = dot(a22,cross(r1a,f1))+dot(a22,cross(r2a,f2))+...
108           dot(a22,cross(r3a,f3))+dot(a22,cross(r4a,f4))+...
109           dot(a22,cross(r4a.fixed,f4.fixed))+...
110           dot(a22,cross(r5a,f5))+dot(a22,cross(r6a,f6));
111
112       if M2(i)>0 % Loop chooses value of L4 to prevent tip-over
113           L4.long(k,i)=L4;
114           break
115       end
116 end
117 %-----
118 if B(i)≥theta1 && B(i)≤theta2 % Tip over axis is a1
119     pa1 = [0 w/2 0]';           % Location of a point on axis a1
120     % Vectors pointing from mass centers to the point on a1
121     r1a = c1-pa1;
122     r2a = c2-pa1;
123     r3a = c3-pa1;
124     r4a = c4-pa1;
125     r4a.fixed = c4.fixed-pa1;
126     r5a = c5-pa1;
127     r6a = c6-pa1;
128
129     % Calculating sum of moments about axis a1:
130     M1(i) = dot(a11,cross(r1a,f1))+dot(a11,cross(r2a,f2))+...
131             dot(a11,cross(r3a,f3))+dot(a11,cross(r4a,f4))+...
132             dot(a11,cross(r4a.fixed,f4.fixed))+...
133             dot(a11,cross(r5a,f5))+dot(a11,cross(r6a,f6));
134

```



```

135         if M1(i)>0 % Loop chooses value of L4 to prevent tip-over
136             L4_long(k,i)=L4;
137             break
138         end
139     end
140 %-----
141 if B(i)>theta2 % Tip over axis is a4
142     pa4 = [-L1/2 0 0]'; % Location of a point on axis a4
143     % Vectors pointing from mass centers to the point on a4
144     r1a = c1-pa4;
145     r2a = c2-pa4;
146     r3a = c3-pa4;
147     r4a = c4-pa4;
148     r4a_fixed = c4_fixed-pa4;
149     r5a = c5-pa4;
150     r6a = c6-pa4;
151
152     % Calculating sum of moments about axis a4:
153     M4(i) = dot(a44,cross(r1a,f1))+dot(a44,cross(r2a,f2))+...
154             dot(a44,cross(r3a,f3))+dot(a44,cross(r4a,f4))+...
155             dot(a44,cross(r4a_fixed,f4_fixed))+...
156             dot(a44,cross(r5a,f5))+dot(a44,cross(r6a,f6));
157
158     if M4(i)>0
159         L4_long(k,i)=L4;
160         break
161     end
162 end
163     end
164 end
165 end
166

```

```

167 %% Plotting
168 figure
169 for k = 1:length(m4i)
170     x = [B,B];
171     y = [L4_long(k,:),-fliplr(L4_long(k,:))];
172     polar(x,y)
173     xlabel('Slew Angle \beta [deg]')
174     ylabel('Counterweight Position [m]')
175     legend('m_4 = 150 t','m_4 = 200 t','m_4 = 300 t')
176     hold on
177 end

```

Listing A.8: Backward Tip-over Analysis for the jib configuration (m_4 is the variable)

```

1 % This code calculates the counterweight displacement with ...
   respect to
2 % different slew angles in order to prevent backward tip-over, ...
   this is done
3 % for three values of moveable counterweight mass (jib configuration)
4
5 clear
6
7 %% Defining all parameters
8 g=9.8; % Gravitational acceleration [m/s^2]
9 % Defining Lengths of different components
10 L1 = 10.33; % Length of Base Body [m]
11 L2 = 96; % Length of boom [m]
12 L3 = 30; % Length of mast [m]
13 L4_fixed = 7; % Position of fixed counterweight [m]
14 L5 = 50; % Length of payload hoist [m]
15 L6 = 96; % Length of jib [m]

```

```

16 L4_min = 0; % Minimum position of moveable ...
    counterweight [m]
17 L4_max = 100; % Maximum position of moveable ...
    counterweight [m]
18 % Range of allowed locations for counterweight [m]
19 L4_range = linspace(L4_min,L4_max,500);
20 % Other dimensions
21 w = 8.4; % Width of base [m]
22 h = 2.45; % Height of base [m]
23 % Mass parameters
24 m1 = 125; % Mass of Car Body [tons]
25 m2 = 56; % Mass of boom [tons]
26 m3 = 12.5; % Mass of mast [tons]
27 m4i = [150 200 300]; % Different masses of moveable ...
    counterweight [tons]
28 m4_fixed = 240; % Mass of fixed counterweight [tons]
29 m5 = 0 ; % Mass of Payload [tons]
30 m6 = 40; % Mass of jib [tons]
31 % Angles
32 p1 = 65*pi/180; % Boom Luffing Angle [rad]
33 p3 = p1-15*pi/180; % Jib angle wrt x-axis [rad]
34 B = linspace(0,pi,50); % Slewing Angle [rad]
35
36 %% Calculating maximum location for counterweight to ensure safety
37
38 for k=1:length(m4i) % Loop repeats for each value of m4
39     m4 = m4i(k);
40     for i=1:length(B) % Loop repeats for every slew angle
41         for j = 1:length(L4_range) % Loop repeats for every value ...
42             of L4
43                 L4 = L4_range(j);
44                 p2 = acos(L4/L3); % Mast angle

```

```

44 %Set up coordinate systems for mass centers
45 c1 = [0 0 h/2]'; % Car Body mass center
46 c2 = [L2*cos(p1)*cos(B(i))/2,...
47       L2*cos(p1)*sin(B(i))/2,...
48       (L2*sin(p1)/2)+h]'; % Boom mass center
49 c3 = [-L3*cos(p2)*cos(B(i))/2,...
50       -L3*cos(p2)*sin(B(i))/2,...
51       (L3*sin(p2)/2)+h]'; % Mast mass center
52 c4 = [-L4*cos(B(i)),...
53       -L4*sin(B(i)), h]'; % Moving counterweight mass center
54 c4_fixed = [-7*cos(B(i)),...
55             -7*sin(B(i)), 3]'; % Fixed counterweight mass center
56 c5 = [L2*cos(p1)*cos(B(i)),...
57       L2*cos(p1)*sin(B(i)),...
58       L2*sin(p1)+h-L5]'; % Payload mass center
59 c6 = [(L2*cos(p1)+0.5*L6*cos(p3))*cos(B(i)),...
60       (L2*cos(p1)+.5*L6*cos(p3))*sin(B(i)),...
61       L2*sin(p1)+.5*L6*sin(p3)+h]'; % Jib mass center
62
63 % Forces:
64 G = [0 0 -1]'; % Direction of gravitational force
65 f1 = m1*g*G; % Weight of car body
66 f2 = m2*g*G; % Weight of boom
67 f3 = m3*g*G; % Weight of mast
68 f4 = m4*g*G; % Weight of moveable counterweight
69 f4_fixed = m4_fixed*g*G; % Weight of fixed counterweight
70 f5 = m5*g*G; % Weight of payload
71 f6 = m6*g*G; % Weight of jib
72
73 % Instantaneous inertial location of the ith ground contact point
74 p01 = [-L1/2 w/2 0]';
75 p02 = [L1/2 w/2 0]';

```

```

76 p03 = [L1/2 -w/2 0]';
77 p04 = [-L1/2 -w/2 0]';
78
79 % ith tip-over mode axis
80 a1 = p02-p01;
81 a2 = p03-p02;
82 a3 = p04-p03;
83 a4 = p01-p04;
84
85 % Expressing each ith tip-over mode axis as a unit vector
86 a11 = -a1/norm(a1);
87 a22 = -a2/norm(a2);
88 a33 = -a3/norm(a3);
89 a44 = -a4/norm(a4);
90
91 % Deciding which is the tip-over axis based on the value of the ...
    slew angle
92 theta1 = atan((w/2)/(L1/2));
93 theta2 = pi-theta1;
94 %-----
95 if B(i)<theta1 % Tip over axis is a4
96     pa4 = [-L1/2 0 0]'; % Location of a point on axis a4
97     % Vectors pointing from mass centers to the point on a4
98     r1a = c1-pa4;
99     r2a = c2-pa4;
100    r3a = c3-pa4;
101    r4a = c4-pa4;
102    r4a.fixed = c4.fixed-pa4;
103    r5a = c5-pa4;
104    r6a = c6-pa4;
105
106    % Calculating sum of moments about axis a4:

```

```

107 M4(i) = dot(a44,cross(r1a,f1))+dot(a44,cross(r2a,f2))+...
108       dot(a44,cross(r3a,f3))+dot(a44,cross(r4a,f4))+...
109       dot(a44,cross(r4a_fixed,f4_fixed))+...
110       dot(a44,cross(r5a,f5))+dot(a44,cross(r6a,f6));
111
112     if M4(i)>0 % Loop chooses value of L4 to prevent tip-over
113         L4_short(k,i)=L4;
114         break
115     end
116 end
117 %-----
118 if B(i)≥theta1 && B(i)≤theta2 % Tip over axis is a3
119     pa3 = [0 -w/2 0]'; % Location of a point on axis a3
120     % Vectors pointing from mass centers to the point on a3
121     r1a = c1-pa3;
122     r2a = c2-pa3;
123     r3a = c3-pa3;
124     r4a = c4-pa3;
125     r4a_fixed = c4_fixed-pa3;
126     r5a = c5-pa3;
127     r6a = c6-pa3;
128
129     % Calculating sum of moments about axis a3:
130     M3(i) = dot(a33,cross(r1a,f1))+dot(a33,cross(r2a,f2))+...
131           dot(a33,cross(r3a,f3))+dot(a33,cross(r4a,f4))+...
132           dot(a33,cross(r4a_fixed,f4_fixed))+...
133           dot(a33,cross(r5a,f5))+dot(a33,cross(r6a,f6));
134
135     if M3(i)>0 % Loop chooses value of L4 to prevent tip-over
136         L4_short(k,i)=L4;
137         break
138     end

```

```

139 end
140 %-----
141 if B(i)>theta2 % Tip over axis is a2
142     pa2 = [L1/2 0 0]'; % Location of a point on axis a2
143     % Vectors pointing from mass centers to the point on a2
144     r1a = c1-pa2;
145     r2a = c2-pa2;
146     r3a = c3-pa2;
147     r4a = c4-pa2;
148     r4a.fixed = c4.fixed-pa2;
149     r5a = c5-pa2;
150     r6a = c6-pa2;
151
152     % Calculating sum of moments about axis a2:
153     M2(i) = dot(a22,cross(r1a,f1))+dot(a22,cross(r2a,f2))+...
154             dot(a22,cross(r3a,f3))+dot(a22,cross(r4a,f4))+...
155             dot(a22,cross(r4a.fixed,f4.fixed))+...
156             dot(a22,cross(r5a,f5))+dot(a22,cross(r6a,f6));
157
158     if M2(i)>0 % Loop chooses value of L4 to prevent tip-over
159         L4_short(k,i)=L4;
160         break
161     end
162 end
163     end
164 end
165 end
166
167 %% Plotting
168 figure
169 for k = 1:length(m4i)
170     x = [B,B];

```

```

171     y = [L4_short(k,:),-fliplr(L4_short(k,:))];
172     polar(x,y)
173     xlabel('Slew Angle \beta [deg]')
174     ylabel('Counterweight Position [m]')
175     legend('m_4 = 150 t','m_4 = 200 t','m_4 = 300 t')
176     hold on
177 end

```

Listing A.9: Forward Tip-over Analysis for the jib configuration (ϕ_1 is the variable)

```

1 % This code calculates the counterweight displacement with ...
   respect to
2 % different slew angles in order to prevent forward tip-over, ...
   this is done
3 % for three values of luffing angle (jib configuration)
4
5 clear
6
7 %% Defining all parameters
8 g=9.8;           % Gravitational acceleration [m/s^2]
9 % Defining Lengths of different components
10 L1 = 10.33;     % Length of Base Body [m]
11 L2 = 96;       % Length of boom [m]
12 L3 = 30;       % Length of mast [m]
13 L4_fixed = 7;  % Position of fixed counterweight [m]
14 L5 = 50;       % Length of payload hoist [m]
15 L6 = 96;       % Length of jib [m]
16 L4_min = 0;    % Minimum position of moveable ...
   counterweight [m]
17 L4_max = 100;  % Maximum position of moveable ...
   counterweight [m]
18 % Range of allowed locations for counterweight [m]

```



```

19 L4_range = linspace(L4_min,L4_max,500);
20 % Other dimensions
21 w = 8.4;           % Width of base [m]
22 h = 2.45;         % Height of base [m]
23 % Mass parameters
24 m1 = 125;         % Mass of Car Body [tons]
25 m2 = 56;         % Mass of boom [tons]
26 m3 = 12.5;       % Mass of mast [tons]
27 m4 = 200;        % Mass of moveable counterweight [tons]
28 m4_fixed = 240;  % Mass of fixed counterweight [tons]
29 m5 = 110 ;       % Mass of Payload [tons]
30 m6 = 40;         % Mass of jib [tons]
31 % Angles
32 pli = [30 45 65]*pi/180;% Different values of boom Luffing Angle ...
    [rad]
33 p3i = pli-15*pi/180; % Jib angle wrt x-axis [rad]
34 B = linspace(0,pi,50); % Slewing Angle [rad]
35
36 %% Calculating minimum location of counterweight to ensure safety
37
38 for k=1:length(pli) % Loop repeats for each value of m4
39     p1 = pli(k);
40     p3 = p3i(k);
41     for i=1:length(B) % Loop repeats for every slew angle
42         for j = length(L4_range):-1:1 % Loop repeats for every ...
            value of L4
43             L4 = L4_range(j);
44             p2 = acos(L4/L3); % Mast angle
45 % Set up coordinate systems for mass centers
46 c1 = [0 0 h/2]';           % Car Body mass center
47 c2 = [L2*cos(p1)*cos(B(i))/2,...
48       L2*cos(p1)*sin(B(i))/2,...

```

```

49     (L2*sin(p1)/2)+h]';           % Boom mass center
50 c3 = [-L3*cos(p2)*cos(B(i))/2,...
51     -L3*cos(p2)*sin(B(i))/2,...
52     (L3*sin(p2)/2)+h]';           % Mast mass center
53 c4 = [-L4*cos(B(i)),...
54     -L4*sin(B(i)), h]';           % Moving counterweight mass center
55 c4.fixed = [-7*cos(B(i)),...
56     -7*sin(B(i)), 3]';           % Fixed counterweight mass center
57 c5 = [L2*cos(p1)*cos(B(i)),...
58     L2*cos(p1)*sin(B(i)),...
59     L2*sin(p1)+h-L5]';           % Payload mass center
60 c6 = [(L2*cos(p1)+0.5*L6*cos(p3))*cos(B(i)),...
61     (L2*cos(p1)+.5*L6*cos(p3))*sin(B(i)),...
62     L2*sin(p1)+.5*L6*sin(p3)+h]'; % Jib mass center
63
64 % Forces:
65 G = [0 0 -1]';                   % Direction of gravitational force
66 f1 = m1*g*G;                       % Weight of car body
67 f2 = m2*g*G;                       % Weight of boom
68 f3 = m3*g*G;                       % Weight of mast
69 f4 = m4*g*G;                       % Weight of moveable counterweight
70 f4.fixed = m4.fixed*g*G;           % Weight of fixed counterweight
71 f5 = m5*g*G;                       % Weight of payload
72 f6 = m6*g*G;                       % Weight of jib
73
74 % Instantaneous inertial location of the ith ground contact point
75 p01 = [-L1/2 w/2 0]';
76 p02 = [L1/2 w/2 0]';
77 p03 = [L1/2 -w/2 0]';
78 p04 = [-L1/2 -w/2 0]';
79
80 % ith tip-over mode axis

```

```

81 a1 = p02-p01;
82 a2 = p03-p02;
83 a3 = p04-p03;
84 a4 = p01-p04;
85
86 % Expressing each ith tip-over mode axis as a unit vector
87 a11 = -a1/norm(a1);
88 a22 = -a2/norm(a2);
89 a33 = a3/norm(a3);
90 a44 = -a4/norm(a4);
91
92 % Deciding which is the tip-over axis based on the value of the ...
    slew angle
93 theta1 = atan((w/2)/(L1/2));
94 theta2 = pi-theta1;
95 %-----
96 if B(i)<theta1 % Tip over axis is a2
97     pa2 = [L1/2 0 0]'; % Location of a point on axis a2
98     % Vectors pointing from mass centers to the point on a2
99     r1a = c1-pa2;
100    r2a = c2-pa2;
101    r3a = c3-pa2;
102    r4a = c4-pa2;
103    r4a.fixed = c4.fixed-pa2;
104    r5a = c5-pa2;
105    r6a = c6-pa2;
106
107    % Calculating sum of moments about axis a2:
108    M2(i) = dot(a22,cross(r1a,f1))+dot(a22,cross(r2a,f2))+...
109            dot(a22,cross(r3a,f3))+dot(a22,cross(r4a,f4))+...
110            dot(a22,cross(r4a.fixed,f4.fixed))+...
111            dot(a22,cross(r5a,f5))+dot(a22,cross(r6a,f6));

```

```

112
113     if M2(i)>0 % Loop chooses value of L4 to prevent tip-over
114         L4_long(k,i)=L4;
115         break
116     end
117 end
118 %-----
119 if B(i)≥theta1 && B(i)≤theta2 % Tip over axis is a1
120     pa1 = [0 w/2 0]'; % Location of a point on axis a1
121     % Vectors pointing from mass centers to the point on a1
122     r1a = c1-pa1;
123     r2a = c2-pa1;
124     r3a = c3-pa1;
125     r4a = c4-pa1;
126     r4a_fixed = c4_fixed-pa1;
127     r5a = c5-pa1;
128     r6a = c6-pa1;
129
130     % Calculating sum of moments about axis a1:
131     M1(i) = dot(a11,cross(r1a,f1))+dot(a11,cross(r2a,f2))+...
132             dot(a11,cross(r3a,f3))+dot(a11,cross(r4a,f4))+...
133             dot(a11,cross(r4a_fixed,f4_fixed))+...
134             dot(a11,cross(r5a,f5))+dot(a11,cross(r6a,f6));
135
136     if M1(i)>0 % Loop chooses value of L4 to prevent tip-over
137         L4_long(k,i)=L4;
138         break
139     end
140 end
141 %-----
142 if B(i)>theta2 % Tip over axis is a4
143     pa4 = [-L1/2 0 0]'; % Location of a point on axis a4

```

```

144 % Vectors pointing from mass centers to the point on a4
145 r1a = c1-pa4;
146 r2a = c2-pa4;
147 r3a = c3-pa4;
148 r4a = c4-pa4;
149 r4a_fixed = c4_fixed-pa4;
150 r5a = c5-pa4;
151 r6a = c6-pa4;
152
153 % Calculating sum of moments about axis a4:
154 M4(i) = dot(a44,cross(r1a,f1))+dot(a44,cross(r2a,f2))+...
155         dot(a44,cross(r3a,f3))+dot(a44,cross(r4a,f4))+...
156         dot(a44,cross(r4a_fixed,f4_fixed))+...
157         dot(a44,cross(r5a,f5))+dot(a44,cross(r6a,f6));
158
159     if M4(i)>0
160         L4_long(k,i)=L4;
161         break
162     end
163 end
164     end
165 end
166 end
167
168 %% Plotting
169 figure
170 for k = 1:length(pli)
171     x = [B,B];
172     y = [L4_long(k,:),-fliplr(L4_long(k,:))];
173     polar(x,y)
174     xlabel('Slew Angle \beta [deg]')
175     ylabel('Counterweight Position [m]')

```

```

176     legend('\phi_1 = 30', '\phi_1 = 45', '\phi_1 = 65')
177     hold on
178 end

```

Listing A.10: Forward Tip-over Analysis for the jib configuration (m_5 is the variable)

```

1  % This code calculates the counterweight displacement with ...
    respect to
2  % different slew angles in order to prevent forward tip-over, ...
    this is done
3  % for three values of payload mass (jib configuration)
4
5  clear
6
7  %% Defining all parameters
8  g=9.8;                % Gravitational acceleration [m/s^2]
9  % Defining Lengths of different components
10 L1 = 10.33;           % Length of Base Body [m]
11 L2 = 96;              % Length of boom [m]
12 L3 = 30;              % Length of mast [m]
13 L4_fixed = 7;         % Position of fixed counterweight [m]
14 L5 = 50;              % Length of payload hoist [m]
15 L6 = 96;              % Length of jib [m]
16 L4_min = 0;          % Minimum position of moveable ...
    counterweight [m]
17 L4_max = 100;        % Maximum position of moveable ...
    counterweight [m]
18 % Range of allowed locations for counterweight [m]
19 L4_range = linspace(L4_min,L4_max,500);
20 % Other dimensions
21 w = 8.4;              % Width of base [m]
22 h = 2.45;            % Height of base [m]

```

```

23 % Mass parameters
24 m1 = 125;           % Mass of Car Body [tons]
25 m2 = 56;           % Mass of boom [tons]
26 m3 = 12.5;        % Mass of mast [tons]
27 m4 = 200;         % Mass of moveable counterweight [tons]
28 m4_fixed = 240;   % Mass of fixed counterweight [tons]
29 m5i = [60 85 110]; % Different Masses of Payload [tons]
30 m6 = 40;          % Mass of jib [tons]
31 % Angles
32 p1 = 65*pi/180;    % Boom Luffing Angle [rad]
33 p3 = p1-15*pi/180; % Jib angle wrt x-axis [rad]
34 B = linspace(0,pi,50); % Slewing Angle [rad]
35
36 %% Calculating minimum location of counterweight to ensure safety
37
38 for k=1:length(m5i) % Loop repeats for each value of m4
39     m5 = m5i(k);
40     for i=1:length(B) % Loop repeats for every slew angle
41         for j = length(L4_range):-1:1 % Loop repeats for every ...
42             value of L4
43             L4 = L4_range(j);
44             p2 = acos(L4/L3); % Mast angle
45 % Set up coordinate systems for mass centers
46 c1 = [0 0 h/2]';           % Car Body mass center
47 c2 = [L2*cos(p1)*cos(B(i))/2,...
48       L2*cos(p1)*sin(B(i))/2,...
49       (L2*sin(p1)/2)+h]';   % Boom mass center
50 c3 = [-L3*cos(p2)*cos(B(i))/2,...
51       -L3*cos(p2)*sin(B(i))/2,...
52       (L3*sin(p2)/2)+h]';   % Mast mass center
53 c4 = [-L4*cos(B(i)),...
54       -L4*sin(B(i)), h]';   % Moving counterweight mass center

```

```

54 c4.fixed = [-7*cos(B(i)),...
55             -7*sin(B(i)), 3]'; % Fixed counterweight mass center
56 c5 = [L2*cos(p1)*cos(B(i)),...
57       L2*cos(p1)*sin(B(i)),...
58       L2*sin(p1)+h-L5]'; % Payload mass center
59 c6 = [(L2*cos(p1)+0.5*L6*cos(p3))*cos(B(i)),...
60       (L2*cos(p1)+.5*L6*cos(p3))*sin(B(i)),...
61       L2*sin(p1)+.5*L6*sin(p3)+h]'; % Jib mass center
62
63 % Forces:
64 G = [0 0 -1]'; % Direction of gravitational force
65 f1 = m1*g*G; % Weight of car body
66 f2 = m2*g*G; % Weight of boom
67 f3 = m3*g*G; % Weight of mast
68 f4 = m4*g*G; % Weight of moveable counterweight
69 f4.fixed = m4.fixed*g*G; % Weight of fixed counterweight
70 f5 = m5*g*G; % Weight of payload
71 f6 = m6*g*G; % Weight of jib
72
73 % Instantaneous inertial location of the ith ground contact point
74 p01 = [-L1/2 w/2 0]';
75 p02 = [L1/2 w/2 0]';
76 p03 = [L1/2 -w/2 0]';
77 p04 = [-L1/2 -w/2 0]';
78
79 % ith tip-over mode axis
80 a1 = p02-p01;
81 a2 = p03-p02;
82 a3 = p04-p03;
83 a4 = p01-p04;
84
85 % Expressing each ith tip-over mode axis as a unit vector

```



```

86 a11 = -a1/norm(a1);
87 a22 = -a2/norm(a2);
88 a33 = a3/norm(a3);
89 a44 = -a4/norm(a4);
90
91 % Deciding which is the tip-over axis based on the value of the ...
    slew angle
92 theta1 = atan((w/2)/(L1/2));
93 theta2 = pi-theta1;
94 %-----
95 if B(i)<theta1 % Tip over axis is a2
96     pa2 = [L1/2 0 0]'; % Location of a point on axis a2
97     % Vectors pointing from mass centers to the point on a2
98     r1a = c1-pa2;
99     r2a = c2-pa2;
100    r3a = c3-pa2;
101    r4a = c4-pa2;
102    r4a_fixed = c4.fixed-pa2;
103    r5a = c5-pa2;
104    r6a = c6-pa2;
105
106    % Calculating sum of moments about axis a2:
107    M2(i) = dot(a22,cross(r1a,f1))+dot(a22,cross(r2a,f2))+...
108            dot(a22,cross(r3a,f3))+dot(a22,cross(r4a,f4))+...
109            dot(a22,cross(r4a_fixed,f4_fixed))+...
110            dot(a22,cross(r5a,f5))+dot(a22,cross(r6a,f6));
111
112    if M2(i)>0 % Loop chooses value of L4 to prevent tip-over
113        L4_long(k,i)=L4;
114        break
115    end
116 end

```

```

117 %-----
118 if B(i)≥theta1 && B(i)≤theta2 % Tip over axis is a1
119     pa1 = [0 w/2 0]'; % Location of a point on axis a1
120     % Vectors pointing from mass centers to the point on a1
121     r1a = c1-pa1;
122     r2a = c2-pa1;
123     r3a = c3-pa1;
124     r4a = c4-pa1;
125     r4a_fixed = c4_fixed-pa1;
126     r5a = c5-pa1;
127     r6a = c6-pa1;
128
129     % Calculating sum of moments about axis a1:
130     M1(i) = dot(a11,cross(r1a,f1))+dot(a11,cross(r2a,f2))+...
131             dot(a11,cross(r3a,f3))+dot(a11,cross(r4a,f4))+...
132             dot(a11,cross(r4a_fixed,f4_fixed))+...
133             dot(a11,cross(r5a,f5))+dot(a11,cross(r6a,f6));
134
135     if M1(i)>0 % Loop chooses value of L4 to prevent tip-over
136         L4.long(k,i)=L4;
137         break
138     end
139 end
140 %-----
141 if B(i)>theta2 % Tip over axis is a4
142     pa4 = [-L1/2 0 0]'; % Location of a point on axis a4
143     % Vectors pointing from mass centers to the point on a4
144     r1a = c1-pa4;
145     r2a = c2-pa4;
146     r3a = c3-pa4;
147     r4a = c4-pa4;
148     r4a_fixed = c4_fixed-pa4;

```

```

149   r5a = c5-pa4;
150   r6a = c6-pa4;
151
152   % Calculating sum of moments about axis a4:
153   M4(i) = dot(a44,cross(r1a,f1))+dot(a44,cross(r2a,f2))+...
154           dot(a44,cross(r3a,f3))+dot(a44,cross(r4a,f4))+...
155           dot(a44,cross(r4a_fixed,f4_fixed))+...
156           dot(a44,cross(r5a,f5))+dot(a44,cross(r6a,f6));
157
158       if M4(i)>0
159           L4_long(k,i)=L4;
160           break
161       end
162 end
163     end
164 end
165 end
166
167 %% Plotting
168 figure
169 for k = length(m5i):-1:1
170     x = [B,B];
171     y = [L4_long(k,:),-fliplr(L4_long(k,:))];
172     polar(x,y)
173     xlabel('Slew Angle \beta [deg]')
174     ylabel('Counterweight Position [m]')
175     legend('m_5 = 110 t','m_5 = 85 t','m_5 = 60 t')
176     hold on
177 end

```

Listing A.11: Simulation of Payload Swing Angle Resulting from Straight Base Motion

```

1 % This code plots the swing angle of the payload vs. time for ...
   different
2 % base acceleration values, it also calculates the maximum swing ...
   angle in
3 % each case
4
5 clear
6 g = 9.81; % Gravitational Acceleration [m/s^2]
7 t = [0:0.1:80]; % Simulation time [s]
8 v_max = 0.6 * 1000/3600; % Maximum Velocity of the crane [m/s]
9 t2 = 7; % Time needed to accelerate to full ...
   speed [s]
10 A = v_max/1; % Maximum Acceleration [m/s^2]
11 L5 = 50; % Hoist Length [m]
12 wn = sqrt(g/L5); % Natural frequency of payload [rad/s]
13 t3 = 21; % Time to apply deceleration [s]
14 t4 = 28; % Time when crane stops [s]
15 a = A*(heaviside(t)-heaviside(t-t2)-heaviside(t-t3)+heaviside(t-t4));
16
17 theta1 = -(A/(L5*wn^2))*((1-cos(wn*t))-((1-cos(wn*(t-t2)))...
18     .*heaviside(t-t2))-((1-cos(wn*(t-t3))).*heaviside(t-t3))+...
19     ((1-cos(wn*(t-t4))).*heaviside(t-t4)));
20
21 theta1=theta1'*180/pi;
22
23 t=t';
24 a=a';
25 max(theta1)
26
27 figure(1)

```

```

28 plot(t,theta1)
29 xlabel('Time (s)')
30 ylabel('Payload Swing Angle (deg)')
31 figure(2)
32 plot(t,a)
33 xlabel('Time (s)')
34 ylabel('Acceleration Command (m/s^2)')

```

Listing A.12: Forward Tip-over Analysis for the Case of Straight Base Motion (m_4 is the variable)

```

1 % This code calculates the counterweight displacement with ...
   respect to
2 % different slew angles in order to prevent forward tip-over, ...
   this is done
3 % for three values of moveable counterweight mass (Straight Base ...
   Motion)
4
5 clear
6
7 %% Defining all parameters
8 g=9.8;           % Gravitational acceleration [m/s^2]
9 % Defining Lengths of different components
10 L1 = 10.33;      % Length of Base Body [m]
11 L2 = 102;       % Length of boom [m]
12 L3 = 30;        % Length of mast [m]
13 L4.fixed = 7;   % Position of fixed counterweight [m]
14 L5 = 20;        % Length of payload hoist [m]
15 L4_min = 0;     % Minimum position of moveable ...
   counterweight [m]
16 L4_max = 100;   % Maximum position of moveable ...
   counterweight [m]

```

```

17 % Range of allowed locations for counterweight [m]
18 L4_range = linspace(L4_min,L4_max,500);
19 % Other dimensions
20 w = 8.4; % Width of base [m]
21 h = 2.45; % Height of base [m]
22 % Mass parameters
23 m1 = 125; % Mass of Car Body [tons]
24 m2 = 60; % Mass of boom [tons]
25 m3 = 12.5; % Mass of mast [tons]
26 m4i = [150 200 300]; % Different masses of moveable ...
    counterweight [tons]
27 m4_fixed = 240; % Mass of fixed counterweight [tons]
28 m5 = 110 ; % Mass of Payload [tons]
29 % Angles
30 p1 = 62*pi/180; % Boom Luffing Angle [rad]
31 B = linspace(0,pi,50); % Slewing Angle [rad]
32 q = 3.89*pi/180; % Maximum Payload Swing Angle [rad]
33 %% Calculating minimum location of counterweight to ensure safety
34
35 for k=1:length(m4i) % Loop repeats for each value of m4
36     m4 = m4i(k);
37     for i=1:length(B) % Loop repeats for every slew angle
38         for j = length(L4_range):-1:1 % Loop repeats for every ...
            value of L4
39             L4 = L4_range(j);
40             p2 = acos(L4/L3); % Mast angle
41 % Set up coordinate systems for mass centers
42 c1 = [0 0 h/2]'; % Car Body mass center
43 c2 = [L2*cos(p1)*cos(B(i))/2,...
44     L2*cos(p1)*sin(B(i))/2,...
45     (L2*sin(p1)/2)+h]'; % Boom mass center
46 c3 = [-L3*cos(p2)*cos(B(i))/2,...

```

```

47     -L3*cos(p2)*sin(B(i))/2,...
48     (L3*sin(p2)/2)+h]';           % Mast mass center
49 c4 = [-L4*cos(B(i)),...
50     -L4*sin(B(i)), h]';         % Moving counterweight mass center
51 c4_fixed = [-7*cos(B(i)),...
52     -7*sin(B(i)), 3]';         % Fixed counterweight mass center
53 c5 = [(L2*cos(p1)+L5*sin(q))*cos(B(i)),...
54     (L2*cos(p1)+L5*sin(q))*sin(B(i)),...
55     L2*sin(p1)+h-L5*cos(q)]';   % Payload mass center
56
57
58 Pc = (c1*m1+c2*m2+c3*m3+c4*m4+c4_fixed*m4_fixed+c5*m5)/...
59     (m1+m2+m3+m4_fixed+m4+m5);
60
61
62 % Forces:
63 G = [0 0 -1]';                 % Direction of gravitational force
64 f1 = m1*g*G;                   % Weight of car body
65 f2 = m2*g*G;                   % Weight of boom
66 f3 = m3*g*G;                   % Weight of mast
67 f4 = m4*g*G;                   % Weight of moveable counterweight
68 f4_fixed = m4_fixed*g*G;       % Weight of fixed counterweight
69 f5 = m5*g*G;                   % Weight of payload
70 fi = 0.167*(m1+m2+m3+m4_fixed+m4+m5)*[1 0 0]'; % Inertial Force
71 % Instantaneous inertial location of the ith ground contact point
72 p01 = [-L1/2 w/2 0]';
73 p02 = [L1/2 w/2 0]';
74 p03 = [L1/2 -w/2 0]';
75 p04 = [-L1/2 -w/2 0]';
76
77 % ith tip-over mode axis
78 a1 = p02-p01;

```

```

79 a2 = p03-p02;
80 a3 = p04-p03;
81 a4 = p01-p04;
82
83 % Expressing each ith tip-over mode axis as a unit vector
84 a11 = -a1/norm(a1);
85 a22 = -a2/norm(a2);
86 a33 = a3/norm(a3);
87 a44 = -a4/norm(a4);
88
89 % Deciding which is the tip-over axis based on the value of the ...
    slew angle
90 theta1 = atan((w/2)/(L1/2));
91 theta2 = pi-theta1;
92 %-----
93 if B(i)<theta1 % Tip over axis is a2
94     pa2 = [L1/2 0 0]'; % Location of a point on axis a2
95     % Vectors pointing from mass centers to the point on a2
96     r1a = c1-pa2;
97     r2a = c2-pa2;
98     r3a = c3-pa2;
99     r4a = c4-pa2;
100    r4a.fixed = c4.fixed-pa2;
101    r5a = c5-pa2;
102    ria = Pc-pa2;
103
104    % Calculating sum of moments about axis a2:
105    M2(i) = dot(a22,cross(r1a,f1))+dot(a22,cross(r2a,f2))+...
106            dot(a22,cross(r3a,f3))+dot(a22,cross(r4a,f4))+...
107            dot(a22,cross(r4a.fixed,f4.fixed))+...
108            dot(a22,cross(r5a,f5))+dot(a22,cross(ria,fi));
109

```



```

110     if M2(i)>0 % Loop chooses value of L4 to prevent tip-over
111         L4_long(k,i)=L4;
112         break
113     end
114 end
115 %-----
116 if B(i)>theta1 && B(i)<=theta2 % Tip over axis is a1
117     pa1 = [0 w/2 0]'; % Location of a point on axis a1
118     % Vectors pointing from mass centers to the point on a1
119     r1a = c1-pa1;
120     r2a = c2-pa1;
121     r3a = c3-pa1;
122     r4a = c4-pa1;
123     r4a_fixed = c4_fixed-pa1;
124     r5a = c5-pa1;
125     ria = Pc -pa1;
126
127     % Calculating sum of moments about axis a1:
128     M1(i) = dot(a11,cross(r1a,f1))+dot(a11,cross(r2a,f2))+...
129             dot(a11,cross(r3a,f3))+dot(a11,cross(r4a,f4))+...
130             dot(a11,cross(r4a_fixed,f4_fixed))+...
131             dot(a11,cross(r5a,f5))+dot(a11,cross(ria,fi));
132
133     if M1(i)>0 % Loop chooses value of L4 to prevent tip-over
134         L4_long(k,i)=L4;
135         break
136     end
137 end
138 %-----
139 if B(i)>theta2 % Tip over axis is a4
140     pa4 = [-L1/2 0 0]'; % Location of a point on axis a4
141     % Vectors pointing from mass centers to the point on a4

```

```

142   r1a = c1-pa4;
143   r2a = c2-pa4;
144   r3a = c3-pa4;
145   r4a = c4-pa4;
146   r4a_fixed = c4_fixed-pa4;
147   r5a = c5-pa4;
148   ria = Pc-pa4;
149
150   % Calculating sum of moments about axis a4:
151   M4(i) = dot(a44,cross(r1a,f1))+dot(a44,cross(r2a,f2))+...
152           dot(a44,cross(r3a,f3))+dot(a44,cross(r4a,f4))+...
153           dot(a44,cross(r4a_fixed,f4_fixed))+...
154           dot(a44,cross(r5a,f5))+dot(a44,cross(ria,fi));
155
156       if M4(i)>0
157           L4_long(k,i)=L4;
158           break
159       end
160 end
161     end
162 end
163 end
164
165 %% Plotting
166 figure
167 for k = 1:length(m4i)
168     x = [B,B];
169     y = [L4_long(k,:),-fliplr(L4_long(k,:))];
170     polar(x,y)
171     xlabel('Slew Angle \beta [deg]')
172     ylabel('Counterweight Position [m]')
173     legend('m_4 = 150 t','m_4 = 200 t','m_4 = 300 t')

```

```

174     hold on
175 end

```

Listing A.13: Simulation of Payload Swing Angle Resulting from Boom Luffing Motion

```

1  % This code is used to calculate the radial swinging angle of the
2  % payload carried by a crawler crane for boom luffing motion
3
4  clear
5  L2 = 102;                % Boom Length [m]
6  L5 = 30;                % Hoist Length [m]
7  L = L2/L5;
8  g = 9.81;              % Gravitational Acceleration ...
   [m/s^2]
9  t_gap = .75;           % Time between the 2 Acc. ...
   Pulses [s]
10 tp = 1;                % Acceleration Pulse Duration [s]
11 t_tot = t_gap+(2*tp);  % Total Command Time [s]
12 A = -0.02;            % Luffing Acc. Amplitude [rad/s^2]
13 t = [0:0.1:50];       % Simulation Time Interval [s]
14 %-----
15 % Solving the system of coupled differential equations
16 for i = 1:length(t)
17     if t(i) ≤ tp
18         u(i)=A;
19         couplode = @(t,x) [x(2);...
20             ((L*(x(4)^2)*cos(x(3)))+(L*u(i)*sin(x(3)))...
21             -(L*u(i)*x(1)*cos(x(3)))+(L*x(1)*(x(4)^2)*sin(x(3)))...
22             -(g*x(1)/L5));...
23             x(4); ...
24             u(i)];

```

```

25     [t1,y1] = ode45(couplode, [0 tp],...
26         [10^-8,10^-8,(80*pi/180),10^-8]);
27
28     elseif t(i)>tp & t(i)≤tp+t_gap
29         u(i) = 0;
30         couplode = @(t,x) [x(2);...
31             ((L*(x(4)^2)*cos(x(3)))+(L*u(i)*sin(x(3)))...
32             -(L*u(i)*x(1)*cos(x(3)))+(L*x(1)*(x(4)^2)*sin(x(3)))...
33             -(g*x(1)/L5));...
34             x(4); ...
35             u(i)];
36         [t2,y2] = ode45(couplode, [tp tp+t_gap], ...
37             [y1(end,1),y1(end,2),y1(end,3),y1(end,4)]);
38
39     elseif t(i)>tp+t_gap & t(i)≤t_tot
40         u(i) = -A;
41         couplode = @(t,x) [x(2);...
42             ((L*(x(4)^2)*cos(x(3)))+(L*u(i)*sin(x(3)))...
43             -(L*u(i)*x(1)*cos(x(3)))+(L*x(1)*(x(4)^2)*sin(x(3)))...
44             -(g*x(1)/L5));...
45             x(4); ...
46             u(i)];
47         [t3,y3] = ode45(couplode, [tp+t_gap t_tot],...
48             [y2(end,1),y2(end,2),y2(end,3),y2(end,4)]);
49
50     elseif t(i)>t_tot
51         u(i) = 0;
52         couplode = @(t,x) [x(2);...
53             ((L*(x(4)^2)*cos(x(3)))+(L*u(i)*sin(x(3)))...
54             -(L*u(i)*x(1)*cos(x(3)))+(L*x(1)*(x(4)^2)*sin(x(3)))...
55             -(g*x(1)/L5));...
56             x(4); ...

```

```

57         u(i)];
58         [t4,y4] = ode45(couplode, [t_tot 50], ...
59             [y3(end,1),y3(end,2),y3(end,3),y3(end,4)]);
60     end
61 end
62
63 tx = [t1;t2;t3;t4];
64 y = [y1;y2;y3;y4];
65 y = y*180/pi;
66
67 displacement = min(y(:,3))
68 y_residual = y(find(tx==t_tot)+1:end,:);
69 max_resid_radial = max(y_residual(:,1))
70
71
72 % figure(1)
73 % plot(tx,y(:,1))
74 % xlabel('Time (s)')
75 % ylabel('Radial Residual Swinging Angle (deg)')

```

Listing A.14: Forward Tip-over Analysis for the Case of Boom Luffing Motion (m_4 is the variable)

```

1 % This code calculates the counterweight displacement with ...
   respect to
2 % different slew angles in order to prevent forward tip-over, ...
   this is done
3 % for three values of moveable counterweight mass (Boom Luffing ...
   Motion)
4
5 clear
6

```

```

7 %% Defining all parameters
8 g=9.8; % Gravitational acceleration [m/s^2]
9 % Defining Lengths of different components
10 L1 = 10.33; % Length of Base Body [m]
11 L2 = 102; % Length of boom [m]
12 L3 = 30; % Length of mast [m]
13 L4.fixed = 7; % Position of fixed counterweight [m]
14 L5 = 50; % Length of payload hoist [m]
15 L4_min = 0; % Minimum position of moveable ...
    counterweight [m]
16 L4_max = 100; % Maximum position of moveable ...
    counterweight [m]
17 % Range of allowed locations for counterweight [m]
18 L4_range = linspace(L4_min,L4_max,500);
19 % Other dimensions
20 w = 8.4; % Width of base [m]
21 h = 2.45; % Height of base [m]
22 % Mass parameters
23 m1 = 125; % Mass of Car Body [tons]
24 m2 = 60; % Mass of boom [tons]
25 m3 = 12.5; % Mass of mast [tons]
26 m4i = [150 200 300]; % Different masses of moveable ...
    counterweight [tons]
27 m4.fixed = 240; % Mass of fixed counterweight [tons]
28 m5 = 125 ; % 110, 125, 140, Mass of Payload [tons]
29 % Angles
30 p1 = 62*pi/180; % Boom Luffing Angle [rad]
31 B = linspace(0,pi,50); % Slewing Angle [rad]
32 q = 11.27*pi/180; % Swing angle [rad]
33
34 %% Calculating minimum location of counterweight to ensure safety
35

```

```

36 for k=1:length(m4i) % Loop repeats for each value of m4
37     m4 = m4i(k);
38     for i=1:length(B) % Loop repeats for every slew angle
39         for j = length(L4_range):-1:1 % Loop repeats for every ...
40             value of L4
41             L4 = L4_range(j);
42             p2 = acos(L4/L3); % Mast angle
43 % Set up coordinate systems for mass centers
44 c1 = [0 0 h/2]'; % Car Body mass center
45 c2 = [L2*cos(p1)*cos(B(i))/2,...
46       L2*cos(p1)*sin(B(i))/2,...
47       (L2*sin(p1)/2)+h]'; % Boom mass center
48 c3 = [-L3*cos(p2)*cos(B(i))/2,...
49       -L3*cos(p2)*sin(B(i))/2,...
50       (L3*sin(p2)/2)+h]'; % Mast mass center
51 c4 = [-L4*cos(B(i)),...
52       -L4*sin(B(i)), h]'; % Moving counterweight mass center
53 c4_fixed = [-7*cos(B(i)),...
54             -7*sin(B(i)), 3]'; % Fixed counterweight mass center
55 c5 = [(L2*cos(p1)+L5*sin(q))*cos(B(i)),...
56       (L2*cos(p1)+L5*sin(q))*sin(B(i)),...
57       L2*sin(p1)+h-L5*cos(q)]'; % Payload mass center
58 % Forces:
59 G = [0 0 -1]'; % Direction of gravitational force
60 f1 = m1*g*G; % Weight of car body
61 f2 = m2*g*G; % Weight of boom
62 f3 = m3*g*G; % Weight of mast
63 f4 = m4*g*G; % Weight of moveable counterweight
64 f4_fixed = m4_fixed*g*G; % Weight of fixed counterweight
65 f5 = m5*g*G; % Weight of payload
66

```

```

67 % Instantaneous inertial location of the ith ground contact point
68 p01 = [-L1/2 w/2 0]';
69 p02 = [L1/2 w/2 0]';
70 p03 = [L1/2 -w/2 0]';
71 p04 = [-L1/2 -w/2 0]';
72
73 % ith tip-over mode axis
74 a1 = p02-p01;
75 a2 = p03-p02;
76 a3 = p04-p03;
77 a4 = p01-p04;
78
79 % Expressing each ith tip-over mode axis as a unit vector
80 a11 = -a1/norm(a1);
81 a22 = -a2/norm(a2);
82 a33 = a3/norm(a3);
83 a44 = -a4/norm(a4);
84
85 % Deciding which is the tip-over axis based on the value of the ...
      slew angle
86 theta1 = atan((w/2)/(L1/2));
87 theta2 = pi-theta1;
88 %-----
89 if B(i)<theta1 % Tip over axis is a2
90     pa2 = [L1/2 0 0]'; % Location of a point on axis a2
91     % Vectors pointing from mass centers to the point on a2
92     r1a = c1-pa2;
93     r2a = c2-pa2;
94     r3a = c3-pa2;
95     r4a = c4-pa2;
96     r4a.fixed = c4.fixed-pa2;
97     r5a = c5-pa2;

```



```

98
99 % Calculating sum of moments about axis a2:
100 M2(i) = dot(a22,cross(r1a,f1))+dot(a22,cross(r2a,f2))+...
101         dot(a22,cross(r3a,f3))+dot(a22,cross(r4a,f4))+...
102         dot(a22,cross(r4a_fixed,f4_fixed))+dot(a22,cross(r5a,f5));
103
104     if M2(i)>0 % Loop chooses value of L4 to prevent tip-over
105         L4_long(k,i)=L4;
106         break
107     end
108 end
109 %-----
110 if B(i)≥thetal && B(i)≤theta2 % Tip over axis is a1
111     pa1 = [0 w/2 0]'; % Location of a point on axis a1
112     % Vectors pointing from mass centers to the point on a1
113     r1a = c1-pa1;
114     r2a = c2-pa1;
115     r3a = c3-pa1;
116     r4a = c4-pa1;
117     r4a_fixed = c4_fixed-pa1;
118     r5a = c5-pa1;
119
120 % Calculating sum of moments about axis a1:
121 M1(i) = dot(a11,cross(r1a,f1))+dot(a11,cross(r2a,f2))+...
122         dot(a11,cross(r3a,f3))+dot(a11,cross(r4a,f4))+...
123         dot(a11,cross(r4a_fixed,f4_fixed))+dot(a11,cross(r5a,f5));
124
125     if M1(i)>0 % Loop chooses value of L4 to prevent tip-over
126         L4_long(k,i)=L4;
127         break
128     end
129 end

```

```

130 %-----
131 if B(i)>theta2 % Tip over axis is a4
132     pa4 = [-L1/2 0 0]'; % Location of a point on axis a4
133     % Vectors pointing from mass centers to the point on a4
134     r1a = c1-pa4;
135     r2a = c2-pa4;
136     r3a = c3-pa4;
137     r4a = c4-pa4;
138     r4a_fixed = c4_fixed-pa4;
139     r5a = c5-pa4;
140
141     % Calculating sum of moments about axis a4:
142     M4(i) = dot(a44,cross(r1a,f1))+dot(a44,cross(r2a,f2))+...
143             dot(a44,cross(r3a,f3))+dot(a44,cross(r4a,f4))+...
144             dot(a44,cross(r4a_fixed,f4_fixed))+dot(a44,cross(r5a,f5));
145
146         if M4(i)>0
147             L4_long(k,i)=L4;
148             break
149         end
150     end
151         end
152     end
153 end
154
155 %% Plotting
156 figure
157 for k = 1:length(m4i)
158     x = [B,B];
159     y = [L4_long(k,:),-fliplr(L4_long(k,:))];
160     polar(x,y)
161     xlabel('Slew Angle \beta [deg]')

```

```

162     ylabel('Counterweight Position [m]')
163     legend('m_4 = 150 t', 'm_4 = 200 t', 'm_4 = 300 t')
164     hold on
165 end

```

Listing A.15: Simulation of Payload Swing Angle Resulting from Slewing Motion of the Tower Crane

```

1  % This code is used to simulate the behavior of the tower crane, to
2  % compare it with the results obtained in the experiment.
3
4  clear
5  R = .908; % Radius of Slewing [m]
6  L5 = .902; % Hoist Length [m]
7  g = 9.81; % Gravitational Acceleration [m/s^2]
8  t_gap = 2.272; % Time between the 2 Acc. Pulses [s]
9  tp = .728; % Acceleration Pulse Duration [s]
10 t_tot = t_gap+(2*tp); % Total Command Time [s]
11 A = 0.482; % Slewing Acc. Amplitude [rad/s^2]
12 t = [0:0.01:15]; % Simulation Time Interval [s]
13 %-----
14 % Solving the system of coupled differential equations
15 for i = 1:length(t)
16     if t(i) ≤ tp
17         u(i) = A;
18         couplode = @(t,x) [x(2); ...
19             ((R/L5)*cos(x(1))*x(6)^2) ...
20             + ((R/L5)*u(i)*sin(x(1))*sin(x(3))) ...
21             - (2*x(4)*x(6)*(cos(x(1))^2*cos(x(3)))) ...
22             - (u(i)*sin(x(3)))+(sin(x(1)) ...
23             *(cos(x(3))^2*cos(x(1))*x(6)^2) ...
24             - ((g/L5)*sin(x(1))*cos(x(3)))-...

```

```

25         (cos(x(1))*sin(x(1))*x(4)^2);...
26         x(4); ...
27         ((R/L5)*u(i)*cos(x(3))/cos(x(1)))...
28         +(2*x(6)*x(2)*cos(x(1))*cos(x(3)))...
29         +(u(i)*sin(x(1))*cos(x(3))/cos(x(1)))...
30         +(sin(x(3))*cos(x(1))*cos(x(3))*x(6)^2)...
31         +(2*sin(x(1))*x(2)*x(4)/cos(x(1)))...
32         -((g/L5)*sin(x(3))/cos(x(1))));...
33         x(6);...
34         u(i)];
35         [t1,y1] = ode45(couplode, [0 tp], [1;1;1;1;1;1]*10^-8);
36
37     elseif t(i)>tp & t(i)≤tp+t_gap
38         u(i) = 0;
39         couplode = @(t,x) [x(2);...
40             ((R/L5)*cos(x(1))*x(6)^2)...
41             +(R/L5)*u(i)*sin(x(1))*sin(x(3))...
42             -(2*x(4)*x(6)*(cos(x(1))^2)*cos(x(3)))...
43             -(u(i)*sin(x(3)))+(sin(x(1))...
44             *(cos(x(3))^2)*cos(x(1))*x(6)^2)...
45             -((g/L5)*sin(x(1))*cos(x(3)))-...
46             (cos(x(1))*sin(x(1))*x(4)^2);...
47             x(4); ...
48             ((R/L5)*u(i)*cos(x(3))/cos(x(1)))...
49             +(2*x(6)*x(2)*cos(x(1))*cos(x(3)))...
50             +(u(i)*sin(x(1))*cos(x(3))/cos(x(1)))...
51             +(sin(x(3))*cos(x(1))*cos(x(3))*x(6)^2)...
52             +(2*sin(x(1))*x(2)*x(4)/cos(x(1)))...
53             -((g/L5)*sin(x(3))/cos(x(1))));...
54             x(6);...
55             u(i)];
56         [t2,y2] = ode45(couplode, [tp tp+t_gap], ...

```

```

57         [y1(end,1),y1(end,2),y1(end,3),y1(end,4),...
58         y1(end,5),y1(end,6)];
59
60     elseif t(i)>tp+t_gap & t(i)≤t_tot
61         u(i) = -A;
62         couplode = @(t,x) [x(2);...
63             ((R/L5)*cos(x(1))*x(6)^2)...
64             +((R/L5)*u(i)*sin(x(1))*sin(x(3)))...
65             -(2*x(4)*x(6)*(cos(x(1))^2*cos(x(3))))...
66             -(u(i)*sin(x(3)))+(sin(x(1))...
67             *(cos(x(3))^2*cos(x(1))*x(6)^2)...
68             -(g/L5)*sin(x(1))*cos(x(3))-...
69             (cos(x(1))*sin(x(1))*x(4)^2)];...
70         x(4); ...
71         ((R/L5)*u(i)*cos(x(3))/cos(x(1)))...
72         +(2*x(6)*x(2)*cos(x(1))*cos(x(3)))...
73         +(u(i)*sin(x(1))*cos(x(3))/cos(x(1)))...
74         +(sin(x(3))*cos(x(1))*cos(x(3))*x(6)^2)...
75         +(2*sin(x(1))*x(2)*x(4)/cos(x(1)))...
76         -(g/L5)*sin(x(3))/cos(x(1))];...
77         x(6);...
78         u(i)];
79     [t3,y3] = ode45(couplode, [tp+t_gap t_tot],...
80     [y2(end,1),y2(end,2),y2(end,3),y2(end,4),...
81     y2(end,5),y2(end,6)];
82
83     elseif t(i)>t_tot
84         u(i) = 0;
85         couplode = @(t,x) [x(2);...
86             ((R/L5)*cos(x(1))*x(6)^2)...
87             +((R/L5)*u(i)*sin(x(1))*sin(x(3)))...
88             -(2*x(4)*x(6)*(cos(x(1))^2*cos(x(3))))...

```

```

89         -(u(i)*sin(x(3)))+(sin(x(1))...
90         *(cos(x(3))^2)*cos(x(1))*x(6)^2)...
91         -((g/L5)*sin(x(1))*cos(x(3)))-...
92         (cos(x(1))*sin(x(1))*x(4)^2));...
93         x(4); ...
94         ((R/L5)*u(i)*cos(x(3))/cos(x(1)))...
95         +(2*x(6)*x(2)*cos(x(1))*cos(x(3)))...
96         +(u(i)*sin(x(1))*cos(x(3))/cos(x(1)))...
97         +(sin(x(3))*cos(x(1))*cos(x(3))*x(6)^2)...
98         +(2*sin(x(1))*x(2)*x(4)/cos(x(1)))...
99         -((g/L5)*sin(x(3))/cos(x(1))));...
100        x(6);...
101        u(i)];
102    [t4,y4] = ode45(couplode, [t_tot 15], ...
103        [y3(end,1),y3(end,2),y3(end,3),y3(end,4),...
104        y3(end,5),y3(end,6)]);
105    end
106 end
107
108 tx = [t1;t2;t3;t4];
109 y = [y1;y2;y3;y4];
110 y = y*180/pi;
111
112 displacement = max(y(:,5))
113 y_residual = y(find(tx==t_tot)+1:end,:);
114 max_resid_radial = max(y_residual(:,1))
115 max_resid_tangential = max(y_residual(:,3))
116
117 figure(1)
118 plot(tx,y(:,1))
119 xlabel('Time (s)')
120 ylabel('Radial Residual Swinging Angle (deg)')

```

```

121
122 figure(2)
123 plot(tx,y(:,3))
124 xlabel('Time (s)')
125 ylabel('Tangential Residual Swinging Angle (deg)')

```

Listing A.16: Simulation of Payload Swing Angle Resulting from Boom Slewing Motion

```

1 % This code is used to calculate the radial and tangential swinging
2 % angles of the payload carried by a crawler crane for boom slewing
3
4 clear
5 R = 102*cos(70*pi/180);           % Radius of Slewing [m]
6 L5 = 70;                          % Hoist Length [m]
7 g = 9.81;                          % Gravitational Acceleration ...
   [m/s^2]
8 t_gap = 20.5;                      % Time between the 2 Acc. ...
   Pulses [s]
9 t_tot = t_gap+2;                   % Total Command Time [s]
10 tp = 1;                            % Acceleration Pulse Duration [s]
11 t_tot = t_gap+(2*tp);              % Total Command Time [s]
12 A = 0.0733;                        % Slewing Acc. Amplitude [rad/s^2]
13 t = [0:0.1:150];                  % Simulation Time Interval [s]
14 %-----
15 % Solving the system of coupled differential equations
16 for i = 1:length(t)
17     if t(i)≤tp
18         u(i)=A;
19         couplode = @(t,x) [x(2);...
20                             ((R/L5)*cos(x(1))*x(6)^2)...
21                             +((R/L5)*u(i)*sin(x(1))*sin(x(3)))]...

```

```

22         - (2*x(4) *x(6) * (cos(x(1))^2 *cos(x(3))) ...
23         - (u(i) *sin(x(3))) + (sin(x(1)) ...
24         * (cos(x(3))^2 *cos(x(1)) *x(6)^2) ...
25         - ((g/L5) *sin(x(1)) *cos(x(3))) - ...
26         (cos(x(1)) *sin(x(1)) *x(4)^2); ...
27         x(4); ...
28         ((R/L5) *u(i) *cos(x(3)) /cos(x(1))) ...
29         + (2*x(6) *x(2) *cos(x(1)) *cos(x(3))) ...
30         + (u(i) *sin(x(1)) *cos(x(3)) /cos(x(1))) ...
31         + (sin(x(3)) *cos(x(1)) *cos(x(3)) *x(6)^2) ...
32         + (2*sin(x(1)) *x(2) *x(4) /cos(x(1))) ...
33         - ((g/L5) *sin(x(3)) /cos(x(1))) ); ...
34         x(6); ...
35         u(i)];
36         [t1,y1] = ode45(couplode, [0 tp], [1;1;1;1;1;1]*10^-8);
37
38     elseif t(i)>tp & t(i)≤tp+t_gap
39         u(i) = 0;
40         couplode = @(t,x) [x(2); ...
41             ((R/L5) *cos(x(1)) *x(6)^2) ...
42             + ((R/L5) *u(i) *sin(x(1)) *sin(x(3))) ...
43             - (2*x(4) *x(6) * (cos(x(1))^2 *cos(x(3))) ...
44             - (u(i) *sin(x(3))) + (sin(x(1)) ...
45             * (cos(x(3))^2 *cos(x(1)) *x(6)^2) ...
46             - ((g/L5) *sin(x(1)) *cos(x(3))) - ...
47             (cos(x(1)) *sin(x(1)) *x(4)^2); ...
48             x(4); ...
49             ((R/L5) *u(i) *cos(x(3)) /cos(x(1))) ...
50             + (2*x(6) *x(2) *cos(x(1)) *cos(x(3))) ...
51             + (u(i) *sin(x(1)) *cos(x(3)) /cos(x(1))) ...
52             + (sin(x(3)) *cos(x(1)) *cos(x(3)) *x(6)^2) ...
53             + (2*sin(x(1)) *x(2) *x(4) /cos(x(1))) ...

```



```

54         - ((g/L5)*sin(x(3))/cos(x(1))));...
55         x(6);...
56         u(i)];
57     [t2,y2] = ode45(couplode, [tp tp+t_gap], ...
58         [y1(end,1),y1(end,2),y1(end,3),y1(end,4),...
59         y1(end,5),y1(end,6)]);
60
61     elseif t(i)>tp+t_gap & t(i)≤t_tot
62         u(i) = -A;
63         couplode = @(t,x) [x(2);...
64             ((R/L5)*cos(x(1))*x(6)^2)...
65             +((R/L5)*u(i)*sin(x(1))*sin(x(3)))...
66             -(2*x(4)*x(6)*(cos(x(1))^2)*cos(x(3)))...
67             -(u(i)*sin(x(3)))+(sin(x(1))...
68             *(cos(x(3))^2)*cos(x(1))*x(6)^2)...
69             -((g/L5)*sin(x(1))*cos(x(3)))-...
70             (cos(x(1))*sin(x(1))*x(4)^2)];...
71         x(4); ...
72         ((R/L5)*u(i)*cos(x(3))/cos(x(1)))...
73         +(2*x(6)*x(2)*cos(x(1))*cos(x(3)))...
74         +(u(i)*sin(x(1))*cos(x(3))/cos(x(1)))...
75         +(sin(x(3))*cos(x(1))*cos(x(3))*x(6)^2)...
76         +(2*sin(x(1))*x(2)*x(4)/cos(x(1)))...
77         -((g/L5)*sin(x(3))/cos(x(1))));...
78         x(6);...
79         u(i)];
80     [t3,y3] = ode45(couplode, [tp+t_gap t_tot],...
81         [y2(end,1),y2(end,2),y2(end,3),y2(end,4),...
82         y2(end,5),y2(end,6)]);
83
84     elseif t(i)>t_tot
85         u(i) = 0;

```

```

86     couplode = @(t,x) [x(2);...
87         ((R/L5)*cos(x(1))*x(6)^2)...
88         +((R/L5)*u(i)*sin(x(1))*sin(x(3)))...
89         -(2*x(4)*x(6)*(cos(x(1))^2*cos(x(3)))...
90         -(u(i)*sin(x(3)))+(sin(x(1))...
91         *(cos(x(3))^2*cos(x(1))*x(6)^2)...
92         -((g/L5)*sin(x(1))*cos(x(3)))-...
93         (cos(x(1))*sin(x(1))*x(4)^2)];...
94         x(4); ...
95         ((R/L5)*u(i)*cos(x(3))/cos(x(1)))...
96         +(2*x(6)*x(2)*cos(x(1))*cos(x(3)))...
97         +(u(i)*sin(x(1))*cos(x(3))/cos(x(1)))...
98         +(sin(x(3))*cos(x(1))*cos(x(3))*x(6)^2)...
99         +(2*sin(x(1))*x(2)*x(4)/cos(x(1)))...
100        -((g/L5)*sin(x(3))/cos(x(1)))]);...
101        x(6);...
102        u(i)];
103    [t4,y4] = ode45(couplode, [t_tot 150], ...
104        [y3(end,1),y3(end,2),y3(end,3),y3(end,4),...
105        y3(end,5),y3(end,6)]);
106    end
107 end
108
109 tx = [t1;t2;t3;t4];
110 y = [y1;y2;y3;y4];
111 y = y*180/pi;
112
113 displacement = max(y(:,5))
114 y_residual = y(find(tx==t_tot)+1:end,:);
115 max_resid_radial = max(y_residual(:,1))
116 max_resid_tangential = max(y_residual(:,3))
117

```

```

118 figure(1)
119 plot(tx,y(:,1))
120 xlabel('Time (s)')
121 ylabel('Radial Residual Swinging Angle (deg)')
122
123 figure(2)
124 plot(tx,y(:,3))
125 xlabel('Time (s)')
126 ylabel('Tangential Residual Swinging Angle (deg)')

```

Listing A.17: Forward Tip-over Analysis for the Case of Boom Slewing Motion (m_4 is the variable)

```

1 % This code calculates the counterweight displacement with ...
    respect to
2 % different slew angles in order to prevent forward tip-over, ...
    this is done
3 % for three values of moveable counterweight mass (Boom Luffing ...
    Motion)
4
5 clear
6
7 %% Defining all parameters
8 g=9.8; % Gravitational acceleration [m/s^2]
9 % Defining Lengths of different components
10 L1 = 10.33; % Length of Base Body [m]
11 L2 = 102; % Length of boom [m]
12 L3 = 30; % Length of mast [m]
13 L4.fixed = 7; % Position of fixed counterweight [m]
14 L5 = 70; % Length of payload hoist [m]
15 L4.min = 0; % Minimum position of moveable ...
    counterweight [m]

```

```

16 L4_max = 100;           % Maximum position of moveable ...
    counterweight [m]
17 % Range of allowed locations for counterweight [m]
18 L4_range = linspace(L4_min,L4_max,500);
19 % Other dimensions
20 w = 8.4;               % Width of base [m]
21 h = 2.45;              % Height of base [m]
22 % Mass parameters
23 m1 = 125;               % Mass of Car Body [tons]
24 m2 = 60;                % Mass of boom [tons]
25 m3 = 12.5;              % Mass of mast [tons]
26 m4i = [150, 200, 300]; % Different masses of moveable ...
    counterweight [tons]
27 m4_fixed = 240;        % Mass of fixed counterweight [tons]
28 m5 = 156 ;              % 110, 125, 140, Mass of Payload [tons]
29 % Angles
30 p1 = 70*pi/180;        % Boom Luffing Angle [rad]
31 B = [6.30 8.4 10.5 12.6 14.7...
32       16.8 18.9 20.99 23.1 25.2 ...
33       27.3 29.4 31.5 33.6 35.7 ...
34       37.8 39.9 42 44.1 46.2 ...
35       48.3 50.4 52.5 54.6 56.7 ...
36       58.8 60.9 63 65.1 67.2 ...
37       69.3 71.4 73.5 75.6 77.7 ...
38       79.8 81.9 84 86.1 88.2]*pi/180;    % Slewing Angle [rad]
39 q1i = [.17 .3 .47 .66 .89 ...
40        1.13 1.41 1.7 2 2.31 ...
41        2.64 2.97 3.3 3.63 3.95 ...
42        4.26 4.55 4.83 5.08 5.3 ...
43        5.48 5.58 5.67 5.77 5.83 ...
44        5.88 5.97 6.03 6.03 5.94 ...
45        5.77 5.54 5.3 5.12 4.97 ...

```

```

46         4.86 4.74 4.67 4.64 4.66]*pi/180; % Radial Swing angle [rad]
47 q2i = [3.06 4.04 4.97 5.86 6.69 ...
48         7.45 8.14 8.78 9.32 9.8 ...
49         10.18 10.47 10.67 10.83 10.86...
50         10.76 10.65 10.41 10.06 9.64...
51         9.18 8.64 8.02 7.36 6.66 ...
52         5.96 5.43 4.94 4.53 4.22 ...
53         4.01 3.92 3.93 4.12 4.33 ...
54         4.51 4.63 4.66 4.65 4.64]*pi/180; % Tangential Swing ...
           angle [rad]
55
56 %% Calculating minimum location of counterweight to ensure safety
57
58 for k=1:length(m4i) % Loop repeats for each value of m4
59     m4 = m4i(k);
60     for i=1:length(B) % Loop repeats for every slew angle
61         q1 = q1i(i);
62         q2 = q2i(i);
63         syms L4
64         p2 = acos(L4/L3); % Mast angle
65 % Set up coordinate systems for mass centers
66 c1 = [0 0 h/2]'; % Car Body mass center
67 c2 = [L2*cos(p1)*cos(B(i))/2,...
68       L2*cos(p1)*sin(B(i))/2,...
69       (L2*sin(p1)/2)+h]'; % Boom mass center
70 c3 = [-L3*cos(p2)*cos(B(i))/2,...
71       -L3*cos(p2)*sin(B(i))/2,...
72       (L3*sin(p2)/2)+h]'; % Mast mass center
73 c4 = [-L4*cos(B(i)),...
74       -L4*sin(B(i)), h]'; % Moving counterweight mass center
75 c4.fixed = [-7*cos(B(i)),...
76            -7*sin(B(i)), 3]'; % Fixed counterweight mass center

```

```

77 c5 = [(L2*cos(p1)+L5*sin(q1))*cos(B(i))+L5*sin(q2)*sin(B(i)),...
78       (L2*cos(p1)+L5*sin(q1))*sin(B(i))-L5*sin(q2)*cos(B(i)),...
79       L2*sin(p1)+h-L5*sqrt(1-(sin(q1))^2-(sin(q2))^2)]';
80                                     % Payload mass center
81
82 % Forces:
83 G = [0 0 -1]';                       % Direction of gravitational force
84 f1 = m1*g*G;                          % Weight of car body
85 f2 = m2*g*G;                          % Weight of boom
86 f3 = m3*g*G;                          % Weight of mast
87 f4 = m4*g*G;                          % Weight of moveable counterweight
88 f4_fixed = m4_fixed*g*G;              % Weight of fixed counterweight
89 f5 = m5*g*G;                          % Weight of payload
90
91 % Instantaneous inertial location of the ith ground contact point
92 p01 = [-L1/2 w/2 0]';
93 p02 = [L1/2 w/2 0]';
94 p03 = [L1/2 -w/2 0]';
95 p04 = [-L1/2 -w/2 0]';
96
97 % ith tip-over mode axis
98 a1 = p02-p01;
99 a2 = p03-p02;
100 a3 = p04-p03;
101 a4 = p01-p04;
102
103 % Expressing each ith tip-over mode axis as a unit vector
104 a11 = -a1/norm(a1);
105 a22 = -a2/norm(a2);
106 a33 = a3/norm(a3);
107 a44 = -a4/norm(a4);
108

```

```

109 % Deciding which is the tip-over axis based on the value of the ...
    slew angle
110 theta1 = atan((w/2)/(L1/2));
111 theta2 = pi-theta1;
112 %-----
113 pa2 = [L1/2 0 0]'; % Location of a point on axis a2
114 % Vectors pointing from mass centers to the point on a2
115 r1a = c1-pa2;
116 r2a = c2-pa2;
117 r3a = c3-pa2;
118 r4a = c4-pa2;
119 r4a_fixed = c4_fixed-pa2;
120 r5a = c5-pa2;
121
122 % Calculating sum of moments about axis a2:
123 equ = dot(a22,cross(r1a,f1))+dot(a22,cross(r2a,f2))+...
124       dot(a22,cross(r3a,f3))+dot(a22,cross(r4a,f4))+...
125       dot(a22,cross(r4a_fixed,f4_fixed))+...
126       dot(a22,cross(r5a,f5))==0;
127 L4_long = solve(equ,L4);
128 L4_long1(k,i) = double(vpa(L4_long));
129 if L4_long1(k,i)<0
130     L4_long1(k,i) = 0;
131 end
132 %-----
133 pa1 = [0 w/2 0]'; % Location of a point on axis a1
134 % Vectors pointing from mass centers to the point on a1
135 r1a = c1-pa1;
136 r2a = c2-pa1;
137 r3a = c3-pa1;
138 r4a = c4-pa1;
139 r4a_fixed = c4_fixed-pa1;

```

```

140 r5a = c5-pa1;
141
142 % Calculating sum of moments about axis a1:
143 equ = dot(a11,cross(r1a,f1))+dot(a11,cross(r2a,f2))+...
144       dot(a11,cross(r3a,f3))+dot(a11,cross(r4a,f4))+...
145       dot(a11,cross(r4a_fixed,f4_fixed))+...
146       dot(a11,cross(r5a,f5))==0;
147 L4_long = solve(equ,L4);
148 L4_long2(k,i) = double(vpa(L4_long));
149 if L4_long2(k,i)<0
150     L4_long2(k,i) = 0;
151 end
152 %-----
153     end
154 end
155
156 %% Plotting
157 figure
158 for k = 1:length(m4i)
159     x = [B*180/pi];
160     y1 = [L4_long1(k,:)];
161     y2 = [L4_long2(k,:)];
162     plot(x,y1,x,y2)
163     xlabel('Slew Displacement [deg]')
164     ylabel('Counterweight Position [m]')
165     legend('m_4 = 150 t','m_4 = 200 t','m_4 = 300 t')
166     hold on
167 end

```

Listing A.18: Forward Tip-over Analysis for the Case of Tandem Cranes (ϕ_1 is the variable)


```

1 % This code calculates the boom luffing angle and swinging angle ...
    limits
2 % for two tandem cranes to prevent forward tipping-over
3
4 clear
5
6 %% Defining all parameters
7 g=9.8;                % Gravitational acceleration [m/s^2]
8 % Defining Lengths of different components
9 L1 = 10.33;           % Length of Base Body [m]
10 L2 = 102;            % Length of boom [m]
11 L3 = 7;              % Position of counterweight [m]
12 L4 = 80;            % Length of payload hoist [m]
13 % Other dimensions
14 w = 8.4;            % Width of base [m]
15 h = 2.45;           % Height of base [m]
16 % Mass parameters
17 m1 = 125;           % Mass of Car Body [tons]
18 m2 = 60;            % Mass of boom [tons]
19 m3 = 160;           % Mass of counterweight [tons]
20 m4_range = [120 170 220 270 320] ;    % Mass of Payload [tons]
21 % Defining range of swinging angles [rad]
22 t_range = [0:20]*pi/180;
23 x = [0:35];
24 syms p1
25
26 %% Calculating minimum luffing angle to ensure safety of crane A
27
28 for u = 1:length(m4_range)
29     m4 = m4_range(u);
30
31     %This loop repeats for all values of swing angle

```

```

32     for k = 1:length(t_range)
33         %t = 0.5*x(k)/L4;
34         t = t_range(k);
35
36         % Set up coordinate systems for mass centers
37         c1 = [0 0 h/2]';           % Car Body mass center
38         c2 = [L2*cos(p1)/2,0,...
39             (L2*sin(p1)/2)+h]';   % Boom mass center
40         c3 = [-7,0,3]';          % Counterweight mass center
41         c4 = [L2*cos(p1),0,...
42             L2*sin(p1)+h]';      % Payload mass center
43
44         % Forces:
45         G = [0 0 -1]';           % Direction of gravitational ...
46         force
47         f1 = m1*g*G;             % Weight of car body
48         f2 = m2*g*G;             % Weight of boom
49         f3 = m3*g*G;             % Weight of counterweight
50         D = [sin(t) 0 -cos(t)]'; % Direction of tension in ...
51         the chord
52         f4 = (.5*m4*g/cos(t))*D;  % Tension in the chord
53
54         % Instantaneous inertial location of the ith ground contact point
55         p01 = [-L1/2 w/2 0]';
56         p02 = [L1/2 w/2 0]';
57         p03 = [L1/2 -w/2 0]';
58         p04 = [-L1/2 -w/2 0]';
59
60         % ith tip-over mode axis
61         a1 = p02-p01;
62         a2 = p03-p02;
63         a3 = p04-p03;

```

```

62     a4 = p01-p04;
63
64     % Expressing each ith tip-over mode axis as a unit vector
65     a11 = -a1/norm(a1);
66     a22 = -a2/norm(a2);
67     a33 = -a3/norm(a3);
68     a44 = -a4/norm(a4);
69
70     % Tip over axis is a2
71     pa2 = [L1/2 0 0]';           % Location of a point on axis a4
72
73     % Vectors pointing from mass centers to the point on a2
74     r1a = c1-pa2;
75     r2a = c2-pa2;
76     r3a = c3-pa2;
77     r4a = c4-pa2;
78
79     % Calculating sum of moments about axis a2:
80     Ma(k) = dot(a22,cross(r1a,f1))+dot(a22,cross(r2a,f2))+...
81             dot(a22,cross(r3a,f3))+dot(a22,cross(r4a,f4))==0;
82     plsol(:,k)=double(vpa(solve(Ma(k),p1)));
83
84     if plsol(1,k)>0
85         plfina(u,k)=plsol(1,k);
86     else
87         plfina(u,k)=plsol(2,k);
88     end
89
90     plfina = real(plfina);
91     end
92 end
93

```

```

94 for j=1:length(t_range)
95     p1_max(j)=82;
96     p1_min(j)=43.5;
97 end
98
99 %% Calculating minimum luffing angle to ensure safety of crane B
100
101 for u=1:length(m4_range)
102     m4=m4_range(u);
103
104     %This loop repeats for all values of swing angle
105     for k = 1:length(t_range)
106         %t = 0.5*x(k)/L4;
107         t = t_range(k);
108
109         % Set up coordinate systems for mass centers
110         c1 = [0 0 h/2]'; % Car Body mass center
111         c2 = [L2*cos(p1)/2,0,...
112             (L2*sin(p1)/2)+h]'; % Boom mass center
113         c3 = [-7,0,3]'; % Counterweight mass center
114         c4 = [L2*cos(p1),0,...
115             L2*sin(p1)+h]'; % Payload mass center
116
117         % Forces:
118         G = [0 0 -1]'; % Direction of gravitational ...
119             force
120         f1 = m1*g*G; % Weight of car body
121         f2 = m2*g*G; % Weight of boom
122         f3 = m3*g*G; % Weight of counterweight
123         D = [-sin(t) 0 -cos(t)]'; % Direction of tension in ...
124             the chord
125         f4 = (.5*m4*g/cos(t))*D; % Tension in the chord

```

```

124
125 % Instantaneous inertial location of the ith ground contact point
126 p01 = [-L1/2 w/2 0]';
127 p02 = [L1/2 w/2 0]';
128 p03 = [L1/2 -w/2 0]';
129 p04 = [-L1/2 -w/2 0]';
130
131 % ith tip-over mode axis
132 a1 = p02-p01;
133 a2 = p03-p02;
134 a3 = p04-p03;
135 a4 = p01-p04;
136
137 % Expressing each ith tip-over mode axis as a unit vector
138 a11 = -a1/norm(a1);
139 a22 = -a2/norm(a2);
140 a33 = -a3/norm(a3);
141 a44 = -a4/norm(a4);
142
143 % Tip over axis is a2
144 pa2 = [L1/2 0 0]'; % Location of a point on axis a4
145
146 % Vectors pointing from mass centers to the point on a2
147 r1a = c1-pa2;
148 r2a = c2-pa2;
149 r3a = c3-pa2;
150 r4a = c4-pa2;
151
152 % Calculating sum of moments about axis a2:
153 Mb(k) = dot(a22,cross(r1a,f1))+dot(a22,cross(r2a,f2))+...
154         dot(a22,cross(r3a,f3))+dot(a22,cross(r4a,f4))==0;
155 plsol(:,k)=double(vpa(solve(Mb(k),p1)));

```

```

156
157     if plsol(1,k)>0
158         plfinb(u,k)=plsol(1,k);
159     else
160         plfinb(u,k)=plsol(2,k);
161     end
162
163     plfinb = real(plfinb);
164     end
165 end
166
167 plfina=plfina'*180/pi;
168 plfinb=plfinb'*180/pi;
169
170 figure
171 plot(t_range*180/pi,plfina,t_range*180/pi,plfinb,...
172      t_range*180/pi,pl_max)
173 xlabel('Swing Angle \theta (deg)')
174 ylabel('Boom Luffing Angle \phi_1 (deg)')
175 legend('\phi_1 of Crane A','\phi_1 of Crane B','Maximum \phi_1')

```

Listing A.19: Forward Tip-over Analysis for the Case of Tandem Cranes (m_4 is the variable)

```

1 % This code calculates the boom luffing angle and swinging angle ...
   limits
2 % for two tandem cranes to prevent forward tipping-over
3
4 clear
5
6 %% Defining all parameters
7

```

```

8 g=9.8; % Gravitational acceleration [m/s^2]
9
10 % Defining Lengths of different components
11 L1 = 10.33; % Length of Base Body [m]
12 L2 = 102; % Length of boom [m]
13 L3 = 7; % Position of counterweight [m]
14 L4 = 80; % Length of payload hoist [m]
15
16 % Other dimensions
17 w = 8.4; % Width of base [m]
18 h = 2.45; % Height of base [m]
19
20 % Mass parameters
21 m1 = 125; % Mass of Car Body [tons]
22 m2 = 60; % Mass of boom [tons]
23 m3 = 160; % Mass of counterweight [tons]
24 syms m4
25
26 % Defining range of swinging angles [rad]
27 t_range = [0:20]*pi/180;
28 p1_range = [57 62 67 72 77]*pi/180;
29
30 %% Calculating minimum luffing angle to ensure safety of crane A
31 for u = 1:length(p1_range)
32
33     p1 = p1_range(u);
34
35     %This loop repeats for all values of swing angle
36     for k = 1:length(t_range)
37         t = t_range(k);
38
39     % Set up coordinate systems for mass centers

```

```

40     c1 = [0 0 h/2]'; % Car Body mass center
41     c2 = [L2*cos(p1)/2,0,...
42           (L2*sin(p1)/2)+h]'; % Boom mass center
43     c3 = [-7,0,3]'; % Counterweight mass center
44     c4 = [L2*cos(p1),0,...
45           (L2*sin(p1))+h]'; % Payload mass center
46
47     % Forces:
48     G = [0 0 -1]'; % Direction of gravitational ...
           force
49     f1 = m1*g*G; % Weight of car body
50     f2 = m2*g*G; % Weight of boom
51     f3 = m3*g*G; % Weight of counterweight
52     D = [sin(t) 0 -cos(t)]'; % Direction of tension in ...
           the chord
53     f4 = (.5*m4*g/cos(t))*D; % Tension in the chord
54
55     % Instantaneous inertial location of the ith ground contact point
56     p01 = [-L1/2 w/2 0]';
57     p02 = [L1/2 w/2 0]';
58     p03 = [L1/2 -w/2 0]';
59     p04 = [-L1/2 -w/2 0]';
60
61     % ith tip-over mode axis
62     a1 = p02-p01;
63     a2 = p03-p02;
64     a3 = p04-p03;
65     a4 = p01-p04;
66
67     % Expressing each ith tip-over mode axis as a unit vector
68     a11 = -a1/norm(a1);
69     a22 = -a2/norm(a2);

```



```

70     a33 = -a3/norm(a3);
71     a44 = -a4/norm(a4);
72
73     % Tip over axis is a2
74     pa2 = [L1/2 0 0]';           % Location of a point on axis a4
75
76     % Vectors pointing from mass centers to the point on a2
77     r1a = c1-pa2;
78     r2a = c2-pa2;
79     r3a = c3-pa2;
80     r4a = c4-pa2;
81
82     % Calculating sum of moments about axis a2:
83     Ma(k) = dot(a22,cross(r1a,f1))+dot(a22,cross(r2a,f2))+...
84             dot(a22,cross(r3a,f3))+dot(a22,cross(r4a,f4))==0;
85     m4sola(u,k)=double(vpa(solve(Ma(k),m4)));
86
87     end
88 end
89
90 m4sola=m4sola';
91
92 t_range=t_range'*180/pi;
93 plot(t_range,m4sola)
94 xlabel('Swing Angle \theta (deg)')
95 ylabel('Payload Mass (tons)')

```

REFERENCES

- [1] ABO-SHANAB, R. and SEPEHRI, N., “Tip-over stability of manipulator-like mobile hydraulic machines,” *Journal of Dynamic Systems, Measurements and Control*, vol. 127, pp. 295–301, Jun. 1, 2005.
- [2] ASME-B30.5, “The american society of mechanical engineers: Mobile and locomotive cranes,” 2014.
- [3] BERMAN, M., “The washington post.” <https://www.washingtonpost.com/news/post-nation/wp/2016/02/05/crane-collapse-in-new-york-city-kills-one-person-injures-two-others/>. Accessed: 1:35am, March 1, 2016.
- [4] CRANEACCIDENTS.COM, “Crane accidents.” <http://www.craneaccidents.com/>. Accessed: 12:20pm, July 31, 2015.
- [5] FUJIOKA, D., “Tip-over stability analysis for mobile boom cranes with single- and double-pendulum payloads,” Master’s thesis, Georgia Institute of Technology, Atlanta, GA, 2010.
- [6] GHASEMPOOR, A. and N, S., “A measure of stability for mobile manipulators with application to heavy-duty hydraulic machines,” *Journal of Dynamic Systems, Measurements and Control*, vol. 120, pp. 360–369, Sep. 1, 1998.
- [7] GOTTWALD, “Gottwald port technology: Safe solutions for lifting project cargoes.” www.porttechnology.org.
- [8] JENG, S., YANG, C., and CHIENG, W., “Outrigger force measure for mobile crane safety based on linear programming optimization,” *Mechanics Based Design of Structures and Machines*, vol. 38, pp. 145–170, Apr. 1, 2010.
- [9] JONES, M., “What does a crawler crane do?.” <http://www.gorge.net.au/what-does-a-crawler-crane-do/>. Published: March 5, 2014, Accessed: 7:44pm, March 4, 2015.

- [10] KARBBENDAM, R., “Heavy lift news.” <http://www.heavyliftnews.com/news/tandem-lift-goes-wrong>. Accessed: 6:40pm, March 3, 2016.
- [11] KILIÇASLAN, S., BALKAN, T., and IDER, S., “Tipping loads of mobile cranes with flexible booms,” *Journal of Sound and Vibration*, vol. 223, pp. 645–657, Jun. 17, 1999.
- [12] KORAYEM, M., AZIMIRAD, V., and NIKOOBIN, A., “Maximum load-carrying capacity of autonomous mobile manipulator in an environment with obstacle considering tip-over stability,” *International Journal of Advanced Manufacturing Technology*, vol. 46, pp. 811–829, Jan. 1, 2010.
- [13] LAWRENCE, J., W., *Crane Oscillation Control: Non-linear Elements and Educational Improvements*. PhD thesis, Georgia Institute of Technology, Atlanta, GA, 2006.
- [14] LEE, Y. and YI, S., “Rollover prevention for sport utility vehicle using fuzzy-logic controller,” in *SPIE - The International Society for Optical Engineering*, Dec., 2005.
- [15] LI, Y. and LIU, Y., “Real-time tip-over prevention and path following control for redundant nonholonomic mobile modular manipulators via fuzzy and neural-fuzzy approaches,” *Journal of Dynamic Systems, Measurement and Control*, vol. 128, pp. 753–764, Dec. 1, 2006.
- [16] LIU, H., SINGHOSE, W., and CHENG, W., “Static and dynamic tip-over stability of crawler cranes with movable counterweights,” in *VIII International Conference "Heavy Machinery-HM2014"*, (Zlatibor, Serbia), June 25-28, 2014.
- [17] MACCOLLUM, D., “Critical hazard analysis of crane design,” *Professional Safety*, vol. 24, pp. 31–36, 1980.
- [18] MACCOLLUM, D., *Crane Hazards and their prevention*. Des Plaines, IL: American Society of Safety Engineers, 1993.
- [19] MALEKI, E., PRIDGEN, B., SINGHOSE, W., and SEERING, W., “Educational use of a small-scale cherrypicker,” *International Journal of Mechanical Engineering Education*, vol. 40, pp. 104–120, Apr. 1, 2012.

- [20] MANNING, R., CLEMENT, J., KIM, D., and SINGHOSE, W., “Dynamics and control of bridge cranes transporting distributed-mass payloads,” *ASME J. Dynamic Systems, Measurement, and Control*, vol. 132, no. 1, pp. 014505–3, 2010.
- [21] MORGAN, J., “Exploring the middle-east’s crawler crane market.” <http://www.constructionweekonline.com/article-26943-exploring-the-middle-east-s-crawler-crane-market/3/>. Published: March 7, 2014, Accessed: 6:45pm, July 30, 2015.
- [22] NEITZEL, R., SEIXAS, N., and REN, K., “A review of crane safety in the construction industry,” *Applied Occupational and Environmental Hygiene*, vol. 16, pp. 1106–1117, 2001.
- [23] PALMERLAW, “The law offices of palmer oliver.” <http://www.palmerlaw.com/index.php/case-history/stimpson-v-maxim-et-al>. Accessed: 10:28pm, August 12, 2015.
- [24] PAPADOPOULOS, E. and REY, D., “The force-angle measure of tip-over stability margin for mobile manipulators,” *Vehicle System Dynamics*, vol. 33, pp. 29–48, 2000.
- [25] PAPADOPOULOS, E. and REY, D., “A new measure of tip-over stability margin for mobile manipulators,” in *IEEE International Conference on Robotics and Automation*, (Minneapolis, MN), Apr., 1996.
- [26] PASCO, “Pasco structure systems - large structures set me-7003.” https://www.pasco.com/prodCatalog/ME/ME-7003_large-structures-set/index.cfm. Accessed: 9:08pm, March 4, 2016.
- [27] PECH, D. J., “Lift crane with moveable counterweight,” 2011. US Patent 2011/0031202 A1.
- [28] PECH, D. J., “Mobile lift crane with variable position counterweight,” 2011. US Patent 7,967,158 B2.
- [29] RAUCH, A., SINGHOSE, W., FUJIOKA, D., and JONES, T., “Tip-over stability analysis of mobile cranes with swinging payloads,” *Journal of Dynamic Systems, Measurement and Control*, vol. 135, Jan. 1, 2013.

- [30] RAUCH, A., “Stability analysis of mobile boom cranes,” Master’s thesis, Georgia Institute of Technology, Atlanta, GA, 2008.
- [31] SHAPIRA, A., LUCKO, G., and SCHEXNAYDER, C., “Cranes for building construction projects,” *Journal of Construction Engineering and Management*, vol. 9, pp. 690–700, September, 2007.
- [32] SHOPMADEINCHINA, “Sany scc8000 crawler crane toy.” http://www.shopmadeinchina.com/product-image/1-50-SANY-SCC8000-CRAWLER-CRANE-toy_13124925.shtml. Accessed: 8:39pm, July 30, 2015.
- [33] SUN, L., “Moveable weight counterbalance apparatus of crawler crane containing apparatus thereof,” 2013. US Patent 2013/0161278 A1.
- [34] TEREX, “Terex cranes.” <http://www.terex.com/>. Accessed: 5:20pm, March 4, 2015.
- [35] TRADEGET.COM, “Tower crane qtz125.” <http://www.tradeget.com/listing/jinan-jinkui-architecture-machinery-co-ltd/product-services-detail/66460/21121/1/>. Accessed: 6:40pm, July 30, 2015.
- [36] VERTIKAL, “Seven gmk 6300l western australia.” <http://www.vertikal.net/en/news/story/17539/>. Accessed: 8:32pm, September 18, 2015.
- [37] WIGGLESWORTH, E., “Improvements in or relating to cranes,” 1922. GB Patent 190,594.
- [38] WIKIPEDIA, “Crane (machine).” http://en.wikipedia.org/wiki/Crane_%28machine%29#Mechanical_principles. Accessed: 7:36pm, March 4, 2015.
- [39] WORKCOVER, “Using mobile cranes in ‘pick and carry’ operations.” www.workcover.nsw.gov.au, 2013.
- [40] YERAL, J.-M., “Lifting appliance,” 2006. US Patent 2006/0283826 A1.

- [41] ZHAOFA, Z., FENG, L., and XIANXIANG, H., “Safety monitoring method of hoisting equipment based on pressure measuring,” in *International Conference on Electronic Measurement And Instruments*, pp. 2504–2507, 2007.